

CRANFIELD UNIVERSITY

SAMUEL M GRICE

IS THE THERMODYNAMIC EFFICIENCY OF SOIL  
MICROBIAL COMMUNITIES RELATED TO ECOSYSTEM  
MATURITY AND STRESS?

SCHOOL OF APPLIED SCIENCE

PhD THESIS  
Academic year: 2013-14

Supervisors: James A Harris & Karl Ritz  
July 2014

CRANFIELD UNIVERSITY

SCHOOL OF APPLIED SCIENCE

PhD THESIS

Academic Year 2013-2014

SAMUEL M GRICE

Is the thermodynamic efficiency of soil microbial communities related to ecosystem maturity and stress?

Supervisors: James A Harris & Karl Ritz

July 2014

This thesis is submitted in partial fulfilment of the requirements for the degree of Doctor of Philosophy

© Cranfield University 2014. All rights reserved. No part of this document may be reproduced without the written permission of the copyright owner.

In memory of Dr Rodger Barnes

~

In gratitude to Mr John Miles

~

“The mediocre teacher tells. The good teacher explains.  
The superior teacher demonstrates. The great teacher  
inspires.” -William Arthur Ward

## Abstract

According to the second law of thermodynamics, no process can be 100% efficient and all processes must increase the total entropy of the system they occupy. Therefore, living systems require a constant influx of low-entropy energy to survive, giving an evolutionary advantage to those that produce less waste. Odum suggested that ecosystems would therefore develop mechanisms for reducing entropy production per unit biomass, as they matured.

Isothermal calorimetry allows the direct measurement of waste heat emitted from any system, including soils and the life within them. However, upon review it became apparent that current methods employed in the analysis of soil microbial communities via isothermal calorimetry are outdated and in need of review. An experiment was conducted to troubleshoot the method and appropriate modifications were made. A second experiment was conducted to test the microbial community response to pre-incubation prior to calorimetric analysis at 20°C, concluding that samples should be pre-incubated for ten to sixteen days prior to analysis at 20°C.

Subsequently, experiments were carried out to establish how much waste heat was produced by soil microbial communities in the context of various ecological gradients, following glucose amendment. Results for enthalpy efficiency ( $\eta_{\text{eff}}$ ) proved inconclusive, whereas results for substrate induced heat production (SIHP), where heat output is expressed per unit biomass, indicated that soil microbial communities produced significantly more waste heat when subjected to

long-term metals induced stress and short-term copper-induced stress. In addition, a reduction in the production of waste heat generated by soil microbial communities associated with primary succession along a glacier foreland was observed. This provides evidence that living systems do indeed evolve towards greater thermodynamic efficiency, manifest via the reduction of energetic waste.

# Acknowledgements

I would like to thank the National Environmental Research Council of the UK (NERC) and The Swedish Research Council Formas for providing the funding for this project.

I would also like to thank the following people:

My parents, David and Angela Grice, for providing additional funding, helping with fieldwork, sampling, proofreading, providing dietary sustenance and continuous support in more ways than I could ever possibly mention.

My supervisors Jim Harris and Karl Ritz for giving me the opportunity to do this PhD, for helping me develop and grow my academic and professional skills, for encouraging me to strive for excellence and for taking every problem that I have dealt them in their stride with good humour.

My subject advisor Mark Pawlett for teaching me the ways of the laboratory, providing helpful insight and feedback on my project and for giving his time to help with the PhD process.

The lab technicians Mirsada Kulenovic and Bernt at MVM huset at SLU in Uppsala and Richard Andrews, Maria Biskupska and Jane Hubble at Cranfield University for all you help with procuring equipment and reagents and for making sure that I did not cause any lasting damage.

Vadim Kessler, Ingmar Persson, Anke Herrman, Elsa Coucheney and everyone else at The Department of Chemistry at SLU for hosting me and allowing access to their equipment, with a special thank you to Daniel Lundberg, Julia Paraskova,

Kai Wilkinson and Pierre Andersson for your helpful assistance and enjoyable company.

My independent chairmen Richard Wellman and Benny Tjahjono for giving up their time to read various reports, my thesis and sit through review meetings.

The lovely Sophie Hedberg, for helping and encouraging me with my thesis writing, despite her best efforts to distract me.

Finally I would like to thank my friends Louise Malmgren, Florian Zeitler, Joseph Wastie and the rest of the international student community in Uppsala for making my time in Sweden so enjoyable that I had to be forcibly returned to the UK.

# Contents

Abstract .....	i
Acknowledgements .....	iii
List of figures .....	xiii
List of tables .....	xviii
List of equations .....	xix
Glossary .....	xx
Acronyms .....	xx
Mathematical expressions and their units .....	xxi
1 Introduction .....	1
1.1 Ecosystem development .....	1
1.2 The thermodynamics of life .....	3
1.3 What is meant by thermodynamic efficiency? .....	7
1.4 Measurement of entropy minimisation in ecosystems .....	9
1.5 C-substrate use efficiency .....	10
1.6 Aims and hypotheses of this study .....	11
2 Literature review .....	13
2.1 Introduction to isothermal calorimetry .....	13
2.1.1 Previous reviews .....	14
2.1.2 Use of calorimetry in soil science .....	15
2.2 Development of the isothermal calorimetric method .....	16



2.2.1	Establishment of the method .....	16
2.3	Estimating microbial biomass.....	17
2.4	Measuring changes in microbial activity .....	18
2.4.1	From addition of C-substrates.....	19
2.4.2	In relation to soil contaminates .....	20
2.4.3	From biodegradation of organic contaminants.....	22
2.4.4	In relation to soil pH .....	23
2.4.5	In relation to sample storage .....	24
2.4.6	In relation to oxygen availability .....	25
2.4.7	In relation to soil moisture .....	25
2.4.8	In relation to soil type or land use .....	26
2.4.9	In relation to incubation temperature .....	28
2.5	Measuring thermodynamic efficiency .....	28
2.5.1	Caloric quotient ( $qW$ ).....	28
2.5.2	Calorirespirometric ratio.....	29
2.5.3	Metabolic enthalpy change .....	29
2.5.4	Biomass specific heat rate.....	33
2.6	Summary and comment .....	34
3	General methods .....	37
3.1	Basic isothermal microcalorimetric technique .....	37
3.1.1	Sample preparation .....	39

3.1.2	Baseline calibration.....	39
3.1.3	Insertion of samples.....	39
3.1.4	Calculation of thermodynamic indices .....	40
3.2	Phospholipid fatty acid profiling.....	41
3.2.1	Sample preparation .....	44
3.2.2	Lipid extraction.....	45
3.2.3	Lipid fractionation.....	45
3.2.4	Mild alkaline methanolysis .....	46
3.2.5	Gas chromatography .....	47
3.2.6	Multivariate statistical analysis.....	48
3.3	Soil microbial biomass carbon.....	48
3.3.1	Sample preparation .....	49
3.3.2	Fumigation.....	49
3.3.3	Extraction.....	50
3.3.4	Dissolved organic carbon analysis.....	50
3.3.5	Calculation.....	51
3.4	Soil organic carbon and total nitrogen content .....	51
3.4.1	Method.....	52
3.5	Soil pH.....	52
3.5.1	Method.....	53
3.6	Soil gravimetric water content .....	53

3.7	Soil water holding capacity.....	54
4	Preliminary experiment .....	55
4.1	Introduction .....	55
4.1.1	Long term metal induced stress.....	56
4.2	Methodology.....	57
4.2.1	Gusums Bruk.....	57
4.2.2	Sampling.....	58
4.2.3	Sample preparation and pre-incubation.....	60
4.2.4	Moisture and organic matter content .....	60
4.2.5	Soil microbial biomass .....	61
4.2.6	Calorimetric analysis.....	61
4.2.7	Statistical analysis .....	62
4.3	Results .....	63
4.3.1	GWC, WHC, SOM and microbial biomass-C.....	63
4.3.2	Calorimetric analysis.....	63
4.3.3	Additional comments on the method.....	67
4.4	Discussion.....	69
4.4.1	Influence of apparent contamination on thermal output.....	69
4.4.2	Inaccuracies in the methodology .....	70
4.5	Conclusions.....	72
5	Method development.....	73

5.1	Introduction .....	73
5.1.1	Background .....	74
5.1.2	Introduction to the experimental work .....	77
5.2	Experimental method .....	77
5.2.1	Sampling & sample preparation.....	77
5.2.2	Biotic analysis.....	78
5.2.3	Glucose saturation optimisation.....	78
5.2.4	Pre-incubation experiment.....	79
5.2.5	Statistical analysis .....	80
5.3	Results .....	81
5.3.1	Biomass and phenotypic structure.....	81
5.3.2	Glucose concentration optimisation.....	82
5.3.3	Changes in heat flow – time curves.....	82
5.3.4	Enthalpy efficiency.....	87
5.4	Discussion.....	88
5.5	Conclusions.....	91
6	Short term copper sulphate induced stress.....	92
6.1	Introduction .....	92
6.2	Materials and methods.....	94
6.2.1	Soils.....	94
6.2.2	Contamination of samples via Cu spiking.....	95

6.2.3	Microbial biomass-C .....	95
6.2.4	PLFA analysis.....	96
6.2.5	pH.....	96
6.2.6	Microcalorimetry .....	97
6.2.7	Data analysis .....	98
6.3	Results .....	99
6.3.1	Biomass & phenotypic profile.....	99
6.3.2	Power time curve of uncontaminated samples .....	101
6.3.3	Power time curves of Cu contaminated samples.....	102
6.3.4	Enthalpy efficiency & SIHP .....	104
6.4	Discussion.....	105
6.5	Conclusions.....	108
7	Ecosystem maturity.....	109
7.1	Introduction .....	109
7.2	Materials and methods.....	112
7.2.1	Soil sampling .....	112
7.2.2	Sample storage, homogenisation and pre-incubation.....	116
7.2.3	Calorimetric analysis.....	117
7.2.4	Biomass.....	117
7.2.5	PLFA analysis.....	117
7.2.6	End-point glucose determination .....	118

7.2.7	Total C and N.....	119
7.2.8	pH.....	119
7.2.9	Statistical analysis .....	119
7.3	Results .....	120
7.3.1	Generic sample site and soil parameters.....	120
7.3.2	PLFA analysis and PCA .....	122
7.3.3	Fungal: bacterial ratios .....	123
7.3.4	Endpoint glucose determination.....	124
7.3.5	Enthalpy efficiency.....	125
7.3.6	Substrate induced heat production .....	127
7.3.7	Fungal dominance and thermodynamic efficiency .....	128
7.4	Discussion.....	129
7.5	Conclusions.....	132
8	General discussion and conclusions.....	134
8.1	Summary.....	134
8.2	Comment on the methodology .....	135
8.2.1	Improvements to the isothermal calorimetric method .....	135
8.2.2	Calculation of $\eta_{eff}$ .....	136
8.2.3	Calculation of SIHP.....	139
8.3	Thermodynamic efficiency.....	140
8.3.1	Relationship with ecosystem maturity.....	141

8.3.2	Relation to ecological stress .....	142
8.3.3	Relation to fungal dominance .....	143
8.4	Suggestions for future work.....	143
8.5	Concluding remarks .....	144
	References.....	146

## List of figures

Figure 3.1 Diagram of the TAM Air isothermal microcalorimeter, showing; A) cutaway view of the instrument with top insulation lid removed, showing: three of the eight calorimeters (1-3), one with part of the heat sink removed, showing the position of the ampoules (1); the thermostat controls (4); the Peltier element (5); insulation (6); amplifier, data logger and power supply (7); and B) cutaway view of a single constituent calorimeter unit, showing: main aluminium heat sink (8); thermopiles (9); 'sample' ampoule (10); inert 'reference' ampoule (11); heat sink plug (12); secondary aluminium heat sink (13). Part A) after Wadsö (2005); part B) after Ren et al. (2012).....	38
Figure 3.2 Diagram of the phospholipid bilayer within cell membrane, showing: A) location of cell membrane; B) constituents of the cell membrane; C) phospholipid bilayer, and; D) space-filling chemical model of an example phospholipid: phosphatidylcholine; black = C, white = H, red = O, yellow = P and blue = N <sup>+</sup> (Dhatfield, 2008) .....	42
Figure 4.1: Approximate location of the four sample sights (marked A-D in red) in relation to the now defunct Gusums Bruk (marked Old Mill), located near the centre of Gusum, Östergötland, Sweden (after Lantmäteriet (2013), ©Lantmäteriet, Gävle, Sweden) .....	59
Figure 4.2: Power-time curves produced from the lab replicate samples, showing both the glucose amended and water amended samples from each sample pair. ....	64
Figure 4.3: Power-time curves for all field samples. Only one of the four lab replicates couples is presented from each site, corresponding to the same	



calorimeter cells as the other samples from each site. Therefore samples A1, B1, C1 and D1 correspond to Site A Rep 1, Site B Rep 2, Site C Rep 3 and Site D rep 4 respectively in Figure 4.2..... 66

Figure 4.4: Results for: A) mean  $\eta_{\text{eff}}$  and B) mean SIHP from each site (field replicates only) for t=2.5-64 hours, with bars denoting pooled standard error and lower case letters denoting homogenous groups at the P = 0.05 level. .... 67

Figure 5.1: Ordination of first (PC1) and second (PC2) principal components, showing a) the phenotypic differences between the three sites with bars denoting pooled standard error and b) loadings of all identified PLFAs associated with the PCA ..... 81

Figure 5.2: Rate of CO<sub>2</sub> mineralisation resulting from addition of different concentrations of glucose-C on a logarithmic scale to the grassland (solid line), arable (dotted line) and forest (dashed line) soils, with error bars denoting pooled standard error ..... 82

Figure 5.3: Power – time curves produced by both glucose and water amended soil samples from the Fors arable site observed at: 2, 4, 6, 10, 16, 27 & 36 days after sample homogenisation ..... 83

Figure 5.4 Power – time curves produced by both glucose and water amended soil samples from the Jädraås pine forest site observed at: 2, 4, 6, 10, 16, 26 & 36 days after sample homogenisation..... 84

Figure 5.5 Power – time curves produced by both glucose and water amended soil samples from the Nântuna grassland site observed at: 2, 4, 6, 10, 16, 26 & 36 days after sample homogenisation..... 85

Figure 5.6 Mean values for a) peak heat flow amplitude ( $P_{max}$ ) and b) time taken to reach peak heat flow amplitude ( $tP_{max}$ ) against pre-incubation time, with error bars denoting the pooled standard error for each series ..... 87

Figure 5.7 Mean enthalpy efficiency ( $\eta_{eff}$ ) measured at 40 hours after substrate addition, with error bars denoting pooled standard error ..... 88

Figure 6.1: Ordination of the first (PC1) and second (PC2) principal components constructed using the PLFA analysis data, showing; a) the phenotypic variance between Cu contamination levels, with bars denoting pooled standard error and letters indicating homogenous groups identified via an LSD test of the third (PC3) principal component, and b) individual loadings of all PLFAs identified in the analysis ..... 101

Figure 6.2: Power/time curve recorded from 8 glucose amended samples of non-lab contaminated soil for 100 hours after substrate addition ..... 102

Figure 6.3: Typical power/time curves for samples at each Cu contamination level, with both glucose and water amended samples from each replicate .... 103

Figure 6.4: Changes in primary peak amplitude and time taken to reach the primary peak due to increasing Cu contamination with bars denoting pooled standard error..... 104

Figure 6.5: Effect of Cu contamination on a)  $\eta_{eff}$  and b) SIHP with blue and red bars showing index values for 0-40 hours and 0-100 hours respectively, error bars denoting pooled standard error and letters indicating homogenous groups at the  $p = 0.05$  confidence level..... 105

Figure 7.1 Location of the sample site in SE Switzerland (Google Inc., 2011), showing approximate isochrones of equal surface age (from Burga, 1999) and the location of sampling sites (A-E & 1-15)..... 112

Figure 7.2 Map of the Morteratsch Glacier Vorfeld, showing a) dominant vegetation types, and b) Isochrones showing retreat data (Burga et al., 2010) ..... 113

Figure 7.3 Sampling polygon for the 1960-2 area, generated using GPS coordinates plotted into an MS Excel x-y plot, overlaid onto the Google Earth 3D terrain surface (Google Inc., 2011). Sampling positions are shown using Google Earth waypoints, with the red point (№6) identifying the randomly generated sampling position, with green points (№7-10) drawn from it as a ‘W’ of best fit. .... 115

Figure 7.4 Typical above ground ecosystem in each of the sampling areas, showing surface ages of: A) 0 years, B) 8 years, C) 51 years and D) 155 years. .... 120

Figure 7.5 Ordination of first (PC1) and second (PC2) principal components from the PLFA data, showing: A) phenotypic differences between the four sample sites, with bars denoting pooled standard error and letters denoting homogenous groups at the  $p=0.05$  level, and B) individual loading of all PLFAs identified by the PCA. .... 123

Figure 7.6 Ratios of fungal: bacterial biomarkers in the PLFA analysis, with error bars denoting pooled standard error and letters identifying homogenous groups. .... 124

Figure 7.7 Glucose remaining in samples after removal from the calorimeter, as determined by a glucose oxidase assay, with bars denoting pooled standard error and homogenous groups identified by letters. .... 124

Figure 7.8 Mean enthalpy efficiency ( $\eta_{eff}$ ) for surface age groups after 40 and 100 hours calorimeter run time, with bars denoting pooled standard error and homogenous groups marked with letters (upper case: T=0-40; lower case: T=0-100). .... 126

Figure 7.9 Mean enthalpy efficiency ( $\eta_{eff}$ ) for surface age groupings after 100 hours calorimeter run time, accounting for unconsumed glucose. Bars denoting pooled standard error. .... 126

Figure 7.10 Mean substrate induced heat production (SIHP) for surface age groups after 40 and 100 hours calorimeter run time, with bars denoting pooled standard error and homogenous groups marked with letters (upper case: T=0-40; lower case: T=0-100). One sample with a negative biomass value was omitted from the analysis. .... 127

Figure 7.11 Modelled relationship between surface age (x-axis), fungal: bacterial ratios (y-axis) and thermodynamic indices (z-axis), namely: A) enthalpy efficiency for T=0-40h, B) enthalpy efficiency for T=0-100h, C) enthalpy efficiency for T=100h, accounting for unconsumed glucose, D) SIHP for T=0-40h and E) SIHP for T=0-100h. Data points shown as blue circles. .. 128

## List of tables

Table 4.1: Mean observations for GWC, WHC, SOM by LOI and chloroform labile Biomass-C, with standard deviations in brackets. Approximate levels of copper contamination are taken from Almqvist (2010) for sites A, B & D and Tyler (1984) for site C.....	63
Table 4.2: Mean values for total heat output from 2.5 to 64 hours after sample amendment of the lab replicated samples. Pooled standard error was calculated using the samples as categorical predictors. n = 16.....	65
Table 5.1: Mean site values ( $\pm$ standard error) for chloroform liable biomass C and water holding capacity (WHC).....	81
Table 6.1 Mean chloroform labile biomass and fungal: bacterial PLFA index (F:B ratio) at each CuSO <sub>4</sub> contamination level.....	99
Table 7.1 Approximate surface age, dominant vegetation type and soil characteristics of each sampling site.....	121

## List of equations

(1).....	1
(2).....	4
(3).....	8
(4).....	8
(5).....	8
(6).....	10
(7).....	29
(8).....	31
(9).....	31
(10).....	32
(11).....	37
(12).....	40
(13).....	41
(14).....	51

# Glossary

## Acronyms

PLFA	phospholipid fatty acid
FAME	fatty acid methyl ester
GC	gas chromatography
PTFE	polytetrafluoroethylene (aka: Teflon <sup>®</sup> )
SPE	solid phase extraction
FID	flame ionisation detector
PCA	principal component analysis
DOC	dissolved organic carbon
CEC	cation exchange capacity
UV	ultra violet [radiation]
MPN	most probable number
CFU	colony forming unit

## Mathematical expressions and their units

$Q$	[Total] heat flow: J
$P$	Power: W
$\varepsilon_c$	Calibration constant: W
$t$	Time: s, min, hour, day, month, year
$U$	Electrical potential difference (voltage): V
$K_{ec}$	Conversion factor: unitless constant
$\eta_{eff}$	Enthalpy efficiency: unitless index with value 0-1
$\Delta H^0$	Enthalpy of change upon complete combustion: kJ mol <sup>-1</sup>



# 1 Introduction

*Nothing in life is certain except death, taxes and the second law of thermodynamics. All three are processes in which useful or accessible forms of some quantity, such as energy or money, are transformed into useless, inaccessible forms of the same quantity. That is not to say that these three processes don't have fringe benefits: taxes pay for roads and schools; the second law of thermodynamics drives cars, computers and metabolism; and death, at the very least, opens up tenured faculty positions.*

– Seth Lloyd (2004)

## 1.1 Ecosystem development

The science of ecology can be defined as the study of the distribution and abundance of organisms, the interactions between those organisms and the transformations and flux of energy and matter that determine the distribution, abundance and interactions of those organisms (Odum, 1969; Likens, 1992; Begon et al., 2006). As such ecology deals with interactions between organisms as well as the interactions between organisms and their physical environment. Jenny (1980) used a modified version of his soil forming equation (Jenny, 1941) to express how these relationships determine the biological and physical development of terrestrial ecosystems via Equation (1):

$$l, v, a, s = f(cl, \phi, r, p, t, \dots) \quad (1)$$

Where the ecosystem properties:  $l$ , vegetation:  $v$ , animals:  $a$  and soil properties:  $s$  of an ecosystem are a function of the climate:  $cl$ , available genetics:  $\phi$ ,

topography:  $r$ , parent material:  $p$ , age:  $t$  and history: ... of the location of the ecosystem. This 'ecosystem state' equation goes some way to explain how the biotic factors of a site will influence the abiotic factors as an ecosystem develops and *vice versa*. However, Jenny (1980) omits all organisms outside the *Animalia* and *Plantae* kingdoms i.e. the majority of species present in a terrestrial ecosystem, as such it may be more helpful to replace the 'vegetation' and 'animals' factors in Equation (1) with a single biotic factor:  $b$ , to represent all biota within the system.

While commenting on Darwin's (1859) theory of natural selection, Spencer (1864) wrote the following on the relationships between biota and their environment:

*“That is to say, it cannot but happen that those individuals whose functions are most out of equilibrium with the modified aggregate of external forces, will be those to die; and that those will survive whose functions happen to be most nearly in equilibrium with the modified aggregate of external forces.*

*But this survival of the fittest, implies multiplication of the fittest. Out of the fittest thus multiplied, there will, as before, be an overthrowing of the moving equilibrium wherever it presents the least opposing force to the new incident force.”*

This is evident during the process of primary succession, where an abiotic environment is colonised by organisms and then subject to ecosystem formation. At the start of this process, those individuals that are able to rapidly

colonise new substrates, termed pioneers, may be termed 'fittest' as they are able to colonise so rapidly that they temporarily avoid direct competition from other organisms. As competition increases, pioneer communities form and individuals will start to compete against each other, which may result in some individuals or species becoming unable to successfully reproduce, diminishing their genetic heritage, allowing other 'fitter' individuals to thrive. Yet Equation (1) shows us that, over time, the biota will change the physical environment (external forces) around them and therefore what constitutes the 'fittest' is likely to change as an ecosystem develops. As such, some species that were able to thrive during early successional stages may be out competed during later stages by species that are able to better exploit the developing substrate more efficiently (Bastow, 2012).

## **1.2 The thermodynamics of life**

Life can be deceptive. In a universe where every process brings greater disorder, life is able to produce and maintain complex and highly ordered structures such as proteins, enzymes, ribosomes and cells (Alberts et al., 2012). Yet, a mechanical explanation of the second law of thermodynamics, termed the Clausius inequality, states that every process must increase the total disorder of a closed system (Atkins, 2000). The concept of entropy is used to describe the quantity of molecular disorder in a system. A highly ordered system, such as a cell, has low entropy, whereas a highly disordered system such as a hot diffuse gas has high entropy. Using the concept of entropy, the second law of thermodynamics can be expressed using Equation (2):

$$\Delta S_{total} > 0 \quad (2)$$

Where  $S_{total}$  is the total entropy of a system during any process.

Schrödinger (1944) stated that according to the second law of thermodynamics, organisms will continually increase the total entropy of part of the world where they exist. Therefore, in order to avoid reaching a state of maximum entropy, i.e. death, they need to feed on a continuous stream of 'negative entropy'.

Entropy is a well-defined concept, which can be quantified for a closed system, with units given in  $J K^{-1}$  (Atkins, 2000). In the relevant literature, the concept of low entropy energy is variously referred to as negative entropy, free energy, exergy and emergy, depending on the exact context (Schrödinger, 1944; Schneider & Sagan, 2005; Odum, 2007). In this study the term low entropy energy will be used. The term 'negative entropy' used by Schrödinger (1944) is technically incorrect, as the third law of thermodynamics states that a perfect crystal will have an entropy of 0 at absolute zero (0 K), therefore the entropy of a system will always be  $\geq 0$ . Schrödinger made a note on the use of this term in later editions of his book, stating that the term 'free energy' was more appropriate. Schrödinger (1944) used this term to illustrate the fact that we cannot treat life as a closed system, as all organisms and ecosystems are open systems, exchanging matter and energy with their surroundings, with most of the low entropy energy used by life originating as short-wave radiation from the Sun and the biologically degraded high entropy energy being re-emitted into space as long wave infrared radiation (Kleidon, 2004). It is therefore necessary to identify that these systems usually do not operate in thermodynamic equilibrium with their surroundings, often accumulating low entropy energy in

the form of biomass. The study of such systems is referred to as non-equilibrium thermodynamics.

Odum (1969) suggested that ecosystems would work to minimise entropy production, in order to be able to support a greater total biomass within the confines of the available low entropy energy influx. Katchalsky & Curran (1967) and Addiscott (1995, 2010) also suggested that ecosystems minimise entropy production, by decreasing entropy through processes such as photosynthesis and biomass formation. However, the concepts discussed do not actually decrease entropy, as Equation (2) shows that with any process entropy will always increase. Rather they increase the order (exergy) of the system, resulting in the system having lower entropy. This increase in order is accomplished by accumulating low entropy energy (emergy) in the system, while high entropy energy is dissipated from the system as dispersed heat and matter.

Lotka (1922) and Odum (1969) suggested that evolution will favour organisms and ecosystems that are able to capture the greatest available energy flux, in order to maximise biomass production. Ulanowicz & Hannon (1987) suggested that this would lead to ecosystems maximising entropy production. Schneider & Kay (1994) and Schneider & Sagan (2005) expanded this concept, asserting that processes such as biomass development, species richness, cycling of C and nutrient cycling all serve to maximise entropy production, even suggesting that organisms exist simply in order to reduce available entropic gradients, i.e. that life exists as a manifestation of the second law, degrading low entropy energy as rapidly as possible. The concept of ecosystems maximising entropy

production during development was first demonstrated via parameterisation and modelling of the terrestrial surface heat flux of lakes at various stage of ecological succession (Aoki, 1989, 1995). More recently the parameterisation of terrestrial surface heat fluxes has been complemented via the integration of mass and energy balance calculations for the system and enhanced modelling techniques, indicating that total entropy production increases over time with increased vegetation colonisation (Vallino, 2010; Brunsell et al., 2011) and is lower in stressed ecosystems (Holdaway et al., 2010). Models of ecosystems produced using the concept of maximisation of entropy have been able to predict the spatial distribution of vegetation by plant species (Schymanski et al., 2010; White et al., 2012) and the sustainability of growth in developing urban areas (Zhang et al., 2006). Similar models employing the maximisation of entropy production have been produced to examine the energetic functioning of the global biosphere (Kleidon, 2004; Kleidon et al., 2010).

However, in spite of this evidence for the maximisation of entropy production, Odum's (1969) concept of minimisation of entropy production still holds true. If life were to fully maximise entropy production, then we would logically expect to see organisms producing as much heat as possible from a minimal total biomass, yet an increase in total biomass is a well-established trend during ecological succession (Jenny, 1941; Chapin et al., 1994; Burga, 1999).

So how can we reconcile this apparent paradox of simultaneous maximisation and minimisation of entropy production? In fact, they can easily be reconciled as both strategies present evolutionary advantages when considered together.

To borrow the analogy of tax representing entropy from Lloyd (2004), quoted at the beginning of this chapter, then we can compare an ecosystem to a company and how much tax it pays. If we assume that this company operates in a stagnant economy with a flat rate of 30% tax, then we will see an increase in the total tax paid as the company expands its share of the market. This is akin to the concept of entropy maximisation due to increasing the proportion of available energy that is captured and recycled by the biomass. In this instance it is desirable for the company to expand its workforce (biomass) until it achieves a monopoly of the available market. Once a monopoly has been achieved, the only way for the company to employ more staff is by finding loopholes to reduce the percentage of tax paid, or by paying the staff less per capita. This is akin to the ecosystem reducing maintenance costs by increasing thermodynamic efficiency, thereby minimising entropy production per unit biomass and allowing a greater total biomass.

As such, over the course of ecological succession we should be able to observe an increase in the thermodynamic efficiency of communities as they progress from a state of r-strategist domination where total systemic energetic inputs are increased, thereby driving entropy maximisation, to a state of K-strategist domination, where entropy production is minimised per unit biomass.

### **1.3 What is meant by thermodynamic efficiency?**

The first law of thermodynamics states that energy is conserved and that heat and work are both forms of energy (Blundell & Blundell, 2009). This can be expressed using Equation (3):

$$\Delta U = \Delta Q + \Delta W \quad (3)$$

Where  $U$  is the internal energy of the system,  $Q$  is the heat supplied to the system and  $W$  is the work done on the system. The definition of the second law of thermodynamics was given by Lord Kelvin as “No process is possible whose sole result is the complete conversion of heat into work”. Therefore Equation (2) can alternatively be rewritten for any process as:

$$\Delta Q > \Delta W \quad (4)$$

Using the principles of the first and second laws of thermodynamics, it is possible to express the thermodynamic efficiency of a process converting heat into work using Equation (5):

$$\eta = \frac{W}{Q} \quad (5)$$

Where  $\eta$  is the efficiency, a dimensionless index with a value of  $< 100\%$ , as  $Q$  must be  $> W$ .

We should therefore be able to observe a minimisation in the entropy production per unit biomass as an increase in the thermodynamic efficiency of the ecosystem. In this case the heat supplied to the system  $Q$  may take the form of shortwave solar radiation driving photosynthesis in phototrophs, a mineral substrate for chemoautotrophs or a C-substrate for chemoheterotrophs. The value for work  $W$  may be manifested as the driving of metabolism or production of biomass. If Odum's (1969) theory of the minimisation of entropy production is manifest, then we should expect to see a lower value for efficiency in immature or stressed ecosystems, than in steady state, mature ecosystems.



## **1.4 Measurement of entropy minimisation in ecosystems**

As discussed above, there is a wealth of study on the maximisation of entropy in ecosystems, quantified by comparison of the total measured and/or modelled energy budget of ecosystems, with much of this research undertaken since the year 2000. In contrast there are only a few studies that have attempted to quantify minimisation of entropy production by measurement of thermodynamic efficiency of terrestrial ecosystems, most of which were conducted pre-2000.

Anderson & Domsch (1985) developed a method for assessing how much energy is lost from maintenance by calculating the metabolic quotient ( $q_{CO_2}$ ), a ratio of respiration: biomass. Insam & Haselwandter (1989) attempted to examine Odum's (1969) theory by measuring the metabolic quotient along two successional chronosequences arising from glacial retreat. A decrease in  $CO_2$  production per unit biomass over the 0 – 200 year age range was observed, implying that immature ecosystems produced more energetic waste than mature ecosystems. Several studies used the metabolic quotient to try to replicate and expand on Insam & Haselwandter's (1989) findings, however further studies proved inconclusive (Wardle & Ghani, 1995; Merilä, 2003) and the concept now appears to have been abandoned by the scientific community.

More recently, isothermal calorimetry has shown that  $CO_2$  production rates do not always correspond to heat production rates (Barros et al., 2011; Harris et al., 2012), therefore  $CO_2$  mineralisation cannot be used as a proxy for entropy production. Harris et al. (2012) used isothermal calorimetry to directly measure metabolically produced heat from soil microbial communities subjected to

various nutrient input regimes during a long term arable field trail. The data was assessed using a modified version of Equation (5), adapted from Battley (1960) and the substrate induced heat production (SIHP), a measure of heat production per unit biomass. It was observed that values for both enthalpy efficiency  $\eta_{\text{eff}}$  and SIHP indicated that microbial communities under traditional input regimes produced less entropy than those exposed to long term stress, supporting Odum's (1969) theory.

## 1.5 C-substrate use efficiency

Although the concept of minimisation in entropy production has only been subject to limited study, the parallel idea of substrate use efficiency is frequently used in ecology and biochemistry, and provides some evidence for this theory. Although it can be an ambiguous term with several definitions attributed to it (Blagodatskaya et al., 2014), it is generally identified as an organism's efficiency in assimilating C-substrates into new biomass. As such it can be seen as an indicator for the inverse of entropy production. The definition most comparable to the work presented in this thesis assumes that all consumed C-substrate is either absorbed into the biomass or respired as CO<sub>2</sub> (Keiblinger et al., 2010), as defined in Equation (6):

$$\text{C-substrate use efficiency} = \frac{\text{growth in biomass-C}}{\text{growth in biomass-C} + \text{respired C}} \quad (6)$$

Studies on C-substrate use efficiency have provided examples concurrent with the ecological trend of minimisation of entropy production. Studies have indicated that C-substrate use efficiency increases as ecosystems develop

along a chronosequence (Ohtonen et al., 1999; Kashian et al., 2013), decreased in nutrient staved ecosystems (Chambers et al., 2004; Saetre & Stark, 2005; Manzoni et al., 2012; Waring et al., 2014), are higher for K-strategists than in r-strategists (Six et al., 2006; Strickland & Rousk, 2010).

Barros et al. (2000) measured the enthalpy change from the metabolization of glucose by the soil microbial biomass using isothermal calorimetry, in a very similar manner to Harris et al. (2012). Apparently no attempt was made to quantify entropy production and biomass data presented were most probable numbers (MPN) from counts of colony forming units (CFU) counts, a veteran technique incapable of being used to provide a robust conversion to biomass (Ritz, 2007). However, despite methodological issues, discussed more in Chapters 2 & 8, the study did find that Amazonian forest soils which were poor in organic matter had a higher enthalpy change than those rich in organic matter, suggesting that the organic rich soils were able to incorporate more C into their biomass with lower entropic losses.

## **1.6 Aims and hypotheses of this study**

This body of work aims to build on the findings of Harris et al. (2012) by empirically investigating Odum's (1969) theory of minimisation of entropy production via the use of direct calorimetry to measure the thermodynamic efficiency of glucose degradation by the soil microbial biomass. To that end this study will address the following hypotheses:

1. The thermodynamic efficiency of the soil microbial biomass increases as ecosystem development takes place along a successional gradient.

2. The thermodynamic efficiency of the soil microbial biomass will decrease when subjected to ecological stress.
3. The thermodynamic efficiency of the soil microbial biomass will be greater when the fungal (K-strategist) biomass is dominant than when the bacterial (r-strategist) biomass dominates.

In order to achieve this, the dissertation has been divided into eight chapters, as follows; introducing the reader to the thermodynamic principals of ecology (Chapter 1), a review of investigations on the soil microbial biomass by use of isothermal calorimetry (Chapter 2), a general methodology (Chapter 3), refinement of the isothermal calorimetric methodology (Chapters 4 & 5), empirical assessment of the thermodynamic efficiency of the soil microbial biomass subject to anthropogenically produced ecosystem stress (Chapters 4, 5 & 6), empirical assessment of the thermodynamic efficiency of the soil microbial biomass in relation to fungal dominance (Chapters 5, 6 & 7), empirical assessment of the thermodynamic efficiency of the soil microbial biomass during ecological succession (Chapter 7) and a general discussion and synthesis (Chapter 8).

## 2 Literature review

*All science is either physics or stamp collecting*

– Ernest Rutherford

### 2.1 Introduction to isothermal calorimetry

The word 'calorimetry' comes from a combination of the Latin noun '*calor*' meaning 'heat' and the Greek verb '*metria*' meaning to measure. It is used to denote any scientific technique which aims to parameterise the change or flow of heat over time during a process. The vernacular term 'thermal analysis' is synonymous with 'calorimetry' and both are common in scientific literature; however 'calorimetry' is used to denote only those analyses concerned with direct measurement of the flow or transformation of heat, whereas 'thermal analysis' is more encompassing and can be applied to any analysis that measures or uses heat. The work in this study is only concerned with *isothermal* calorimetry, from combining the Greek '*iso*' meaning 'equal' and '*therme*' meaning 'heat', i.e. measuring the flow or transformation of heat at a constant temperature. The use of isothermal calorimetry allows direct measurement of the waste heat produced during metabolic reactions, therefore providing a quantification of thermodynamic efficiency.

Many thermal analysis techniques besides isothermal calorimetry are used in contemporary soil science, including thermogravimetry, differential thermal analysis, differential scanning calorimetry and evolved gas analysis. Detailed

reviews of studies applying these techniques have been written by Barros et al. (2007) and Plante et al. (2009).

### **2.1.1 Previous reviews**

It should be noted that in the application of isothermal calorimetry in soil science, the term 'isothermal microcalorimetry' is often employed, as most measurements are made in the microwatt range. However, as scale is of little importance when assessing the results, the broader term of 'isothermal calorimetry' is preferable (Wadsö, 2010).

Several reviews have been published on the use of isothermal calorimetry in soil science. Arguably the most relevant to the aims of this study is the review by Barros et al. (2007), who provides a history of how the science has evolved since the work of Mortensen et al. (1973), with a focus on the thermodynamics of the microbial biomass, particularly during growth. A more comprehensive overall review is provided by Rong et al. (2007) who divides studies into four key areas; those which determine the microbial activity, including biomass estimation, those that monitor the toxicity and biodegradation of organic pollutants, those that evaluate the risk from metal and metalloid contamination, and those that measure the heat of abiotic processes in the soil. Wadsö (2009) provided a brief review of method development and applications, aimed at highlighting methodological issues prevalent in the literature, with suggestions for improvements. Braissant et al. (2010) discusses the advantages and disadvantages of using isothermal calorimetry for measuring microbial activity in the environmental and medical sciences. Also Dziejowski & Białobrzewski

(2011) reviews the use of the technique to assess the biodegradation of solid wastes, sewage sludge and wastewater, briefly covering their application to soil.

## **2.1.2 Use of calorimetry in soil science**

Isothermal calorimetry has existed as a scientific technique since the invention of the ice calorimeter by Antoine Lavoisier in 1780, whose used the apparatus to observe that equal amounts of ice were melted by a burning candle or a guinea pig when placed in a jar filled with his newly identified gas, oxygen, leading him to conclude that “*la respiration est donc une combustion*” – respiration is therefore a combustion (Buchholz & Schoeller, 2004). Its use to investigate soil microbial biomass activity can be dated back to the 1920s (Wadsö, 2009), however the study that can be considered the seminal paper introducing isothermal calorimetry in the analysis of soil was by Mortensen et al. (1973), who established that the heat produced by the soil microbial biomass could be detected and that clear changes in the metabolic rate could be observed. Since then, the use of isothermal calorimetry has focused on two main areas. The first of these is microbial biomass determination, i.e. quantification of the mass of microbiota in the soil system, further divided into studies developing the biomass estimation method and those that apply these methods for biomass determination. The second area is concerned with using isothermal calorimetry to study how the total metabolic rate of the soil microbial community is influenced by various factors. This second area has been the subject of much study and includes studies aiming to assess the energy use efficiency of the soil microbial biomass. As such, this review of the literature is structured into the following four sections: early proving and development of the

isothermal calorimetric method; use of isothermal calorimetry in biomass estimation; use of isothermal calorimetry to measure microbial activity, and; use of isothermal calorimetry to assess thermodynamic efficiency.

This review is only concerned with experiments that assess a microbial community response, therefore those studies that have used sterilised soil as a culturing medium for individual or combinations of microbial strains in isothermal calorimetric analysis (Fradette et al., 1994; Oliveira et al., 2008; Gruiz et al., 2010; Chen et al., 2010; Hong et al., 2011) have been omitted.

## **2.2 Development of the isothermal calorimetric method**

### **2.2.1 Establishment of the method**

Apparently unaware of the work of Mortensen et al. (1973), a study was published by Pamatmat & Bhagwat (1973) using isothermal calorimetry to calibrate dehydrogenase activity of lake sediment microbial communities, finding a significant ( $P < 0.001$ ) correlation between the two.

Neither of these works were referenced by Konno (1976, 1979) who observed differences in heat production of volcanic soils depending on soil type and concentration of glucose or N amendment. Konno (1976), investigated the effect of temperature on activity, recording Q10 values in the range of 2-3, along with the effect of Se contamination, observing a retardation of peak heat flow and an increase in the time taken to reach peak heat flow with increasing Se concentrations (Konno, 1979).



The group of Mortensen et al. (1973) continued to investigate methodological issues, finding that heat flow was effected by moisture content, the act of wetting, sample homogenisation, sample storage, CO<sub>2</sub> accumulation, O<sub>2</sub> limitation, metabolic inhibition and sterilisation, recommending that samples should be homogenised by sieving and stored in polyethene bags at 4°C for up to 6 months (Ljungholm et al., 1979a). Using this method the group went on to observe a decrease in heat flow due to soil acidification (Ljungholm et al., 1979b, 1980), with some recovery after liming (Ljungholm et al., 1980).

### **2.3 Estimating microbial biomass**

Biomass estimation using isothermal calorimetry started with the work of Sparling (1981a; b, 1983), determining the standard conversion that 1g biomass C produces a heat flow of 180.05 mW immediately after substrate addition and before active growth. This method was then used by Heilmann & Beese (1992) and Raubuch & Beese (1999), who compared Sparling's method to CO<sub>2</sub> mineralisation and O<sub>2</sub> consumption methods of biomass estimation, by testing forest soils sampled across north-western Europe. The results showed a good correlation between the methods for calculating biomass and also basal respiration rates, showing similar patterns of variance between sites and horizons. However the results for caloric quotient showed no correlation to the metabolic quotient.

Cabral & Sigstad (2011) presented a unique take on Sparling's (1983) method that attempted to simultaneously measure CO<sub>2</sub> production by introducing a vial containing NaOH solution half way through the measurement, before

subsequent removal later on. The idea of simultaneously measuring heat flow due to CO<sub>2</sub> mineralisation in NaOH and microbial respiration has also been used by Barros et al. (2010; 2011) to provide insight into metabolic efficiency of soil micro-organisms, by providing a ratio of heat flow per unit CO<sub>2</sub> production, calculated in a similar way to the specific activity per unit biomass developed by Raubuch & Beese (1999).

Subsequent use of these biomass estimation methods appears to have been limited to that of Sparling (1983), which has been used to assess the use of ammonium nitrification of arginine-N as a method for estimation of soil microbial biomass (Alef et al., 1988) and the calculation of microbial biomass in studies not attempting to measure microbial activity using isothermal calorimetry (Priesack & Kisser-Priesack, 1993; Bölker, 1994; Stenger et al., 1996; Lehr et al., 1996; Raubuch & Joergensen, 2002; Stein et al., 2005; Levy et al., 2007; Klier et al., 2008). A study by Barros et al. (2008b) used the method of Sparling (1983) to produce biomass estimations for the arid soils of the Atacama Desert, where biomass is often below the detectable limit of C mineralisation methods.

## **2.4 Measuring changes in microbial activity**

Most of the work using isothermal calorimetry in soil science has focused on how the heat flow from the microbial biomass has been affected by various treatments. The majority of these have achieved this by measuring how these treatments change the C-substrate endued heat flow, usually by amendment with glucose. The use of isothermal microcalorimetry in this way was established by the group of Takahashi et al., who measured changes in glucose

induced heat production in soil containing various contaminants (Kawabata et al., 1983), the heat flow induced by different C-substrates (Yamano & Takahashi, 1983) and the heat produced per unit biomass (Kimura & Takahashi, 1985).

### **2.4.1 From addition of C-substrates**

Yamano & Takahashi (1983) found that various sugar C-substrates produced different power-time curves and that the activation energy of C-substrate degradation was: D-glucose > sucrose > lactose > D-fructose > D-galactose > D-mannose. However, concentration of glucose-C was shown to influence heat flow rates, with increasing concentration resulting in a lower initial heat production rate in the range of 1.25 – 50 mg glucose g<sup>-1</sup> soil in Barja et al. (1999), while increasing with glucose concentration until reaching a maximum after 4 mg glucose g<sup>-1</sup> soil in Critter et al. (2001).

Amendment of a Galician soil with organic matter was observed to increase total heat production (Barros et al., 2009), with increases of total heat flow upon amendment of 3 Brazilian soils found to follow the pattern: cattle manure > earthworm casts > municipal refuse > compost > 2,6-Dinitro-N,N-dipropyl-4-(trifluoromethyl)aniline (Critter et al., 2002a; b, 2004a; Cenciani et al., 2011). Heat flows have also been shown to increase after amendment of soil with both agricultural and municipal wastewater effluent (Dziejowski, 1995; Prado et al., 2011) and rice straw or green manure (Hassan et al., 2013b; a).

## 2.4.2 In relation to soil contaminates

Kawabata et al. (1983) observed an increase in time to peak with increasing concentrations of cadmium sulphate despite little change in peak amplitude, whereas selenic acid reduced peak amplitude with only a minor increase in time to peak and both ethyl mercuric phosphate or iodoacetic acid decreased peak amplitudes and increased time to peak after glucose amendment. Laboratory contamination with copper sulphate has been shown to decrease peak amplitudes and increase the time taken to reach peak amplitude upon stimulation of the microbial biomass with glucose and ammonium sulphate in an Amazonian red Latosol soil (Airoldi & Critter, 1996), with similar trends observed for lab contamination with ethylmercury phosphate (Airoldi, 1998). Soils dosed with  $\text{HgCl}_2$  showed decreased glucose-induced heat production rates, yet these were shown to recover slightly from 7 days after dosing, returning to pre-contamination levels from 21 days after dosing (Tancho et al., 1995). Contamination with cadmium chloride at increasing concentration has been shown to decrease the peak amplitude of glucose induced heat flow and increase the time taken to reach peak heat flow, while an increase in the total heat flow was observed up to a concentration of  $800 \mu\text{g CdCl}_2 \text{ ml}^{-1}$  (Yao et al., 2007, 2009) despite a fall in the total CFU count (Yao et al., 2007). Contamination of soil with hexavalent chromium ( $\text{K}_2\text{Cr}_2\text{O}_7$ ) caused a slight reduction in peak glucose induced heat flow in concentrations between 0.2 and  $2.4 \mu\text{g K}_2\text{Cr}_2\text{O}_7 \text{ ml}^{-1}$ , with substantial reductions in peak heat flow and total heat production associated with an increased time to peak heat flow at concentration above  $5.0 \mu\text{g K}_2\text{Cr}_2\text{O}_7 \text{ ml}^{-1}$  (Yao et al., 2008, 2009). When measuring the

glucose-induced heat flow of soil spiked with various metals at a concentration of  $1 \text{ mg g}^{-1}$  soil, Wang et al. (2010b) found the relative toxicity to be  $\text{Cr} > \text{Pb} > \text{As} > \text{Co} > \text{Zn} > \text{Cd} > \text{Cu}$ . Contamination with Pb of three soils under different management practices resulted in increases in the time to peak heat flow with increasing Pb concentration up to  $80 \text{ } \mu\text{g g}^{-1}$  soil, however no significant decrease in the total heat production was observed and amplitudes of peak heat flow did not appear to follow any pattern (Gai et al., 2011)

Contamination of soil with 2,4-dichlorophenoxyacetic acid resulted in an increase in total glucose induced heat flow at low concentrations, before decreasing at higher concentrations, coupled with a decrease in peak amplitudes and an increase in the time taken to reach peak amplitude (Prado & Airoidi, 2000, 2001; Airoidi & Prado, 2002). However, no priming effect was shown upon contamination with 1,1-dimethyl-4,4-bipyridinium dichlorate, 1,1-ethylene-2,2-bipyridinium dibromide or 2-chloro-2diethylcarboyl-1-dimethyl-vinyl, as all produced decreasing total glucose-induced heat flows at increased concentrations, especially 2-chloro-2diethylcarboyl-1-dimethyl-vinyl (Crittter & Airoidi, 2001). Contamination of soil samples with the pesticide Chlorpyrifos and its oxon derivative were observed to decrease peak heat production rate and increase the time to peak with concentration and reduce total heat production at concentrations above  $5$  and  $0.1 \text{ } \mu\text{g g}^{-1}$  soil respectively (Wang et al., 2010a), whereas the pesticide beta-cypermethrin was found to have no significant effect on heat flows at concentrations up to  $80 \text{ } \mu\text{g g}^{-1}$  soil (Zhuang et al., 2011). Soil spiked with the two pesticides imidacloprid and acetamiprid showed decreases in peak heat flow, increases in time to peak, with values of total heat production

decreasing with concentration for acetamiprid and increasing up to 20  $\mu\text{g g}^{-1}$  soil for imidacloprid, before decreasing at higher concentrations (Wang et al., 2014). Soil contaminated with petroleum hydrocarbons was found to have a lower peak heat flow and higher time to peak with increasing concentration, while the total heat production increased with concentrations of up to 1100 mg hydrocarbon  $\text{kg}^{-1}$  soil (Guo et al., 2012).

Long term incubation of soils subjected to lab contamination with organic pesticides have been observed to occasionally increase the heat flow of various soil types, while inorganic pesticides were shown to decrease heat flow or have no overall effect (Zelles et al., 1986; Hund et al., 1988; Scheunert et al., 1995). Contamination of soil with the three diphenol compounds catechol, resorcinol and hydroquinone increased the total heat production at concentrations of up to 400, 6000 and 200  $\mu\text{g g}^{-1}$  soil, when compared to an uncontaminated reference sample, with concentrations above these resulting in a lower total heat output than the reference sample (Chen et al., 2009)

Contamination of soil with brewer's yeast was found to decrease the glucose-induced heat production (Sigstad et al., 2013).

### **2.4.3 From biodegradation of organic contaminants**

Metabolic heat production rates have been observed to increase by as much as 400% after pentachlorophenol (PCP) exposure (Lamprecht et al., 1990; Drong et al., 1991). Treatment of soil with Sportak fungicide was observed to increase total heat flow over 1 and 24 hour incubation times, yet decrease total heat flow over a 37 day incubation, except at low concentrations (Heilmann et al., 1995).

Increases in the heat production rate of soil samples amended with tetraethyl lead were shown to be due to direct degradation of the amendment by GC-MS of the end-point soil extract (Teeling & Cypionka, 1997). Tissot (1999) found that rate of biodegradation of some long chain hydrocarbons in soil was too slow to allow assessment using isothermal calorimetry, even under a constant flow of nutrient salts and O<sub>2</sub> gas, however biodegradation of sodium succinate, dodecane and dodecene produced high enough heat production rate to allow calculation of degradation rates. Soil spiked with three phthalate esters showed no significant effect on peak heat flow or peak times, however total heat production initially increased with concentrations of up to 50, 100 and 100 µg g<sup>-1</sup> soil for dimethyl phthalate, diethyl phthalate and di-n-octyl phthalate respectively, followed by subsequent decrease at higher concentrations (Chen et al., 2013).

Contamination of soil with 2,4-dichlorophenoxyacetic acid immobilised on silica gel resulted in an continued increase in total glucose induced heat flow at increasing concentrations (Airoldi & Prado, 2002), whereas the contamination with the mobile form produced diminished heat flows after an initial priming effect (Prado & Airoldi, 2000, 2001; Airoldi & Prado, 2002). However, heat flow was observed to decrease upon addition of both mobile and silica gel immobilised 3-(3,4-dichlorophenyl)-1,1-dimethylurea (Prado & Airoldi, 2002).

#### **2.4.4 In relation to soil pH**

Acidification has been show to decrease metabolic heat flow in the O horizons of forest soils (Kreutzer & Zelles, 1986; Zelles et al., 1987a), while liming of the

same soils increased heat production in both long and short term applications (Kreutzer & Zelles, 1986; Zelles et al., 1987a; b, 1990). In all cases the effect differed between the layers of the O horizon. Rice paddy soils have also been shown to have lower heat production rates at low pH (Koga et al., 2003)

Calorimetric measurements have shown a greater level of microbial activity in the O horizons of acidified soils, with less acidified soils having greater activity in the mineral A horizon (Raubuch & Beese, 1995).

#### **2.4.5 In relation to sample storage**

Zelles et al. (1991) observed that there was only a small difference in total heat flow of samples stored at 4, -18 and -140°C, whereas long storage periods were shown to greatly decrease total heat flow. It was therefore recommended that measurements should be carried out on fresh soil otherwise storage periods should be kept to a minimum. Yet Núñez-Regueira et al. (1994a) upon observing similar results of prolonged storage reducing glucose-induced heat production, concluded that samples should be stored at 4°C for 6 months prior to isothermal calorimetric analysis, as this increased reproducibility. However, the recommendations of Núñez-Regueira et al. (1994a) have been accepted as the standard methodology in this area of research, a point that is discussed in more detail in the introduction of Chapter 5. Other studies have shown that prolonged storage or pre-incubation of samples decreases glucose-induced peak heat production and total heat flow (Tancho et al., 1995), which indicates that either there is a drop in the total microbial biomass, or that less heat is produced per unit biomass, potentially undermining results for total biomass



calculated via Sparling's (1983) method for soils stored for several months before analysis.

#### **2.4.6 In relation to oxygen availability**

Glucose induced heat flow was observed to decrease to low but stable rate after oxygen depletion of the calorimetric ampoule, followed by an anaerobic peak after 9-12 days of anoxic conditions (Vor et al., 2002; Dyckmans et al., 2006), although the methodology used in these studies has been questioned (Barros, 2003). It has been suggested that a measurement of the total heat flow relative to the O<sub>2</sub> available in the ampoule, may indicate the proportion of aerobic and anaerobic pathways (Medina et al., 2009).

#### **2.4.7 In relation to soil moisture**

Heat flow rate has been observed to increase with soil moisture content, until reaching a maximum at field capacity (Barros et al., 1995; Barros et al., 2008c), while addition of water to sterile samples has been observed to cause an endothermic reaction (Ljungholm et al., 1979a; Barros et al., 2008b). An increase in the heat flow has also been observed for the addition of water to composts (Laor et al., 2004), as has an endothermic effect due to water amendment during analysis (Medina et al., 2009). Increases in moisture content above 36% of the WHC have been observed to decrease glucose-induced heat flow in a Brazilian red Latosol (Prado & Airoidi, 1999), while increases in moisture content up to 35% of the WHC have been observed to increase glucose-induced heat flow in other South American soils (Crittter et al., 2001;

Sigstad et al., 2002). Exceeding the WHC has been shown to greatly diminish glucose-induced heat production in soils (Hassan et al., 2013b; a).

Observations of samples from Chinese soils have shown decreases in peak heat flow, increases in time to peak and decreases in total heat production of samples taken during the dry season when compared to those taken during the rainy season (Liang et al., 2014).

Isothermal calorimetry has proved effective at measuring the microbial activity of soils from the Atacama Desert, where previous attempts using CO<sub>2</sub> mineralisation were apparently unsuccessful (Barros et al., 2008b).

#### **2.4.8 In relation to soil type or land use**

Total heat production and total glucose-induced heat production have been observed to increase in soils with a high organic matter content (Bölter, 1994; Barros et al., 1997), while time taken to reach peak heat flow increases with decreasing microbial density measured as CFUs g<sup>-1</sup> soil (Barros et al., 1997). Yet later study observed that total glucose-induced heat production showed a better correlation to total CFUs rather than soil organic matter (Barros et al., 1999).

Higher glucose-induced heat production has been observed in cultivated Galician soils than uncultivated soils of a similar type, with calorimetrically determined microbial growth rates observed to decrease in compacted or low-structure soils, as well as soils with a changeable thermal regime (Núñez-regueira et al., 2002). Glucose induced heat production was also observed to be higher in soil from a managed forestry plot than an adjacent unmanaged plot

(Núñez-Regueira et al., 2006b) and higher in soils from eucalyptus forest than in pine forest (Núñez-Regueira et al., 2006c). However, it should be noted that most of the studies from the group of Núñez-Regueira, Barros et al. at the University of Santiago de Compostela only compare one or two soils in each study and employ archaic methodologies (see Section 2.6 for further discussion), therefore it would be inappropriate to draw firm conclusions from these observations in relation to soil type. A synthesis of this group's work under Núñez-Regueira exists in Rodríguez-Añón et al. (2007). The use of similar techniques showed variations in glucose-induced heat production dependant of soil type have also been observed in Amazonian soils (Critter et al., 1994).

Movement of intact soil columns between different environments, subject to varying levels of air pollution produced no effect on the thermal signals produced 21 months after transferral (Coûteaux et al., 1998), indicating that soil type is more influential than climatic or air pollution conditions within the temperate zone.

While assessing the microbial diversity and activity of soils subject to different nutrient input regimes, Ahamadou et al. (2009) found no variation in values of total glucose induced heat production between treatments, suggesting that measurements of peak amplitude and time taken to reach peak amplitude were more suitable indices. This is in contrast to other studies that have observed significant variations in both total glucose induced heat and time to peak heat flow, depending on nutrient input regimes in long term field trials (Zheng et al., 2009; Ge et al., 2011; Harris et al., 2012; Herrmann et al., 2014) and in relation

to vegetation abundance under various cropping regimes (Zheng et al., 2007; Ge et al., 2012).

### **2.4.9 In relation to incubation temperature**

Increases of incubation temperature between 288 and 303 K have been observed to increase microbial activity and result in a small increase in Gibbs free energy, suggesting that soil microbes are able produce slightly more useful work from C-substrate energy at higher temperatures within that range (Barja et al., 1997). This indicates that temperature may affect the thermodynamic efficiency of the soil microbial biomass.

Observations of total heat production have been lower in Galician soils sampled during winter than at other times of the year (Núñez-Regueira et al., 2005, 2006b; c; a), however these observations are not consistent (Salgado et al., 2009) and will almost certainly have been influenced by water content, leaf litter and other seasonal variations as well.

## **2.5 Measuring thermodynamic efficiency**

### **2.5.1 Caloric quotient ( $qW$ )**

The first study to consider the heat production of the soil microbial biomass in an ecophysical context was Raubuch & Beese (1995) who formulated the caloric quotient ( $qW$ ), a measure of heat flow per unit biomass, measured in  $W\ g^{-1}$  microbial biomass-C, adapted from the metabolic quotient ( $qCO_2$ ) devised by Anderson & Domsch (1985) and used in a previous study by this group in comparison to calorimetric results (Heilmann et al., 1995). Measurements of  $qW$

have been observed to increase with soil acidity (Raubuch & Beese, 1995; 1999) and decrease with soil depth (Raubuch & Beese, 1999).

## 2.5.2 Calorirespirometric ratio

A ratio of heat production: CO<sub>2</sub> respiration, variously known as the calorimetric: respirometric or calorirespirometric ratio has been show to follow the pattern of: aerobic > waterlogged > partially gleyed > completely anaerobic for soil samples (Albers et al., 1995), increase after a high concentration treatment with Sportak fungicide (Heilmann et al., 1995) and vary with soil type (Barros et al., 2008a). An attempt was made to simultaneously measure the thermal signature of glucose-induced microbial metabolic heat and dissolution of the metabolically produced CO<sub>2</sub> in a vial of NaOH solution held within the same ampoule, allowing for calculation of the calorirespirometric ratio without the use of a CO<sub>2</sub> meter (Barros et al., 2010). This method was subsequently used to determine that the calorirespirometric ratio varies with soil and/or vegetation cover type (Barros et al., 2011).

## 2.5.3 Metabolic enthalpy change

An efficiency index resembling the equations of Battley (1960, 1995) was used by Critter & Airoidi (2001), using Equation (7):

$$\eta_{rel} = \frac{Q_{gluc\ contam}}{Q_{gluc\ uncontam}} \quad (7)$$

Where  $\eta_{rel}$  is the relative efficiency, a ratio of  $Q_{gluc\ contam}$ : the total glucose-induced heat flow in a contaminated sample, to  $Q_{gluc\ uncontam}$ : the total glucose-induced heat flow in an uncontaminated sample of the same soil. Vales of  $\eta_{rel}$

was found to decrease upon contamination with 1,1-dimethyl-4,4-bipyridinium dichlorate, 1,1-ethylene-2,2-bipyridinium dibromide or 2-chloro-2diethylcarboyl-1-dimethyl-vinyl, with the greatest reduction observed for 2-chloro-2diethylcarboyl-1-dimethyl-vinyl. However this index is misleading, as it does not in fact inform us about the efficiency of the microbial metabolism, although, as it allows relative quantification of metabolic inhibition, it could be used as an ecological stress index.

Barros et al. (2000) assessed the thermodynamic efficiency of the microbial biomass in Amazonian soils using the metabolic enthalpy change,  $\Delta H_{\text{met}}$ , expressed as the enthalpy change per mol added glucose, finding variations due to vegetation type. Microbial growth was stimulated via addition of 1.5 mg glucose and 1.5 mg ammonium sulphate to 1.0 g soil (unstated whether wet or dry mass). The combination of C, N and S fertilisation may account for one of the samples recording a mean  $\Delta H_{\text{met}}$  value greater than the molar enthalpy for complete combustion of glucose. Despite observing changes in  $\Delta H_{\text{met}}$  due to season and soil water content, (Barros et al., 2001) went on to criticize the usefulness of the index, due to its key assumption of complete consumption of the added glucose, finding that glucose concentration influenced the index more than other variables. Both papers (Barros et al., 2000, 2001) mention observations of a water amended reference sample, but are not explicit as to whether this was used for normalisation of the power-time curves. The  $\Delta H_{\text{met}}$  index is calculated in a similar way to the  $\eta_{\text{eff}}$  index from (Harris et al., 2012), using Equation (2) below:

$$\Delta H_{met} = \frac{Q_{total}}{S_0} \quad (8)$$

Where:  $Q_{total}$  is the total observed metabolic heat production of the sample in kJ,  $S_0$  is the molar quantity of added glucose and  $\Delta H_{met}$  is the metabolic enthalpy change in  $\text{kJ mol}^{-1}$ . Using this notation,  $\eta_{eff}$  can be expressed via Equation (9):

$$\eta_{eff} = 1 - \frac{Q_{total}}{S_0 \cdot \Delta H_0^c} \quad (9)$$

Where:  $\Delta H_0^c$  is the enthalpy of change for complete combustion of 1 mol of glucose, in  $\text{kJ mol}^{-1}$ .

After highlighting the issues with calculating enthalpy change per mol of *added* glucose ( $\Delta H_{met}$ ) in Barros et al. (2001), this index was dropped and the enthalpy of the glucose oxidation reaction ( $\Delta_r H_s$ ), a measure of enthalpy change per mol of *metabolised* glucose, was adopted in Barros & Feijóo (2003). These two indexes have the same units ( $\text{kJ mol}^{-1} \text{ C-substrate}$ ), they are both calculated by Equation (2) and no mention is made of accounting for unmetabolised glucose-C in papers using the  $\Delta_r H_s$  index, therefore it is unclear if or how they are different.

Observations of  $\Delta_r H_s$  have been shown to vary with soil type, apparently in relation to stress (Barros & Feijóo, 2003; Barros et al., 2004, 2008a), however the stress effect is not evident from the published results. It has also been observed to increase with addition of ammonium-iron(II) phosphate monohydrate, especially at higher concentrations (Barros et al., 2006), although not consistently (Barros et al., 2008c)

Values of  $\Delta_r H_s$  were used to calculate the thermal yield ( $\eta_H$ ) using a modified Battley (1960, 1995) equation, as follows:

$$\eta_H = \frac{\Delta_r H_{sNC} - \Delta_r H_{sC}}{\Delta_r H_{sNC}} \quad (10)$$

Where the subscript NC indicates the non-conservative reaction, i.e. not subject to C-substrate amendment and the subscript C indicated the conservative reaction, i.e. the glucose induced reaction. This gives the thermal yield ( $\eta_H$ ) as a dimensionless index ranging between 0 and 1, often expressed as %.

Although Equation (10) was the basis for the Harris et al. (2012) equation to calculate  $\eta_{\text{eff}}$ , it is flawed in its key assumption and therefore does not represent thermodynamic efficiency, as it is fundamentally a ratio of total glucose induced heat production ( $Q_{\text{gluc}}$ ) to total non-amended heat production ( $Q_{\text{control}}$ ). As such, it is unsurprising that calculated values of  $\eta_H$  have been found to correlate with the magnitude of  $Q_{\text{gluc}}$  observations (Barros & Feijóo, 2003; Barros et al., 2006, 2008b).

Studies by other group have shown that values for  $\Delta H_{\text{met}}$  correlate with CFU counts (Sigstad et al., 2002). Values for  $\Delta H_{\text{met}}$  have been observed to decrease when the microbial biomass is subjected to stress from contamination with metals (Wang et al., 2010b) or pesticides (Wang et al., 2010a, 2014), suggesting that this is caused by restraint of metabolic activities under stress. Variations in  $\Delta H_{\text{met}}$  have been observed at different sediment depths in lake sediment (Chen et al., 2011).



(Chen et al., 2011) used a cell specific metabolic enthalpy change, observing that it correlated with soil TOC and TN in lake sediments.

Laor et al. (2004) used a calculation of total heat flow per mol added glucose to determine whether observations of compost microbial biomass were operating aerobically or anaerobically, although this was not linked to efficiency.

#### **2.5.4 Biomass specific heat rate**

Several early attempts were made to measure the heat production per unit biomass during microbial growth, often as a way of measuring the total microbial biomass-C (Sparling, 1983; Kimura & Takahashi, 1985; Heilmann & Beese, 1992; Raubuch & Beese, 1999). However, the first attempt to use this as a thermodynamic index was by measurement of the 'cell specific heat rate' (Barros et al., 2003) or 'heat yield' (Barros & Feijóo, 2003), in Amazonian and Galician soils, observing that soils with a lower biomass, lower biomass per unit soil organic-C or lower total-N content had a higher heat production per CFU. This index has indicated that soils under different land uses produce different levels of heat per CFU (Barros et al., 2004, 2007a), with some indication that soils with low organic input regimes produce more heat per CFU (Barros et al., 2004). A crude measurement of glucose-induced heat production  $\text{g}^{-1}$  soil  $\text{CFU}^{-1}$  in  $0.25 \text{ cm}^3$  suspension was used by Critter et al. (2004b) in relation to amendment of the soil with organic residues, observing that the biomass specific heat rate followed the pattern: cattle manure > earthworm casts > municipal refuse > compost > 2,6-Dinitro-N,N-dipropyl-4-(trifluoromethyl)aniline. This is in contrast to our hypothesis that ecological stress should increase heat

production per unit biomass, which may have been caused by substantial microbial growth and subsequent labile organic matter exhaustion during the three month pre-incubation period. Wirén-Lehr et al. (2002) observed that soil samples from a former hop plantation which had been contaminated with Cu from previous fungicide application produced more heat per unit biomass than the other sample sites, upon amendment with plant residues.

Studies have found that soil microbial communities subject to long term stress due to nutrient input regimes produce more heat per unit biomass than those under traditional input regimes, when measured against CFUs (Zheng et al., 2009) and microbial biomass-C (Harris et al., 2012).

## **2.6 Summary and comment**

A large proportion of the available literature on the isothermal calorimetric analysis of soil samples has been presented as a 'proof of concept' study, establishing the usefulness of the method. Unfortunately, few research groups appear to have attempted testing the reaction of the soil microbial community to ecological gradients, using isothermal calorimetry. The majority of work that has set out to assess ecological gradients, has focused on the concentration of contaminants to the soil, which despite employing outdated CFU techniques for biomass estimation (Ritz, 2007) and the arcane method of storing samples for months prior to analysis, these studies have produced some interesting and insightful observations on how the microbial biomass reacts to organic and inorganic contaminants. This is especially true of the research group of Fei Wang et al. at the China University of Geosciences, in Wuhan, China, who

have applied isothermal calorimetry to test the thermodynamic efficiency of soil microbial communities under ecological stress, in similar manor to this study. However, unfortunately the efforts of this group are undermined by the use of the outdated methodologies endemic in the field.

The culture of using these outdated methods is largely due to the dominance of outputs from the research group based at the University of Satiago de Compostela, accounting for roughly one quarter of the studies in this review. The research methods employed in these studies are not consistent with current practice in general soil microbial ecology and are in need of updating, especially the practice of prolonged sample storage before analysis, and estimation of biomass via the most probable number of colony forming units, an inappropriate and highly inaccurate method (Ritz, 2007). However, due to the dominance of the literature by outputs from this group, many of these practices have been adopted in place of more robust methods and attempts by other groups to produce new experimental methodologies have been met with unfavourable reviews (Barros, 2003). The published research of this group has become increasingly complex, with Barros et al. (2008a) reporting 11 different thermodynamic indices, with 9 of them attempting to quantify the thermodynamic efficiency of the soil microbial biomass. Also about a third of the papers produced by this group have been measuring heat flows of, what appear to be, the same half a dozen Galician and Amazonian soils, with many studies simply characterising a single soil sample, producing some ambiguity over what hypotheses they are testing, other than proving that isothermal calorimetry can be used to measure soil microbial heat production. Yet this group has also laid

the ground work for this study to assess the thermodynamic efficiency of the soil microbial biomass in relation to various ecological gradients, by producing useful indices of thermodynamic efficiency which we have been able to improve into the  $\eta_{\text{eff}}$  and SIHP indices of Harris et al. (2012).

Isothermal calorimetry has shown great potential as a method for investigating the workings of the soil microbial community, however methods in the field are in need of review. As such, an additional aim has been added to the work presented in this thesis: to introduce a standardised operating procedure for the isothermal calorimetric analysis of soil samples, in order to bring the research discipline in line with methodologies employed within the broader domain of soil microbiology.

### 3 General methods

*Heat is work and work's a curse  
And all the heat in the Universe  
Is gonna coool down 'cos it can't increase  
Then there'll be no more work and there'll be perfect peace  
Really?  
Yeah - that's entropy, man!*

– Michael Flanders & Donald Swann

#### 3.1 Basic isothermal microcalorimetric technique

As previously stated in Chapter 2, ‘isothermal calorimetry’ or ‘heat conduction calorimetry’ is a very general technique that can be used to study a wide variety of processes. In this study, the instrument used was the TAM Air isothermal microcalorimeter (TA Instruments, Järfälla, Sweden), an eight-channelled, air-cooled heat conduction calorimeter initially designed for use in cement hydration studies (Wadsö, 2005). The TAM Air consists of 8 individual calorimeters, each with their own heat sink (Figure 3.1A) comprising of a ‘sample’ and ‘reference’ side (Figure 3.1B). The heat generated by the sample is conducted through a thermopile into an aluminium heat sink, which is held at a nominally constant temperature by a Peltier heating/cooling element (Wadsö & Goldberg, 2001). Any heat transient across the thermopile will create an electrical potential difference (voltage), which can be measured by a voltmeter at prescribed observation times to calculate the total thermal output over the time interval, by using Equation (11).

$$Q = \varepsilon_c \int_{t_1}^{t_2} U \delta t \quad (11)$$

Where:  $Q$  is the thermal output for the time interval in joules;  $\epsilon_c$  is the calibration constant in Watts;  $t_1$  and  $t_2$  are observation times, with  $\delta t$  the time interval in seconds;  $U$  is the potential difference in Volts (Wadsö & Goldberg, 2001).

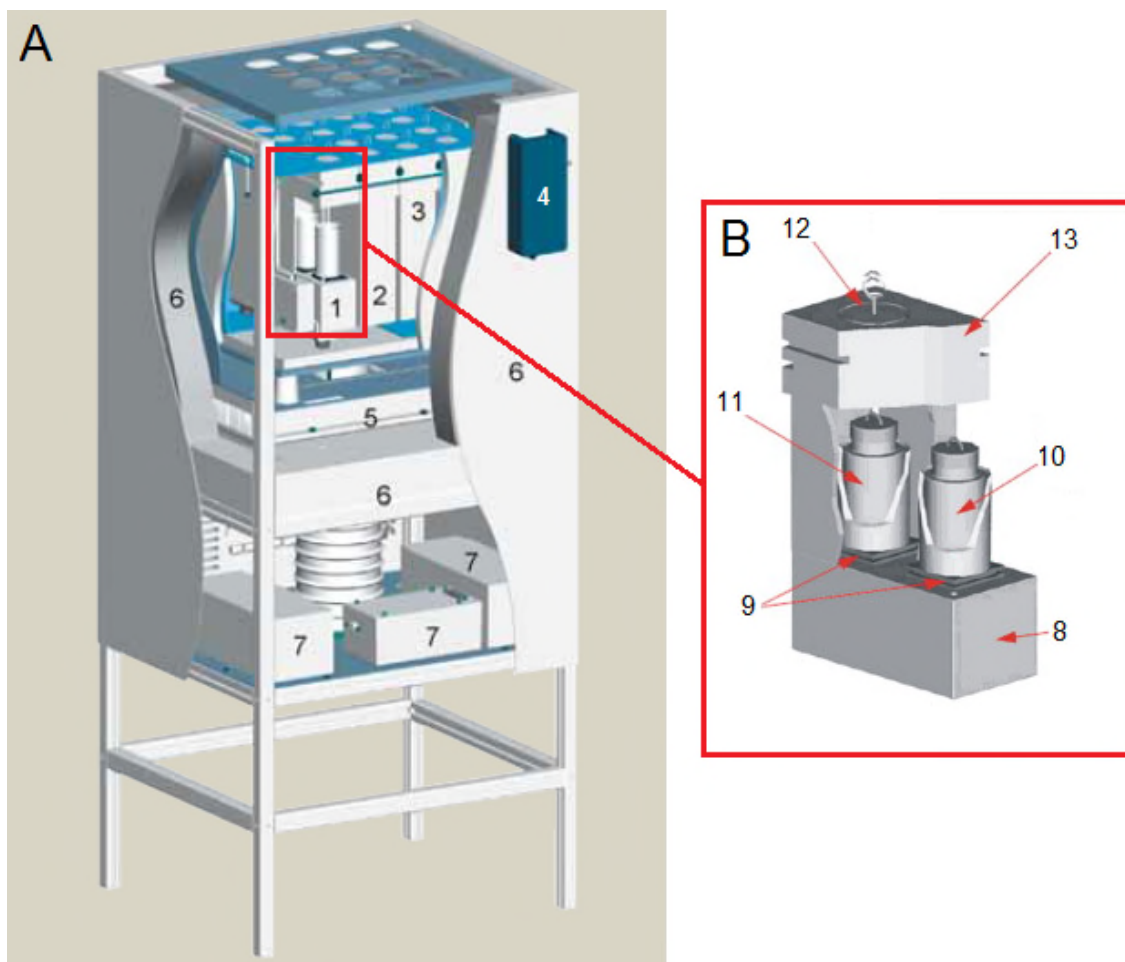


**Figure 3.1** Diagram of the TAM Air isothermal microcalorimeter, showing; A) cutaway view of the instrument with top insulation lid removed, showing: three of the eight calorimeters (1-3), one with part of the heat sink removed, showing the position of the ampoules (1); the thermostat controls (4); the Peltier element (5); insulation (6); amplifier, data logger and power supply (7); and B) cutaway view of a single constituent calorimeter unit, showing: main aluminium heat sink (8); thermopiles (9); 'sample' ampoule (10); inert 'reference' ampoule (11); heat sink plug (12); secondary aluminium heat sink (13). Part A) after Wadsö (2005); part B) after Ren et al. (2012).

### **3.1.1 Sample preparation**

Samples are prepared for the TAM Air in clean glass ampoules of 20 ml internal volume which are lowered directly into the measurement chamber without intermittent staged sample insertion. Each 'sample' ampoule must be accompanied by an inert 'reference' ampoule with a similar heat capacity as the 'sample'. To this end the 'reference' ampoules are usually filled with inert, sterilised media such as glass beads or sand. In all experiments presented in this current study, acid-washed glass beads were used as the inert reference, with estimations of the sample's heat capacity made using standard values of heat capacity for mineral soil, water and organic matter, with the water and organic matter content of the soil determined by oven drying (Section 3.6) and loss on ignition at 500°C (Rowell, 1994) respectively.

### **3.1.2 Baseline calibration**

Prior to sample insertion the TAM Air was allowed 30 min to complete an initial baseline measurement. After the end of the experiment, samples were removed and the calorimeter was allowed at least 45 min to reach thermometric signal stability (signal drift of  $<4 \mu\text{W hour}^{-1}$ ), before the signal was re-measured for the final baseline. The disparity between these two baseline measurements was then automatically integrated by the instrument software in order to obtain the baseline slope for the experimental period.

### **3.1.3 Insertion of samples**

After soil samples had been weighed into their ampoules and the respective inert reference samples made up, the reference ampoules were hermetically

sealed by crimping of an aluminium cap, while the soil sample ampoules were hermetically sealed with either a crimped cap or an 'Admix-ampoule' titration device (TA Instruments, Järfälla, Sweden). The samples were then cleaned all over with tissue paper in order to remove any dust or human secretions arising from handling, before the heat sink plug of the relevant calorimeter channel was opened and the sample lowered into position. The heat sink plug was then replaced and the time of sample insertion noted by the instrument software.

### 3.1.4 Calculation of thermodynamic indices

The heat signals obtained from the calorimeter were then used to calculate two thermal indices using the equations below. Equation (12), a modified version of the growth yield efficiency equations formulated by Battley (1995; 1960), first presented in Harris et al. (2012), was used to determine the thermodynamic enthalpy efficiency of the soil microbial biomass ( $\eta_{eff}$ ), a dimensionless measure of substrate use efficiency.

$$\eta_{eff} = 1 - \left( \frac{Q_{gluc} - Q_{control}}{\Delta H_{gluc}^0} \right) \quad (12)$$

Where:  $\eta_{eff}$  is a dimensionless measure of the total thermodynamic enthalpy efficiency of the soil microbial ecosystem;  $Q_{gluc}$  and  $Q_{control}$  are the total heat production ( $\Delta H_{system}$ ) from the glucose solution amended and water amended samples respectively in  $J\ g^{-1}$  dry wt. soil; and  $\Delta H_{gluc}^0$  is the enthalpy of change for the complete combustion of the added glucose.

Using the same values for  $Q_{gluc}$  and  $Q_{control}$ , Equation (13) was used to calculate the substrate-induced heat production index (SIHP), a simple measure of



thermal output per unit biomass given in  $\text{J g}^{-1}$  microbial biomass-C, used to assess the total waste heat production of the living component of the soil.

$$\text{SIHP} = \frac{Q_{gluc} - Q_{control}}{C_{mic}} \quad (13)$$

Where:  $C_{mic}$  is the mass of microbial biomass-C, in  $\text{g C g}^{-1}$  dry weight soil, as determined by chloroform fumigation extraction (see Section 3.3).

### **3.2 Phospholipid fatty acid profiling**

Phospholipid fatty acid (PLFA) profiling is a taxonomic assay that can be used to assess the phenotypic constitution of a microbial community by way of partially quantifying the chemical composition of phospholipids, the main constituent of cell membranes (Figure 3.2A & B).

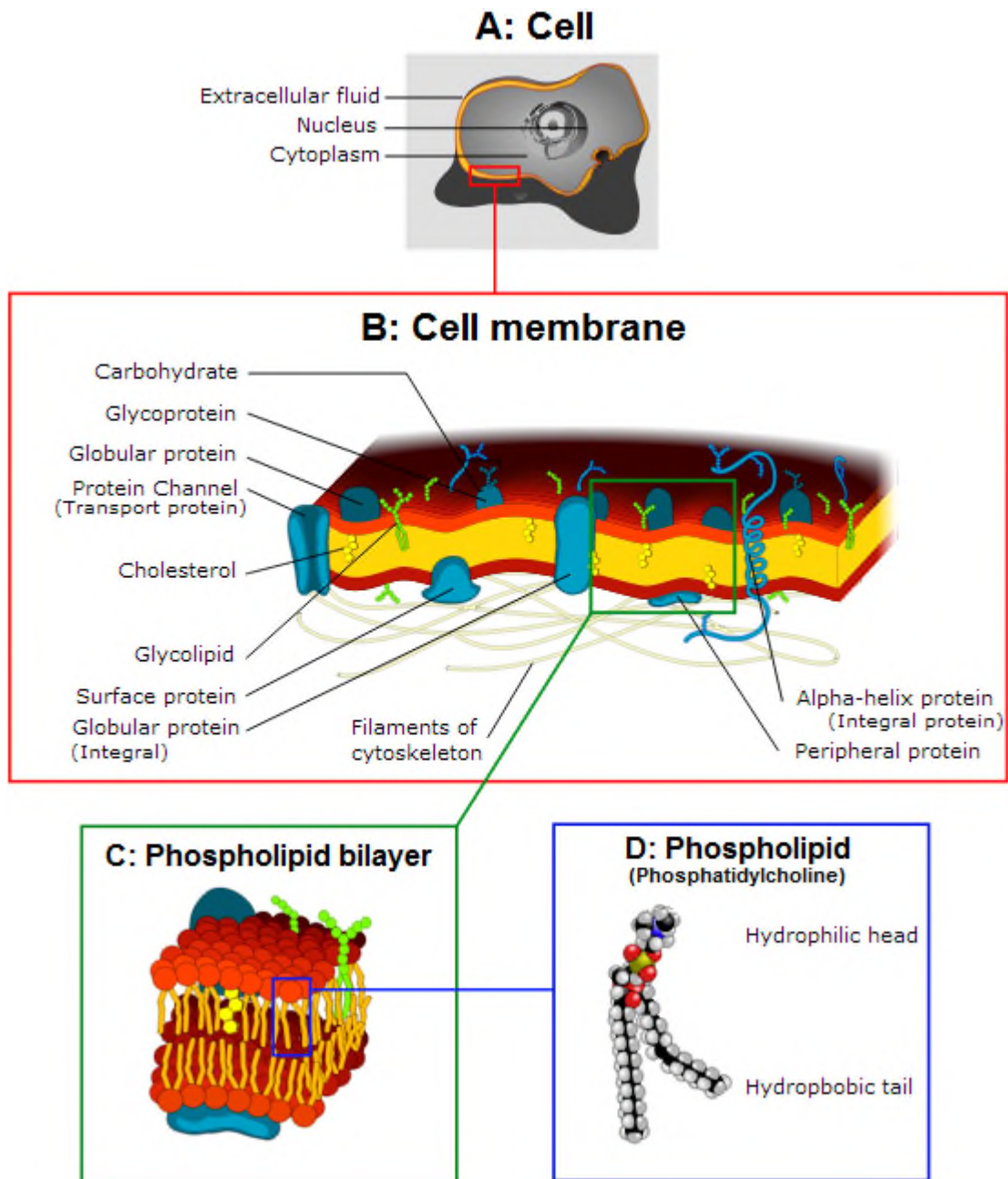


**Figure 3.2** Diagram of the phospholipid bilayer within cell membrane, showing: **A)** location of cell membrane; **B)** constituents of the cell membrane; **C)** phospholipid bilayer, and; **D)** space-filling chemical model of an example phospholipid: phosphatidylcholine; black = C, white = H, red = O, yellow = P and blue = N<sup>+</sup> (Dhatfield, 2008)

Phospholipids consist of a glycerol backbone, connected to a hydrophilic phosphate group, forming the hydrophilic head, and two fatty acids, forming the hydrophobic tail (Figure 3.2D). As phospholipids are highly hydrophilic at one

end and hydrophobic at the other, a property termed amphipathic, upon contact with water they will float with their hydrophobic tails facing the air and their hydrophilic heads in contact with the water. When submerged in water, two such layers will readily combine tail-to-tail, forming a lipid bilayer (Figure 3.2C), which in order to completely avoid contact of the hydrophobic tails with water will then proceed to fold in on itself, forming a spherical liposome, the basic structure of the living cell (Alberts et al., 2012). Phospholipids rapidly decompose upon cell death, make up a relatively constant proportion of the biomass of microbial organisms and are not used to build extra biomass for energetic storage by cells, as such they well suited for phenotypic profiling as they should represent a constant mass fraction of the living biomass, allowing calculation of the proportion of different phenotypes on a microbial biomass-C basis (Zelles, 1999). Many different species and strains of organisms will potentially and actually possess identical phospholipids in their cell membranes and conversely, the phospholipids possessed by a single species may alter in response to environmental conditions (Frostegård et al., 2011). As such phospholipid profiling is unable to assess abundance or changes in the population of individual species, yet when used to assess the whole microbial community it is sensitive to changes between the relative populations of each phospholipid bearing phenotype (Zelles, 1999).

PLFA profiling operates by extracting all lipids present in the microbial assay, isolating the phospholipids, then separating the fatty acid chains from the glycerol backbone by substituting the glycerol site with a methyl group, therefore turning each fatty acid into a fatty acid methyl ester (FAME). The

FAMES can then be identified by gas chromatography (GC) analysis, allowing the source fatty acid chains to be determined. As phospholipids each have two constituent fatty acid chains with many possible combinations, the PLFA method does not allow the identification of the original phospholipids.

The method for assessing the microbial phenotype via PLFA analysis was first undertaken by Tunlid and Hoitink (1989) on an experiment involving bark compost media, using the  $\text{CHCl}_3$  extraction method of Bligh & Dyer (1959). This method was then applied to the soil microbial community using GC-MS and multivariate statistical analysis by Frostegård et al. (1993a; b, 1996), who modified the procedure according to the mild alkaline methanolysis method of Dowling et al. (1986) and by use of a citrate buffer in place of a phosphate buffer. The method used in this study was modified from Frostegård et al. (1993b) and is the same as that of Pawlett et al. (2013). All reagents used were HiPerSolv grade.

### **3.2.1 Sample preparation**

Soil used in the PLFA analysis was taken from the incubated samples at the time of calorimetric analysis and therefore underwent the same storage, homogenisation and pre-incubation regime as the rest of the sample, including passing through a 2 mm sieve and mixing by hand. These subsamples were taken and kept in frozen storage at  $-20^\circ\text{C}$  for up to one month. The samples were then freeze-dried using an Alpha 1-2 LD freeze dryer (Christ Freeze Driers, Osterode-an-Harz, Germany) at the Department of Chemistry at SLU,

Uppsala, Sweden; therefore preserving the lipid bilayer and allowing for transit to Cranfield University, UK.

### **3.2.2 Lipid extraction**

Samples of 7 - 10 g freeze dried soil were placed into a sterile media bottle with a PTFE coated lid and mixed with 20 ml of 0.8:1:2 volumetric ratio citrate buffer: chloroform: methanol, as per the ratios given in Bligh & Dyer (1959). The mixture was then sonicated for 30 min and shaken for another 30 min before separation of the aqueous and hydrophobic layers by centrifugation at 2000 rpm for 10 min. The supernatant hydrophobic layer was transferred to a fresh media bottle by Pasteur pipette. A further 4 ml chloroform and 4 ml citrate buffer were added and the sample was centrifuged again at 2000 rpm for 10 min. The supernatant aqueous layer was then removed and discarded, while the hydrophobic layer was dried under a continuous flow of N<sub>2</sub> gas at 37°C. The lipids were then stored overnight at -20°C under nitrogen.

### **3.2.3 Lipid fractionation**

Sep-pak Vac<sup>TM</sup> solid phase extraction (SPE) cartridges (Waters Chromatography, Elstree, UK) were prepared by the addition of c. 0.5 g anhydrous sodium sulphate to the top of each cartridge. The SPE cartridges were then placed into a SPE manifold, allowing filtration to be aided by a pressure gradient created by the use of a vacuum pump. Prior to the fractionation procedure the SPE cartridges and anhydrous sodium sulphate were washed with 2 ml of each of the three solvents to be used, in order of polarity, being: methanol, acetone, chloroform. The cartridges were then dried

under suction for a few minutes prior to being reconditioned with 2 ml chloroform. After this the SPE cartridges were not allowed to dry out.

The defrosted lipids extracts were resuspended in 1 ml chloroform and transferred to the SPE cartridges by glass Pasteur pipette. The columns were then filtered with 5 ml chloroform in order to elute the neutral lipids. This was followed by 12 ml acetone to elute the glycol lipids. The filtrate was then discarded and a fresh glass media bottle put into the SPE manifold, in order to collect the polar lipids, including the phospholipids, which were eluted with 8 ml methanol. The resultant filtrate was then dried under a continuous flow of N<sub>2</sub> gas at 37°C. The polar lipids were then stored overnight at -20°C under nitrogen.

### **3.2.4 Mild alkaline methanolysis**

The defrosted polar lipids were reconstituted with 1 ml of 1:1 volumetric ratio toluene: methanol solvent mixture and a further 1 ml freshly prepared 0.2 M methanolic potassium hydroxide was added. The mixture was swirled and then incubated at 37°C for 30 min. After 30 min had elapsed, the reaction was quenched by lowering of the pH value to c. pH 6-7, by addition of 0.25 ml of 1 M acetic acid. Afterwards, 5 ml of 4:1 volumetric ratio hexane: chloroform was added along with 3 ml deionised water. The mixture was then sonicated for 30 min, before separation of the aqueous and hydrophobic layers via centrifugation at 2000 rpm for 10 min.

The lower aqueous layer was removed by glass Pasteur pipette and discarded. The hydrophobic phase was supplemented with 3 ml 0.3 M sodium hydroxide

and the mixture was allowed a few minutes to re-separate. The upper hydrophobic layer was then filtered through sodium sulphate, using a Whatman No. 4 filter paper, into a fresh glass media bottle. The filtrate was then dried under a constant flow of nitrogen gas at 20°C. The FAMEs were then stored overnight at -20°C under nitrogen.

### **3.2.5 Gas chromatography**

The FAMEs were prepared for GC analysis by reconstituting with 200 µl hexane, before transferring by glass Pasteur pipette into a GC vial with insert (QMX Laboratories, Donmow, UK). The individual FAMEs were then separated and identified by use of a 6890N GC (Agilent Technologies, California, USA) fitted with a splitless injector and an HP-5 capillary column (30 m length, 0.32 mm internal diameter, 0.25 µm film; Agilent Technologies, California, USA) and an autosampler, programmed to sample 1 µl (Agilent Technologies, California, USA).

The individual FAMEs were separated by use of a temperature programme, with helium used as the carrier gas. This used a starting splitless hold temperature of 50°C for 1 min, before an initial increase of the temperature at a rate of 25°C min<sup>-1</sup> until 160°C, then 2°C min<sup>-1</sup> until 240°C and finally 25°C min<sup>-1</sup> to the maximum temperature of 310°C. FAMEs were then detected using a flame ionisation detector (FID) operating at 320°C.

Peaks from the GC output were identified using the GC operating software G2070 Chemstation (Agilent Technologies, California, USA) and individual FAMEs were identified by comparison with empirically determined retention

times of FAMEs derived from a standard mixture of 26 known PLFAs (Sigma-Aldrich Ltd., Dorset, UK) using the methodology here presented and the CG apparatus in question. Results for individual peaks were then processed as a percentage of the total number of moles (mol %), thereby normalising the dataset.

### **3.2.6 Multivariate statistical analysis**

The resulting PLFA data were analysed using STATISTICA (2010) version 9.1 (StatSoft Inc., Tulsa, Oklahoma, USA). This was achieved by subjecting the data to a principal component analysis (PCA) by use of the correlations matrix. Resulting factor scorings were analysed by a post-hoc one-way ANOVA with a post-hoc Fisher LSD prescribing a significance threshold of 5%.

### **3.3 Soil microbial biomass carbon**

The chloroform fumigation extraction method of Wu et al. (1990), allows for estimation of the microbial biomass by comparing two sub-samples from the same parent sample, one of which has been fumigated with chloroform and the other which has not been fumigated.

When moist soil is placed in an atmosphere of chloroform vapour, the polar chloroform will freely mix with the soil moisture. As chloroform is a strongly polar organic solvent, it is able to interact with both hydrophilic and hydrophobic groups. As such the presence of chloroform in the soil-water matrix allows phospholipids to move freely, therefore disintegrating cell membranes and causing death by cellular breakup. This results in the release of water-soluble organic compounds from the cell's interior, thereby increasing the total



extractable content of water-soluble-C of the sample. As such, quantifying the amount of water-soluble organic compounds in a fumigated and non-fumigated sample, allows for the estimation of the total microbial biomass by use of a conversion ( $k_{ec}$ ) factor that takes into account the percentage of cell components that will be extractable in an aqueous solution.

### **3.3.1 Sample preparation**

As with all other analyses, all samples were homogenised by sieving to 2 mm and mixing by hand. Samples for chloroform liable biomass were taken simultaneously to the samples for PLFA and isothermal microcalorimetric analysis. Two samples of moist soil were taken with a dry weight equivalent of 12.5 g each, and placed into a clean 50 ml glass beaker.

### **3.3.2 Fumigation**

The fumigation samples were placed into a glass vacuum desiccation jar, along with a glass jar containing c. 50 ml ethanol free chloroform with anti-bumping granules. The desiccation jar was lined with moist paper towels, in order to avoid drying out of the soil samples. The desiccation jar was then connected to a vacuum pump and evacuated until the chloroform had been boiling for 2 min. The valve was then closed and the samples left in the chloroform vapour for 24 hours. Subsequently the valve was opened, the desiccation jar allowed to refill with atmospheric air, opened and the chloroform removed. The lid was then replaced, the desiccation jar reconnected to the vacuum pump and turned on for 3 min, in order to create a partial vacuum to remove the remaining chloroform from the soil matrix. The vacuum pump was then removed and the

valve reopened, in order to allow the desiccation jar to refill with air, before the vacuum pump was reattached and the process repeated a further two times.

### **3.3.3 Extraction**

The dissolved organic carbon (DOC) content of both the fumigated and non-fumigated samples was extracted by placement of the sample into a clean plastic 50 ml centrifugation test tube, to which 50 ml 0.25 M  $K_2SO_4$  was added. The test tubes were laterally shaken at 300 oscillations  $min^{-1}$ , before separation of the sample and supernatant extract by centrifugation at 2000 rpm for 2 min. The extract was then filtered through a Whatman No. 4 filter paper into a clean plastic bottle. The extract was then frozen at  $-20^{\circ}C$  until analysis.

### **3.3.4 Dissolved organic carbon analysis**

The DOC of the sample was analysed using a TRAACS 800 autoanalyser (Bran+Luebbe, Norderstedt, Germany). The extract was added to  $K_2PO_4$  buffer solution, containing  $SO_5^{2-}$  to act as an electron donor.  $CO_2$ -free air was bubbled through the solution, in order to displace any dissolved  $CO_2$ . After passing through a glass coil, the solution was subjected to ultra violet (UV) radiation, in order to facilitate oxidation of the organic C into  $CO_3^{2-}$ . An acid surfactant (HCl) was added to convert all C present as  $CO_3^{2-}$  into  $CO_2$ . The  $CO_2$  was dialysed using a silicone rubber membrane and reacted with a buffered phenolphthalein indicator. The C concentration of the sample was then calculated using the absorbance of light at 550 nm wavelength.

### 3.3.5 Calculation

The biomass C was then calculated using Equation (14) of Wu et al. (1990), with an amended  $K_{ec}$  value 0.45 (Dahlin & Witter, 1998).

$$\text{Biomass C} = \frac{(C_{\text{fum}} - C_{\text{non-fum}})}{K_{ec}} \quad (14)$$

Where:  $C_{\text{fum}}$  is the total organic C in the fumigated sample in  $\mu\text{g C}$  and;  $C_{\text{non-fum}}$  is the total organic C in the non-fumigated sample in  $\mu\text{g C}$ . The results for soil microbial biomass are the given as  $\mu\text{g biomass C g}^{-1}$  dry soil weight.

### 3.4 Soil organic carbon and total nitrogen content

Soil organic matter consists of a wide variety of organic (C-based) compounds, both living and dead, including living organisms (biomass), remains of deceased organisms (necromass) and organic compound excreted from current or past metabolism, e.g.; fecal matter and root exudates. Soil organic matter helps to bind mineral particles, giving rise to the soil structure and plays a vitally important role in the chemistry of the soil, despite typically constituting 1 to 6% total mass (Brady & Weil, 2008). Organic C makes up 48 to 58% of total soil organic matter (Rowell, 1994) and therefore provides a good estimate for total organic matter.

Nitrogen, on the other hand, is an essential macronutrient needed for the construction of proteins and amino acids, and is therefore crucial for plant growth. Organic N typically comprises 98-99% of the total N in soils that have not received mineral fertiliser inputs and organic N and can only enter the soil via the process of nitrification, or through the deposition of organic matter,

predominantly necromass or faecal matter (Brady & Weil, 2008). Because of this, total N content increases rapidly in the early stages of primary succession and is a useful tool for investigating the developmental state of the soil-plant ecosystem (Chapin et al., 1994).

### **3.4.1 Method**

Samples of air dried soil were prepared for organic C and N analysis by grinding into powder of <60  $\mu\text{m}$  maximum particle dimension, in order to increase reactive surface area. Samples of c. 20 mg were packed into aluminium envelopes before inserting into a 2400 CHN/O Analyser with AD 6 Ultra Microbalance (PerkinElmer, Waltham, MA, USA). The samples were then oxidised in a stream of pure  $\text{O}_2$  at  $925^\circ\text{C}$  in the presence of hydrochloric acid to act as an oxidation agent, converting the organic C into  $\text{CO}_2$  and the organic N into  $\text{N}_2$ . The gaseous emissions were separated by frontal chromatography and quantified by thermal conductivity detector.

### **3.5 Soil pH**

The pH of a soil can be defined as the inverse log of the concentration of  $\text{H}_3\text{O}^+$  ions in the soil water matrix that will disassociate in solution. Soil pH is dependent on many variables within the soil, such as grain size distribution, mineralogy, cation exchange capacity (CEC), type and quantity of organic matter, hydraulic conductivity and water input regime (Brady & Weil, 2008). The pH will influence CEC and the availability of various ions, especially metals, which will in turn alter the microbial phenotype that the soil will support (Harris et al., 2012).

### **3.5.1 Method**

The pH of soil samples was measured by use of a glass electrode pH meter (ExpotechUSA, Houston, TX, USA) via the method outlined in Rowell (1994). Prior to analysis the pH meter was calibrated using two pre-prepared buffer solutions of pH 4.01 and 7.00 (Sigma-Aldrich Ltd., Dorset, UK). Between each reading the electrode was washed thoroughly with deionised water and dried with tissue paper. All measurements were made at room temperature (20°C).

Samples of 10 g air dried soil were placed into clean plastic centrifugation test tubes, with 25 ml deionised water and laterally shaken for 15 min. The mixture was stirred and the glass electrode pH meter immersed into it. A reading was taken from the pH meter 30 s after immersion. The meter was then removed from the mixture, cleaned with deionised water and dried before analysis of the next sample.

### **3.6 Soil gravimetric water content**

The water content of the soil is a measure of the mass of water contained within the soil matrix at any one given time. In this study, the water content of samples were determined gravimetrically, by comparison of the mass of fresh, moist soil and oven dried soil, via the method outlined in (Rowell, 1994).

Directly after sample homogenisation by passing through a 2 mm sieve and mixing by hand, samples of c. 10 g fresh soil were taken and placed into a clean glass beaker of known mass. The samples were re-weighed in their beakers and the mass recorded, before placing into a drying oven at 105°C overnight. The following day, the samples were removed from the oven and placed into a

desiccation jar containing silica gel crystals until cool. The samples were then reweighed and the mass of oven dried soil determined by subtracting the mass of the glass beaker. The water content of the fresh soil was then calculated as g water  $\text{g}^{-1}$  oven dried soil.

### **3.7 Soil water holding capacity**

The water holding capacity (WHC) of a soil is a measurement of the mass of water retained by the soil matrix against gravity. It is predominantly influenced by soil porosity, grain size distribution, organic matter content and structure.

Directly after sample homogenisation by passing through a 2 mm sieve and mixing by hand, samples of c. 25 g fresh soil were placed into a clean plastic filter funnel, with the spout stuffed with pre-saturated glass wool and stoppered with a rubber bung. The soil was then saturated with deionised water, covered with film to prevent evaporative losses and allowed 30 min for all pores to become inundated. The rubber bung was then removed and the excess water allowed to drain through the glass wool under gravity. After drainage had occurred for at least 8 hours the sample was considered to be at water holding capacity. As such, the sample was transferred into a clean glass beaker of known mass, reweighed and the water content determined gravimetrically by drying overnight at 105°C (see Section 3.6). WHC was then expressed on a g soil moisture  $\text{g}^{-1}$  soil dry mass equivalent (g  $\text{H}_2\text{O}$   $\text{g}^{-1}$  dry soil) basis.

## 4 Preliminary experiment

*Ludwig Boltzmann, who spent much of his life studying statistical mechanics, died in 1906, by his own hand. Paul Ehrenfest, carrying on the work, died similarly in 1933. Now it is our turn to study statistical mechanics. Perhaps it will be wise to approach the subject cautiously.*

– David L. Goodstein (1975)

### 4.1 Introduction

The use of air-cooled calorimeters for the analysis of soil was, as far as we were aware, a completely novel application and the as-yet unused TAM Air instrument arrived at SLU shortly after the present study commenced. Due to the large number of unknowns surrounding the method, a preliminary experiment was undertaken in order to test the working methodology used in the, then unpublished, study of Harris et al. (2012). The calorimetric method employed in Harris et al. (2012), was carried out on our behalf by Dr Malin Suurkuusk (TA Instruments, Sollentuna, Sweden) and as such, this was the first calorimetric lab work carried out by either of the research groups at Cranfield or SLU.

The key aim of this preliminary study was therefore to identify shortcomings of the working methodology that could potentially be addressed. Indeed, several shortcomings were identified (detailed in section 4.5), forming the basis for the method development work presented in Chapter 5. The preliminary experiment also set out to test the level of variance apparent between lab replicates taken

from the same sample. However, the experiment was also designed to test the main hypothesis, by way of investigating the relationship between thermodynamic efficiency and long-term environmental stress due to metal contamination.

#### **4.1.1 Long term metal induced stress**

As discussed in Chapter 1, biological systems under stressed conditions are likely to be less efficient at cycling energy and nutrients than similar soils in unstressed conditions (Addiscott, 1995; Harris et al., 2012). The anthropogenic contamination of soil with metals is known to cause ecological stress to soil microbial communities, resulting in changes to respiration rates, community composition, enzymatic concentrations and total microbial biomass (Kuperman & Carreiro, 1997; Åkerblom et al., 2007; Wang et al., 2007). Some metals such as Cu, Ni and Zn are essential to biological growth and are as such termed 'micronutrients'. However, they are only required in relatively small concentrations and become toxic when available at too high a concentration. Others such as Pb, Hg and Cd have no known biological function yet are readily sequestered by organisms, resulting in a toxic effect (Maier et al., 2009).

Flue gas emissions from heavy industries frequently contain particulate matter rich in metallic and sulphurous aerosols. This is particularly prevalent with smelting works. Long term accumulation of metals in the surrounding soil can cause toxicity to organisms, depending on chemical form and concentration (Hodson, 2004; Brady & Weil, 2008), whereas sulphur is more mobile and less toxic, usually causing toxic effects by soil acidification and mobilisation of



naturally occurring metals such as Al (Brady & Weil, 2008). Due to the high residence time of some metals in the soil, anthropogenic contamination can prevail over many hundreds or even thousands of years. As such, metal working sites offer a unique opportunity to investigate microbial communities that have adapted to survive under long-term anthropogenically caused environmental stress.

## **4.2 Methodology**

In order to test the working methodology for isothermal calorimetric analysis, soil samples were taken from the area surrounding a brass smelter in Gusum, Eastern Sweden. These samples were then used to assess the impact of long-term metal contamination induced ecological stress on the thermodynamic efficiency of soil microbial communities, via the working method.

### **4.2.1 Gusums Bruk**

For at least 300 years, the small Swedish town of Gusum has grown up around the Gusums Bruk brass mill. However, the provision of employment and prosperity was not the only gift from the mill to the surrounding area. A much more sinister gift in the form of flue gas emissions from the brass smelter was bestowed upon the local populace; flue gas containing aerosols rich in toxic metals such as Zn (65% soil metallic contamination), Cu (33%), Pb (2%), Ni, V and Cd (<0.2% collectively), which accumulated in the soil for centuries until emissions controls were implemented in 1982 (Tyler, 1984). In 1988 the mill's holding company was liquidated and the old mill, including the smelter, was closed, before finally being demolished in 2010 (Almqvist, 2010). A buyer was

found for the new part of the mill, built in the 1960s and located c. 1 km away in Gräsdalen (see Figure 4.1), which continues production to this day.

Since the early days of its operational history, Gusums Bruk only undertook secondary smelting of scrap metal. Subsequently the surrounding soils offer a rare example where metal concentrations reach toxic levels, while non-metallic pollutants, such as S, are only present at low concentrations (Tyler, 1984). During the 1970s and 80s this led to many studies on the effects of metal pollution on the surrounding ecology, such as deterioration in vascular vegetation, moss and lichen cover (Folkeson, 1984; Tyler, 1984), reduction of pine litter decomposition rates (Tyler, 1984; Berg et al., 1991), reduction in microbial biomass activity (Tyler, 1984; Nordgren et al., 1988; Bååth et al., 1991), variations in microbial community structure (Rühling et al., 1984; Tyler, 1984) and invertebrate populations (Tyler, 1984; Bengtsson & Rundgren, 1988). Additionally to this there has been much research in the area of Gusum on the fate of metals in the environment.

### **4.2.2 Sampling**

Samples were taken from four sites of varying contamination levels, representing a sight of high, medium, low and negligible (near background) contamination levels, as per the geographic data presented in Tyler (1984) and Almqvist (2010). The location of the four sample sites, marked A-D, are shown in Figure 4.1, with Site A representing the most contaminated site and Site D being the site of negligible contamination.

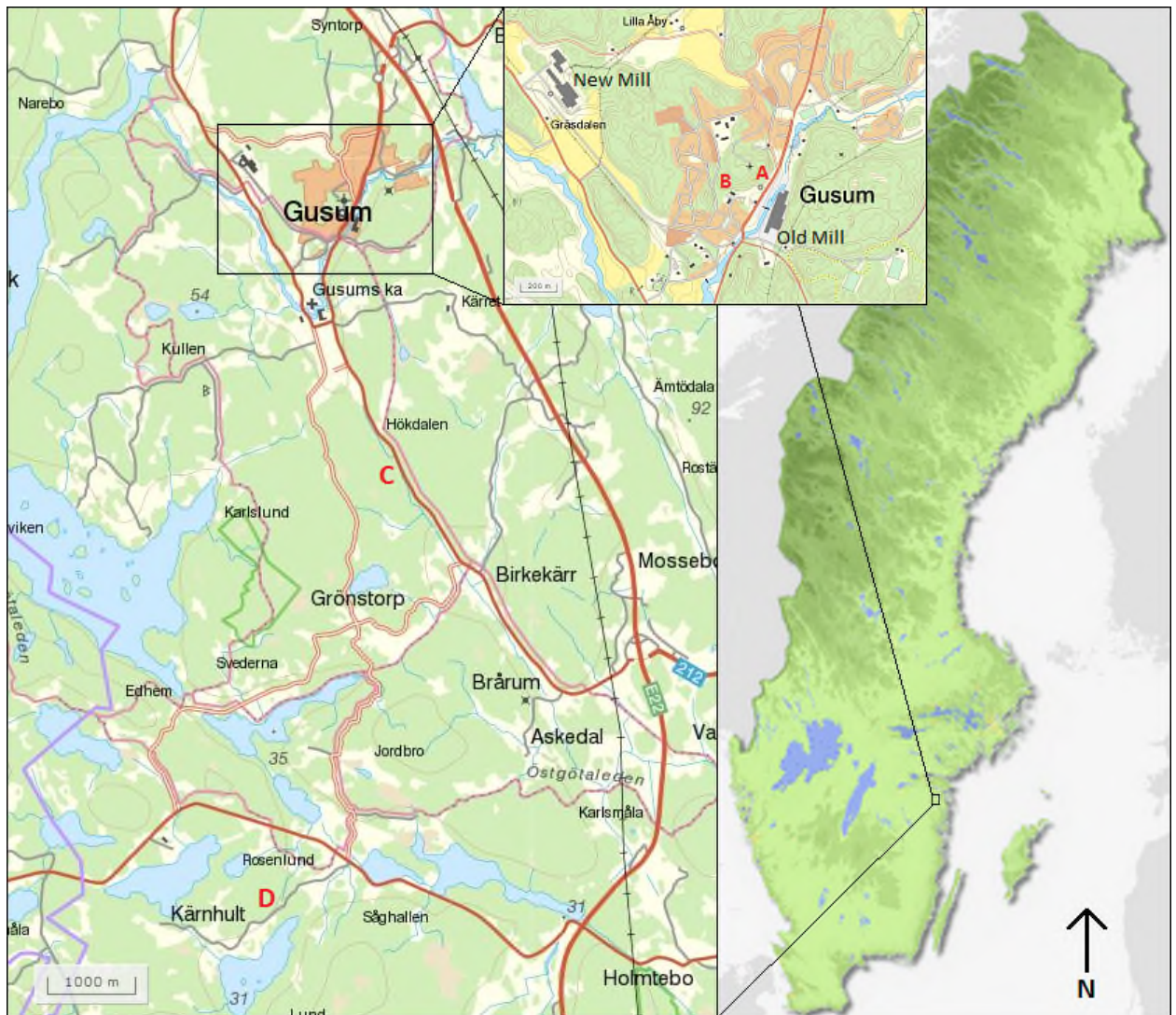


**Figure 4.1: Approximate location of the four sample sights (marked A-D in red) in relation to the now defunct Gusums Bruk (marked Old Mill), located near the centre of Gusum, Östergötland, Sweden (after Lantmäteriet (2013), ©Lantmäteriet, Gävle, Sweden)**

At each site, a topographically similar (c. 10° SE sloping incline) sampling area of 2 m by 2 m was selected. Surface samples of c. 400 g fresh soil were taken from the top 5 cm of the soil profile, from six positions randomly allocated by blind tossing of a glove. The samples were stored in polyethylene bags for road transportation back to the Department of Chemistry at Sveriges Lantbruksuniversitet (SLU) in Uppsala, Sweden.

### **4.2.3 Sample preparation and pre-incubation**

As mentioned in Chapter 2, the literature standard for preparation of soil samples for isothermal calorimetric analysis involved storing samples of soil homogenised by sieving and mixing at 4°C for three to six months. This method had been employed for the work in Harris et al. (2012), but would have been impractical to undertake for this work, as the whole experiment from start to finish was given only one month for completion. As such, it was decided that samples should be individually homogenised by passing through a 2 mm sieve, prior to hand mixing and then pre-incubated at 25°C for exactly one week preceding calorimetric analysis. Samples were pre-incubated at 60% WHC, as microbial metabolic activity has been observed to reach a maximum at around this level, due to substrate diffusion rates being reduced at lower moisture contents and O<sub>2</sub> diffusion rates being hindered above this level (Skopp et al. 1990).

The TAM Air calorimeter has eight channels, therefore allowing simultaneous analysis of four sample pairs, with each pair consisting of a glucose amended and a water amended sample. As such, each run contained one sample selected by a random number generator from each of the samples sites.

### **4.2.4 Moisture and organic matter content**

Measurements of WHC and GWC were made via the methods of Rowell (1994), outlined in Chapter 3.

Crude determinations of soil organic matter (SOM) content were made by measuring loss of mass on ignition at 500°C of c. 10 g soil, which had been previously oven dried at 105°C (Rowell, 1994).

#### **4.2.5 Soil microbial biomass**

Soil microbial biomass estimations were made via the chloroform fumigation-extraction method of Vance et al. (1987) as modified by Wu et al. (1990), detailed in section 3.3.

#### **4.2.6 Calorimetric analysis**

Inert reference samples were made up with acid washed glass beads for each of the soil samples to be run. The mass of glass beads used was calculated to have a similar heat capacity to the soil sample, based on the water, organic and mineral content of the samples, assuming: values of 4.18 J g<sup>-1</sup> K<sup>-1</sup> for water, 1.3 J g<sup>-1</sup> K<sup>-1</sup> for SOM, 0.83 J g<sup>-1</sup> K<sup>-1</sup> for quartz and that the value for quartz was representative for both the glass beads and for the mineral fraction of the soil (Hillel, 1998).

Duplicate samples of 1 g dry soil mass equivalent were placed into clean glass ampoules of 20 cm<sup>3</sup> internal volume. These were then returned to the incubator for an hour at 25°C, to allow the ampoule to reach 25°C, with the uncrimped lids placed onto the ampoules in order to minimise evaporative losses. The soil amendments of either Milli-Q filtered water or 0.07 M aqueous glucose solution were also placed into the incubator at 25°C for an hour prior to use. The soil samples were prepared for analysis by addition of either 100 µl 0.07 M aqueous glucose solution or Milli-Q filtered water, with one sample from each duplicate

pair being glucose amended and the other water amended. After amendment the ampoules were hermetically sealed by crimping of an aluminium cap over a Teflon coated septa, thoroughly cleaned with tissue paper and then lowered into the appropriate calorimeter channels. Calorimetric assessment was then carried out at 25°C for 60 hours after sample amendment, with values of  $Q_{total}$  for  $\eta_{eff}$  and SIHP taken for the period 2.5 – 64 hours after sample amendment.

The samples were analysed in two phases. In the first phase, four lab-replicates of the same sample were run simultaneously, allowing assessment of variations between assays. This was done with only one field sample from each of the four sample sites, constituting a total of four calorimetric runs. In the second phase, only a single analysis was undertaken from each field sample, allowing four field samples to be assessed in each run, one from each sample site. Calculations for  $\eta_{eff}$  and SIHP values and standard errors were made by treating the mean value of the four lab replicates as if it were a single field replicate. During this second phase, the samples from each site were placed into the sample calorimeter cells, i.e. Site A in cells 1 & 5, Site B in cells 2 & 6, Site C in cells 3 & 7 and Site D in cells 4 & 8.

#### **4.2.7 Statistical analysis**

All error values quoted are for pooled standard error, calculated via a one-way factorial ANOVA, using sample sites as categorical predictors.

## 4.3 Results

Due to time restraints, only four of the six samples taken at each site could undergo calorimetric analysis. Only the results obtained from the calorimetrically assessed samples are here presented.

### 4.3.1 GWC, WHC, SOM and microbial biomass-C

Mean values of SOM were similar for all sites, all being in excess of 0.5 g SOM g<sup>-1</sup> dry soil (Table 4.1). However, values for WHC and biomass-C were less uniform, showing highly decreased levels in the most contaminated samples (Site A). However, when looking only at Sites B to D, there was no evident link between apparent contamination level and WHC or biomass-C.

**Table 4.1: Mean observations for GWC, WHC, SOM by LOI and chloroform labile Biomass-C, with standard deviations in brackets. Approximate levels of copper contamination are taken from Almqvist (2010) for sites A, B & D and Tyler (1984) for site C.**

Site	[Cu] (mg-Cu · kg <sup>-1</sup> dry soil)	GWC (g H <sub>2</sub> O g <sup>-1</sup> dry soil)	WHC (g H <sub>2</sub> O g <sup>-1</sup> dry soil)	SOM (g · g <sup>-1</sup> dry soil)	Microbial biomass-C (µg -C g <sup>-1</sup> dry soil)
A	3300	0.75 (±0.15)	1.87(±0.43)	0.51(±0.11)	23.7(±10.2)
B	250	1.18(±0.14)	3.51(±1.47)	0.59(±0.20)	86.0(±38.0)
C	50	1.29(±0.39)	2.59(±1.01)	0.51(±0.20)	118.9(±38.7)
D	10	0.88(±0.33)	2.71(±0.65)	0.50(±0.11)	68.9(±36.5)

### 4.3.2 Calorimetric analysis

#### 4.3.2.1 Assay variance

The variance between lab replicates of the same sample was higher than was expected for such a sensitive instrument. All lab replicates showed similar shaped heat-flow curves to each other, with similar timing for all inflection points

and similar gradients between inflection points, however the relative amplitudes could vary by as much as an order of magnitude. An example of this can be seen for the glucose amended samples in Figure 4.2, yet it was also the case in some of the water-amended samples, with one water amended sample from Site A having  $P$  values greater than three times that of another of its sister lab replicates. However it should be noted that the overall variation between lab replicates was greater at Site A, suggesting that this may have arisen from a lack of homogeneity in the samples at this site arising from disuniform contamination of the soil profile.

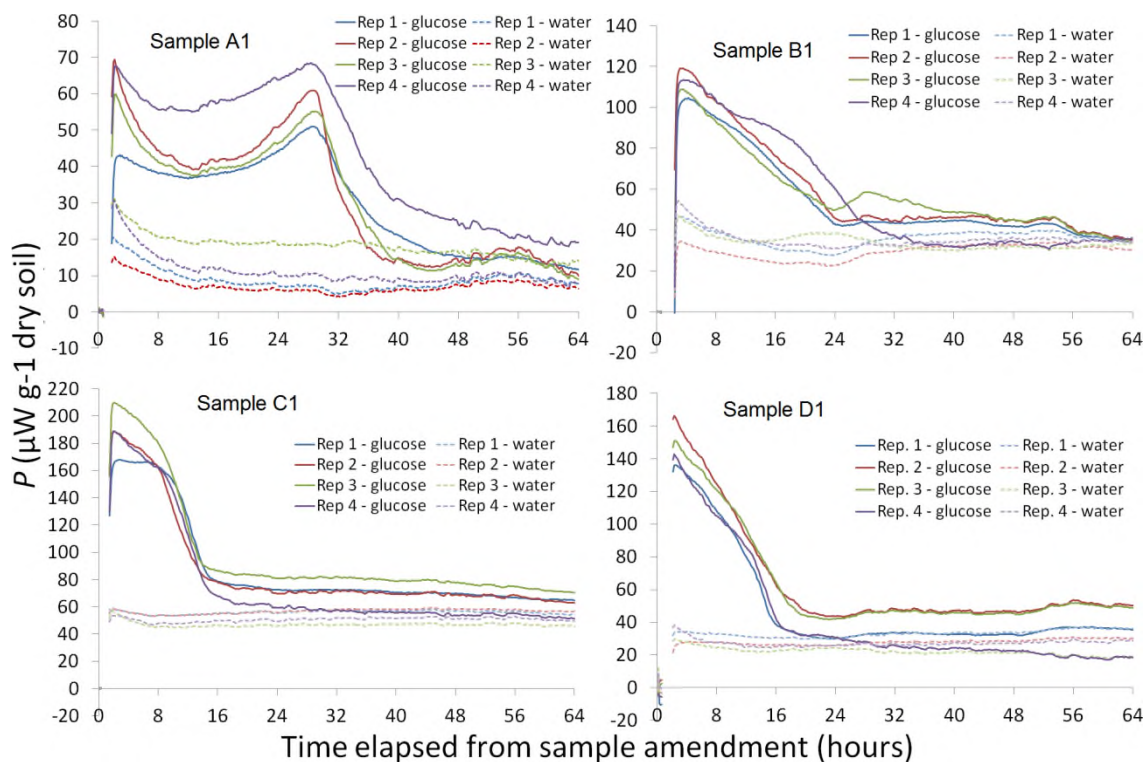


**Figure 4.2: Power-time curves produced from the lab replicate samples, showing both the glucose amended and water amended samples from each sample pair.**

The disparity between  $P$  rates was such that out of a total of 28 sample pairs, in 8 pairs the water amended sample overtook the  $P$  rate of the glucose amended



sample and in 5 of these the  $P$  rate of the water amended sample remained higher than the glucose amended sample over a period of 10 hours or more (see Figure 4.2 & Figure 4.3).

Part of the rationale behind running samples in pairs with a glucose amended and a water amended sample, was for the water amended sample  $Q$  rate to act as a baseline, so that the glucose-induced  $Q$  production rate could be calculated and to counteract any signal instability. However, the relationship between glucose and water amended samples was non-apparent from the results obtained. Values for 'glucose-induced'  $Q_{total}$ , determined by subtracting the baseline  $Q_{ref}$  from  $Q_{gluc}$  and used in both thermodynamic indices, had a greater pooled standard error value than either  $Q_{ref}$  or  $Q_{gluc}$  by themselves (Table 4.2). Normalisation of the datasets resulting in increased error values could indicate a lack of relation between the baseline values and the results for  $Q_{gluc}$ , potentially highlighting an issue with the way the data is collected.

**Table 4.2: Mean values for total and maximum heat output from 2.5 to 64 hours after sample amendment of the lab replicated samples. Standard error values are given in brackets below the mean and were calculated using the samples as categorical predictors. n = 16.**

Sample	$Q_{gluc}$ (J)	$Q_{ref}$ (J)	$Q_{net}$ (J)	$P_{max}$ (mW g <sup>-1</sup> )	Net $P_{max}$ (mW g <sup>-1</sup> )	$tP_{max}$ (h)
A1	7.39 (±0.74)	2.47 (±0.53)	4.92 (±0.95)	62.0 (±4.2)	46.3 (±6.2)	15.38 (±7.62)
B1	12.50 (±0.20)	7.47 (±0.32)	5.03 (±0.51)	111.5 (±3.1)	67.3 (±6.0)	3.79 (±0.18)
C1	18.81 (±0.94)	11.63 (±0.52)	7.18 (±1.22)	188.7 (±8.5)	132.3 (±8.8)	2.29 (±0.24)
D1	11.72 (±1.19)	6.11 (±0.50)	5.62 (±1.48)	149.0 (±6.5)	117.5 (±9.2)	2.42 (±0.05)

### 4.3.2.2 Variation between apparent contamination levels

All glucose amended samples from sites B, C and D followed a similar pattern of a high initial rate of  $P$ , which fell off during the initial 14-32 hours, before stabilising (see Figure 4.3). This was most pronounced with samples from Site C, with samples reaching a more stable state after 14-25 hours, after initial  $P$  rates of 100-210  $\mu\text{W g}^{-1}$  dry soil. At Site B the decrease was slower and less uniform than Sites C & D, with a couple of the samples showing shoulders during their decrease in  $P$  over time. Samples from Site A had more pronounced shoulders or even peaks occurring 22-32 hours after glucose addition.

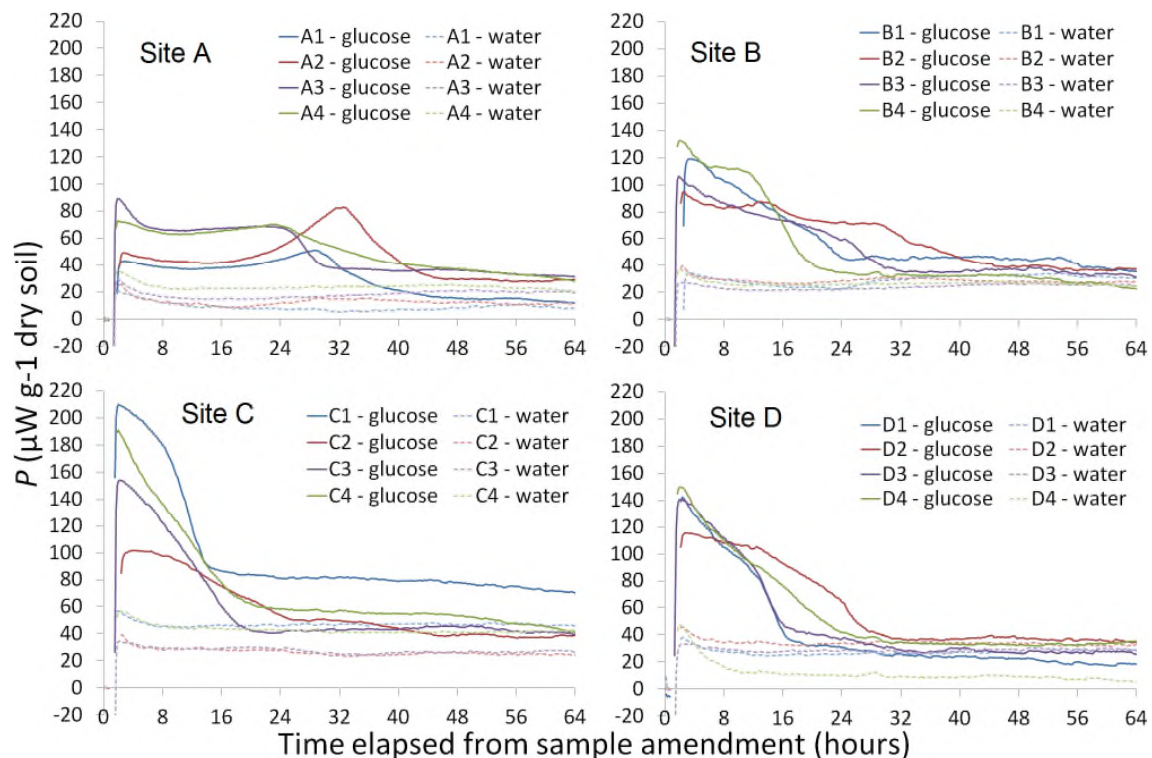


**Figure 4.3: Power-time curves for all field samples. Only one of the four lab replicates couples is presented from each site, corresponding to the same calorimeter cells as the other samples from each site. Therefore samples A1, B1, C1 and D1 correspond to Site A Rep 1, Site B Rep 2, Site C Rep 3 and Site D rep 4 respectively in Figure 4.2.**

All of the water amended samples showed decreasing  $P$  rates during the initial 6-10 hours after sample amendment. This may be an artefact of thermal shock, indicating that the samples may not have reached thermal equilibrium with the calorimeter cells until several hours into the measurements.

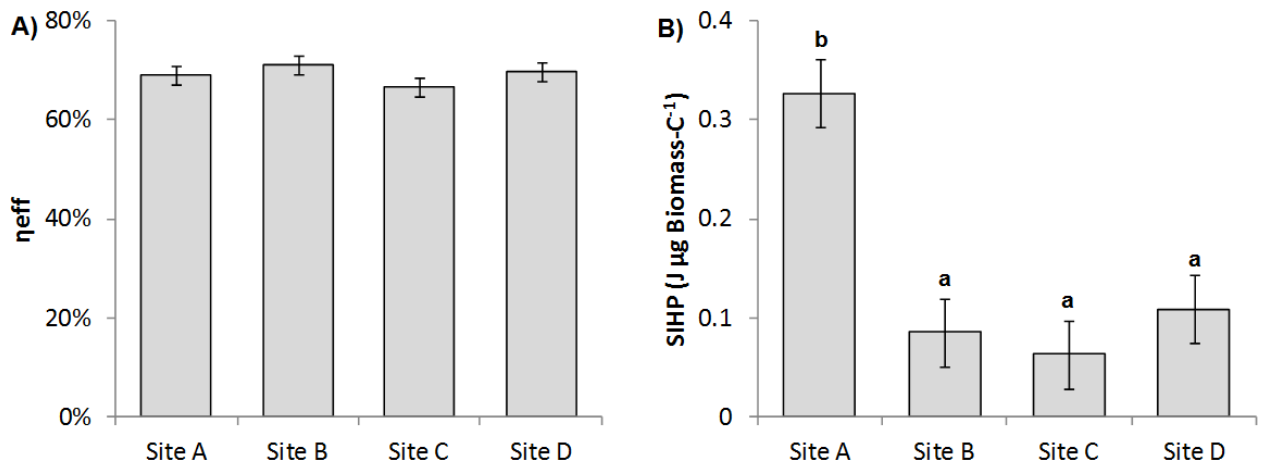


**Figure 4.4: Results for: A) mean  $\eta_{eff}$  and B) mean  $SIHP$  from each site (field replicates only) for  $t=2.5-64$  hours, with bars denoting pooled standard error and lower case letters denoting homogenous groups at the  $P = 0.05$  level.**

Values for  $\eta_{eff}$  did not vary in relation to apparent contamination level, with no significant trend observed at the  $P = 0.1$  level (Figure 4.4). The results for  $SIHP$  however showed a significant difference between Site A and Sites B, C and D at the  $P = 0.05$  level. This indicates that higher levels of soil contamination result in increased heat output per unit Biomass-C.

### 4.3.3 Additional comments on the method

During the experiment, several issues with the method were highlighted. Samples from Site A had a very low density containing a high proportion of pine needles. This would have reduced the head space considerably, reducing the quantity of available  $O_2$ . To address concerns regarding headspace, samples

techniques should aim to avoid including material from the O-horizon when possible. This would not have been possible with this experiment, as the soil profile at Site A only contained a few mm of mineral soil below the O-horizons.

The preparation of soil samples at 65% WHC plus the volume of water or glucose solution amendment caused smearing of the samples upon mixing, suggesting water logging, which could impair diffusion of O<sub>2</sub> within the sample.

Due to the thermal shock arising from inserting the ampoule into the calorimeter chamber, the initial 2.5 hours of data had to be discounted while the instrument and sample reached thermal equilibrium. The power-time curves of the water amended samples suggest that the thermal shock may have lasted as long as 10 hours (Figure 4.2 & Figure 4.3). The loss of the first few hours of thermal data will skew the results towards higher heat production for K-strategist dominated ecosystems, as r-strategists would be expected to use more of the substrate and therefore produce more heat during the initial few hours.

There was a noticeable level of signal instability, common to all channels simultaneously. This is particularly evident in Figure 4.2, where the most visible signal disturbance (due to axis scaling) can be seen with the samples from Site A at c. 50 hours after sample amendment. This is a known issue with air cooled calorimeters (Wadsö, pers. com.) as the temperature regulation of the aluminium heat sink will be effected by environmental conditions, such as room temperature, humidity, air pressure and any air flow. This experiment was conducted in a non-climate controlled room with old metal and glass window frames, which also housed large sample incubators, during a period of

changeable weather. It is possible that the signal instability may have arisen from these conditions. In light of this the calorimeter was moved to a more controlled environment for future experiments.

The end time of 64 hours after sample amendment used for calculation of  $Q_{\text{gluc}}$  and  $Q_{\text{ref}}$  was arbitrary, as all samples showed evidence of a distinct terminal phase, with glucose amended heat signals reaching a relatively stable state by 10-48 hours after sample amendment.

## **4.4 Discussion**

Because the main aim of this experiment was to test and troubleshoot the methodology used by Harris et al. (2012), the discussion section is split between the ecological trends observed and the methodological issues that were highlighted.

### **4.4.1 Influence of apparent contamination on thermal output**

The power-time curves from Sites C & D were similar, reaching a low, stable  $P$ -rate after c. 10-25 and c. 16-28 hours respectively. The results for Site B took c. 22-45 hours to reach a low, stable  $P$ -rate, indicating that the metal contamination was having an inhibitory effect on the microbial community's metabolic rate, especially as Site B had a greater biomass than site D. Yet the thermodynamic indices for Sites B-D were indistinct at the  $p=0.05$  level, showing that despite metal induced stress reducing metabolic rate, it did not reduce system efficiency. Site A, on the other hand, took 30-48 hours to reach a low, stable  $P$ -rate and had a SIHP value three times greater than Sites B-D.

This indicates that the higher apparent contamination levels at Site A not only reduced the metabolic rate, but also decreased the system efficiency.

The results for  $\eta_{eff}$  showed no correlation to apparent contamination level ( $p > 0.1$ ), indicating that despite the differences in heat production per unit biomass, there was no significant change in substrate use efficiency between the sites.

#### **4.4.2 Inaccuracies in the methodology**

- Signal instability

The instability of the  $P$  signals due to environmental factors had a maximum deviation of  $c. \pm 1 \mu W$  and therefore only constitutes a problem with samples that have low absolute amplitudes. The effects of the signal instability are mitigated by the fact that it was observed to affect all channels, simultaneously and to an equal degree. The use of paired samples with one glucose amended and one water amended ampoule used for normalisation, should negate any error arising from this. However this may be an issue when comparing absolute amplitudes between samples from different runs. Regarding this, the lowest peak amplitude for a glucose amended sample in this experiment was  $50.9 \mu W$ , therefore signal instability represents an experimental error of  $c. 2\%$ .

- Thermal shock

The thermal shock arising from the introduction of the ampoule into the calorimeter chamber is by far the most problematic of the issues highlighted in this experiment. Due to the time required for the calorimeter to reach a signal stable enough to run a baseline calibration, the first 1-2.5 hours of the

experiment was not captured in the data log. Also the baseline calibration would have been erroneous, as it would have captured a signal deriving from sample amendment and therefore different for the water amended and the glucose amended samples. This could result in the instrument computer integrating a distorted or sloping baseline, thereby changing the absolute values of the results. The indication from the water amended samples that the thermal shock may have lasted up to 10 hours, which would influence the shape of the power-time curves by inflating absolute values of P in the initial few hours of the experiment.

- O<sub>2</sub> concentration

Concerns have been raised about reduction of the concentration of O<sub>2</sub> in the closed system of the ampoule. It is possible that a reduction in the O<sub>2</sub> content or a corresponding increase in CO<sub>2</sub> could stunt the metabolic rate. However this is unlikely in this experiment, as the 20 ml ampoule should contain enough O<sub>2</sub> to fully oxidise c. 5 mg glucose (Vor et al., 2002), several times greater than the 1.26 mg glucose addition used here.

- Arbitrary nature of 64 hour run times

The run times of 64 hours after sample amendment were completely arbitrary; determined only by the number of samples taken and the time available on the calorimeter. It is therefore questionable as to whether it is appropriate to use values of Q for the period 2.5-64 hours. It may be of more interest to use values of Q for the period 2.5 hours until P reached the terminal phase, evidenced by a low, stable P-rate.

## 4.5 Conclusions

The run through of the working methodology was a success, in that the experiment was conducted with no major setbacks and meaningful data was obtained first time around. It was also successful in that it identified several areas of the method that required improvement.

The data indicated that apparent contamination levels influenced metabolic heat production rates and thermodynamic efficiency, indicated by retardation and delaying of peak thermal power output and an increase in heat production per unit biomass respectively. This in turn indicates that the soil contamination induced stress has lowered the thermodynamic efficiency of the soil microbial community, despite the  $\eta_{eff}$  data not supporting this hypothesis.

Several key areas for improvement of the methodology were identified. Soil sampling should minimise the fraction of O-horizon material included in the samples, when possible, in order to increase O<sub>2</sub> availability and sample stability. The sample pre-incubation process requires refinement; as mentioned in Chapter 2, the method of Núñez-Regueira et al. (1994a) is archaic and the method used here proved to be fairly impractical. Sample amendments should be added *in vitro*, to avoid thermal shock, to allow accurate sample baselines to be taken and to allow observations of the first few hours after sample amendment. The calorimeter should be housed in a controlled environment in order to reduce baseline drift and fluctuations. The length of sample runs should be considered for revising, as successful measurement of the  $\eta_{eff}$  index requires complete consumption of the added glucose by the soil microbial community.



## 5 Method development

*The ultimate aim of the modern movement in biology is in fact to explain all biology in terms of physics and chemistry.*

– Francis Crick

### 5.1 Introduction

Isothermal calorimetry has been demonstrated to be a useful and an increasingly-adopted tool for providing real-time and quantitative data on various aspects of the soil microbial ecosystem, including total biomass estimation (Barros et al., 2008b; Cabral & Sigstad, 2011), metabolic response to environmental stress (Zheng et al., 2009; Gruiz et al., 2010; Zhang et al., 2010; Harris et al., 2012) and measurement of metabolic efficiency (Barros et al., 2010, 2011; Zhang et al., 2010; Harris et al., 2012). However several commentators have remarked that there has been little work done on producing a standard methodology, particularly concerning the areas of sample preparation and storage (Barros et al., 2007b; Wadsö, 2009; Braissant et al., 2010).

As of 2014, the majority of groups publishing in this area have elected to store samples at 4°C for 1-8 months prior to isothermal calorimetric analysis. However, refrigeration for such a long period of time is not commonly practiced within the discipline of soil microbiology when the stated purpose is to capture variance present in the environment. When samples are disassociated from their ecological context for a protracted period, they will begin to acclimatise to

their new circumstance. As such, refrigeration for extended periods will reduce the natural variance in microbial response from the soil, which many experiments aim to capture. Within the discipline of soil microbiology, soil samples are typically pre-incubated for a period of 1-2 weeks prior to the application of microbiological assays (Powlson & Jenkinson, 1976; Wang et al., 2001a; Creamer et al., 2009a). It is therefore necessary to investigate the method, so that research using isothermal calorimetry of soil samples may be compared with results obtained using other complementary techniques. This study evaluates the influence of pre-incubation at 20°C on the microbial response upon fertilisation with glucose-carbon (C), as measured by isothermal calorimetry.

### **5.1.1 Background**

The use of refrigeration to store soil samples prior to analysis is considered by soil microbiologists to be a useful strategy when dealing with many samples collected simultaneously or when using time consuming analytical techniques. In relation to isothermal microcalorimetric analysis, Sparling (Sparling, 1981a; b, 1983) recognised the temporal challenges arising from the low sample throughput, time needed for baseline stabilisation and the long run lengths typically required. To mitigate the effects of this, he used 'stored' samples of soil refrigerated at 5°C in his pioneering work on isothermal microcalorimetric analysis of soil (Sparling, 1981a; b). However, in later studies he also used 'fresh' soil pre-incubated at 21°C for up to 10 days (Sparling et al., 1982; Sparling, 1983), finding that stored soils had less than half the heat output of fresh soils and that the biomass was reduced by over 25% on average in the

stored samples (Sparling, 1983). Yet despite Sparling's refinement of the methodology, the use of refrigeration was subsequently adopted by other groups analysing soils by isothermal calorimetry (Barros et al., 2008b, 2010, 2011; Zheng et al., 2009; Gruiz et al., 2010; Zhang et al., 2010; Cabral & Sigstad, 2011; Harris et al., 2012).

The practice of storing soil samples for several months prior to isothermal microcalorimetric analysis was proposed by the group of Takahashi et al., who stored 'stock' soil, i.e. generic soil to be used in several studies, stored at room temperature for at least 3 months in order to attain a nominal equilibrium (Kawabata et al., 1983; Yamano et al., 1983). This practice is considered acceptable by the soil microbial science community when manipulating stock soils in the lab, as it helps to quell the often intense variability found between responses from samples taken at different field locations. Yet despite this, many of the later works that have used a storage period of at least 3 months have set out to assess variance between field sites or field treatments, when the original concept of storage for such a long time was to reduce such variance.

The combination of storage for at least 3 months and storage by refrigeration were the subject of the seminal paper on method development in this area by Núñez-Regueira et al. (1994a), which analysed soil samples recently after sampling, then again after storing at 4°C for 3 and 6 months. This work found that the signals from samples stored for 6 months produced the most stable results, with a trend of decreased peak amplitudes of heat flow rate ( $P_{\max}$ ), decreased total heat flow and an increase in the time to reach peak heat flow rate ( $tP_{\max}$ ). These results were then used to rationalise storing samples in all

future work for a minimum of 3 months at 4°C (Rodríguez-Añón et al., 2007), as this was observed to produce 'satisfactory reproducibility of the measurements' (Barja et al., 1997) and was subsequently adopted by the isothermal microcalorimetric community at large. However, the data presented by Núñez-Regueira et al. (1994a) shows that after 6 months at 4°C  $P_{\max}$  had decreased to the extent that determination of a distinct metabolic peak was tenuous, with a reported error of  $\pm 1.21$  hours given for the  $tP_{\max}$  value.

The first main issue with this method is that soils are very diverse entities, containing a level of biodiversity greater than that of any other ecosystem (Hågvær, 1998). The metabolic response from the microbial community will alter due to changes in the soil's environment, such as climatic regime, as even the slightest change can give the competitive advantage to a different set of organisms (Petersen & Klug, 1994). This point is well illustrated by Núñez-Regueira et al. (2006c), where large differences were observed in the heat flow – time curves of glucose-induced heat production for the same soils when sampled during different seasons. It is therefore likely that a soil sample stored at 4°C for 3 months will have changed significantly in order to adapt to these new climatic conditions. In terms of microbial ecology, such samples may be considered no longer representative of the ecological circumstances from which they were originally derived. Additionally to this, such soil will have changed chemically due to a storage period of this length, due to the inherent nutrient dynamics of the soil system.

### **5.1.2 Introduction to the experimental work**

In order to put forward a sample preparation method more appropriate for studies involving the highly dynamic soil environment, it was decided to test how glucose-induced thermal responses were affected by pre-incubation at 20°C for up to 36 days after sample homogenisation. The presented methodology was based on practice commonly employed within the discipline of soil microbiology and was undertaken in two parts. The first part established the minimum glucose-C concentration required to ensure glucose-C saturation of the microbial biomass, by measurement of microbial C-mineralisation rates induced by various concentrations of glucose-C. The second part investigated the effects of pre-incubation, by recording the glucose-induced heat flow rate for soil samples pre-incubated at 20°C for periods of 2-36 days after sample homogenisation. This enabled a window of signal stability to be identified within the pre-incubation period, thus identifying an optimum period of soil sample pre-incubation prior to isothermal calorimetric analysis.

## **5.2 Experimental method**

### **5.2.1 Sampling & sample preparation**

Sampling was undertaken at 3 sites in order to observe how pre-incubation affects isothermal microcalorimetric responses from soils under different land use types. The sites selected were a pine forest Podzol (Jädraås: 60° 49' N, 16° 30' E) (Lindahl et al., 2010), an Eutric Cambisol from semi-natural pasture (Nåntuna: 59° 48' N, 17° 38' E) (Sindhøj et al., 2000) and a cultivated silty Udic Haploboroll soil (Fors: 60°20' N, 17° 29' E) (Calgren & Mattsson, 2001).

Sampling of sites was staggered and separate samples were taken for the glucose-C saturation experiment (April 2011) and pre-incubation experiment (June – July 2011). At each sampling event 6 randomly located field samples of 0-7 cm depth and c. 500 g mass were taken from a pre-defined plot of 8 m x 8 m. The field samples were brought to the lab and individually homogenised by passing through a 2 mm sieve with subsequent manual mixing. Subsamples were then taken from each of the homogenised field samples and analysed for water holding capacity (WHC) and gravimetric water content (GWC), using the methods of Rowell (1994) outlined in Chapter 3.6 and 3.7. From each field sample a mass of fresh soil equivalent to 100 g dry soil was taken and pre-incubated in a 500 cm<sup>3</sup> glass jar for 14 days. All subsequent subsamples for biotic, respirometric and calorimetric analyses were taken from the same field samples in each case.

### **5.2.2 Biotic analysis**

Concentrations of soil microbial biomass-C were obtained via the chloroform fumigation extraction method of Vance et al. (1987) as modified by Dahlin & Witter (1998), as per Chapter 3.3.

Phospholipid fatty acid (PLFA) analysis was used to determine the phenotypic structure of the microbial communities using the method of Frostegård et al. (1993), outline in Chapter 3.2.

### **5.2.3 Glucose saturation optimisation**

After pre-incubation samples of 50 g dry weight soil were transferred into gas-tight sealable 500 cm<sup>3</sup> glass jars. Glucose solution was added to produce final

concentrations of 10, 50, 100, 500, 1000, 2000 & 5000  $\mu\text{g}$  glucose-C  $\text{g}^{-1}$  dry soil. The samples were wetted so that addition of the glucose solution would bring their water content up to 65% of the total WHC. The jars were sealed, incubated at 20°C and the CO<sub>2</sub> concentration recorded using an EGM-4 Environmental Gas Monitor (PP Systems, UK). CO<sub>2</sub> measurements were taken immediately after glucose addition and then every hour for the subsequent 7 hours.

#### **5.2.4 Pre-incubation experiment**

Calorimetry runs were undertaken using soil that had been pre-incubated at 20°C for 2, 4, 6, 10, 16, 26 & 36 days after homogenisation. Due to the sample throughput limitations of the TAM Air isothermal microcalorimeter, only four samples could be analysed at the same time. Therefore four of the six field replicate samples taken at each site were randomly selected for calorimetric analysis. Duplicate samples of 3 g dry weight equivalent soil were taken from each field samples and each was placed into glass ampoules of 20 cm<sup>3</sup> internal volume. The water content of the soil was adjusted so that addition of the substrate would bring it to 65% of water holding capacity. The ampoules were sealed with Admix (Wadsö, 2005) attachments containing the substrate in two syringes above the ampoule. Substrate was added at a rate of 100  $\mu\text{l}$   $\text{g}^{-1}$  dry soil equivalent. For each duplicate sample, one ampoule was amended with D-glucose solution at a concentration of 5000  $\mu\text{g}$  glucose-C  $\text{g}^{-1}$  dry soil equivalent, while the second was amended with deionised water. For an inert reference, a closed 20 cm<sup>3</sup> ampoule containing glass beads of equal heat capacity of the wetted sample were used. All ampoules were brought to 20°C for at least one

hour before being inserted into a TAM Air isothermal microcalorimeter (TA Instruments Sollentuna, Sweden) with thermostat set at 20.00°C. The instrument was then allowed at least three hours to reach thermal equilibrium with the samples before the substrates were added by depression and repeated flushing of the Admix syringes. Calorimetry runs of  $\geq 40$  hours were undertaken with the time of substrate addition being recorded as  $t_0$ .

The calorimetric data was then analysed by assessing values for peak height ( $P_{\max}$ ), time to peak ( $tP_{\max}$ ), and total heat production for the initial 40 hours after substrate addition ( $Q_{\text{total}}$ ). Values presented for  $P_{\max}$  were taken from the glucose amended samples, normalised by subtracting the corresponding baseline value from the water amended samples. Values of  $Q_{\text{total}}$  at  $t_{40}$ , given in  $\text{J g}^{-1}$  dry soil equivalent were used to calculate the enthalpy efficiency, via Equation (12) in Chapter 3.1.

### **5.2.5 Statistical analysis**

All observed datasets were analysed via a one-way ANOVA with homogenous groups identified using a post-hoc Fisher LSD test. The phenotypic diversity of the soils was examined by constructing a principal component analysis (PCA) using the values of constituent molarity of known fatty acid methyl esters. Variance of principal components (PC) scores in relation to soil type was assessed via a *post-hoc* one way ANOVA.



## 5.3 Results

### 5.3.1 Biomass and phenotypic structure

**Table 5.1: Mean site values ( $\pm$  standard error) for chloroform liable biomass-C and water holding capacity (WHC)**

Site	Land use	Soil classification	Biomass C ( $\mu\text{g g}^{-1}$ )	WHC ( $\text{g g}^{-1}$ )
Nåntuna	Semi-natural pasture	Eutric Cambisol	917 $\pm$ 10	0.79 $\pm$ 0.01
Fors	Arable	Silty Udic Haploboroll	199 $\pm$ 10	0.48 $\pm$ 0.01
Jädraås	Coniferous forest	Podzol	181 $\pm$ 9	0.50 $\pm$ 0.01

The grassland samples had over four times the chloroform labile biomass-C and a c. 60% greater WHC than the arable and forest samples, while the arable and forest samples were similar on both counts (Table 5.1).

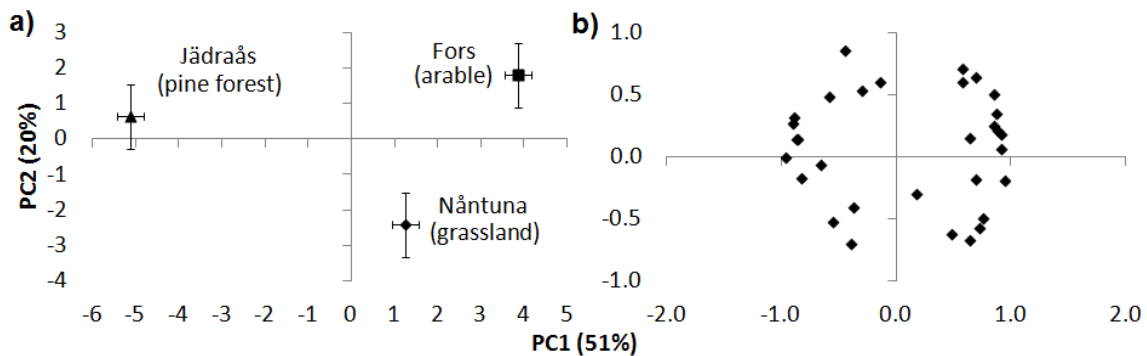


**Figure 5.1: Ordination of first (PC1) and second (PC2) principal components, showing a) the phenotypic differences between the three sites with bars denoting pooled standard error and b) loadings of all identified PLFAs associated with the PCA**

Principal component analysis of the PLFA profiles demonstrated that the community phenotypic structures were highly distinct between the three soils with respect to both the first and second PCs (Figure 5.1a). Loadings showed that the basis of such differences was attributed to a wide range of individual PLFA types (Figure 5.1b).

### 5.3.2 Glucose concentration optimisation

The results from the C-mineralisation experiment showed that the forest, arable and grassland soils became saturated with glucose-C at c. 500, c. 1000 and c. 2000  $\mu\text{g}$  glucose-C  $\text{g}^{-1}$  dry soil equivalent respectively (Figure 5.2).

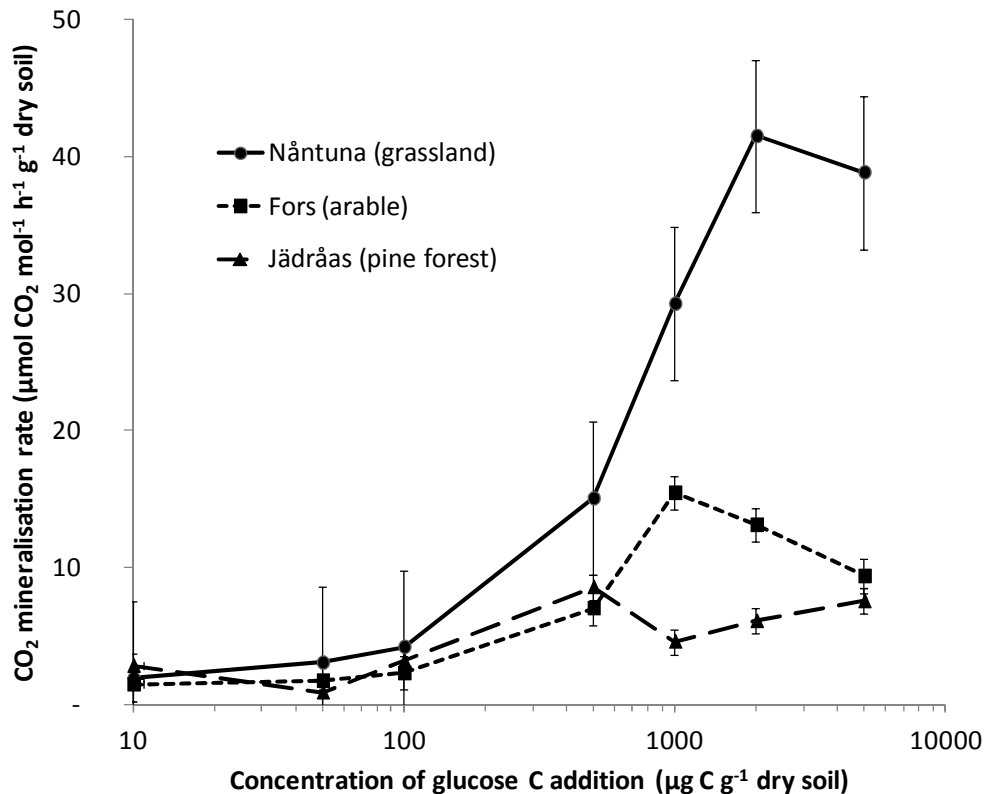
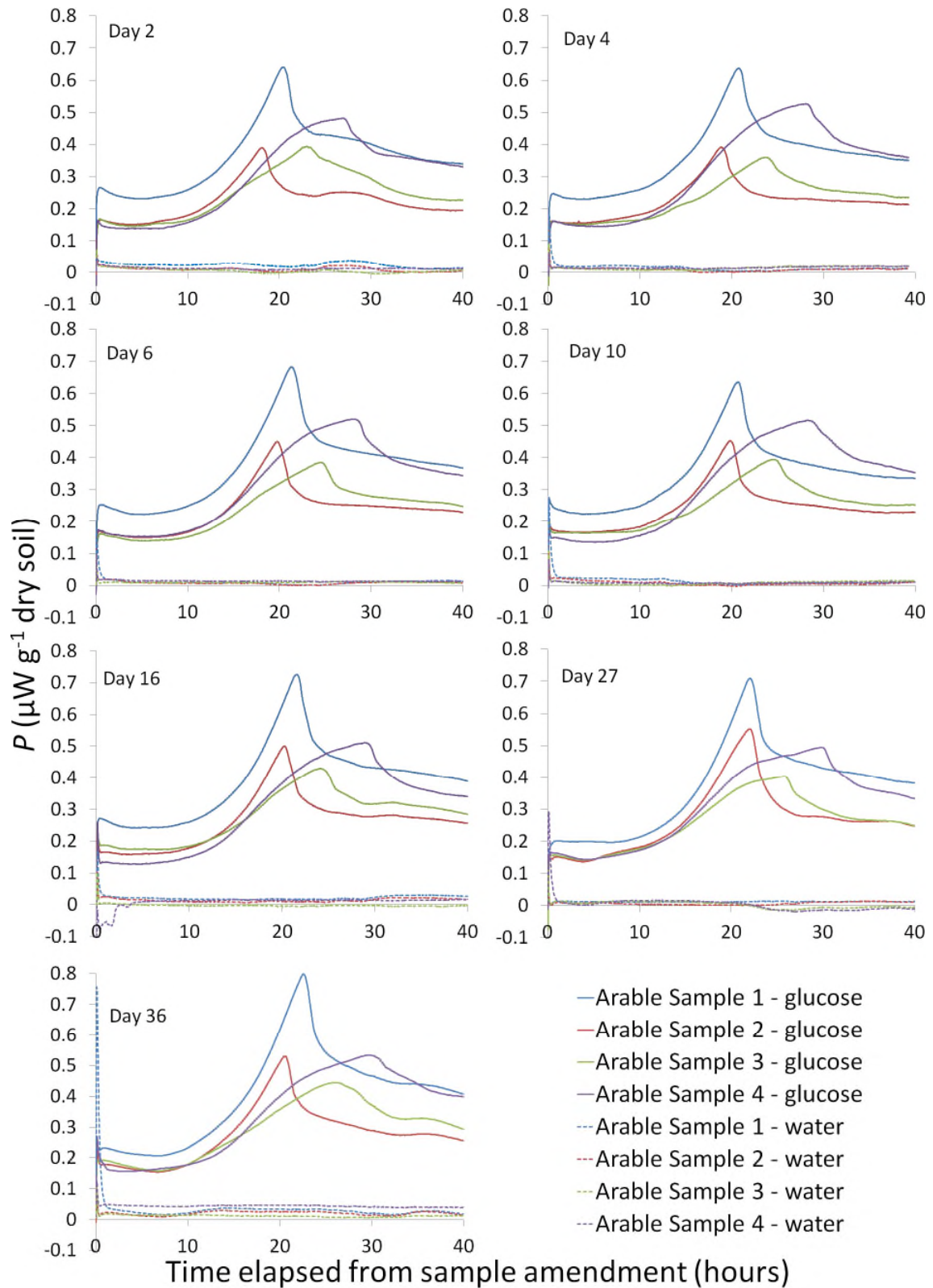


Figure 5.2: Rate of CO<sub>2</sub> mineralisation resulting from addition of different concentrations of glucose-C on a logarithmic scale to the grassland (solid line), arable (dotted line) and forest (dashed line) soils, with error bars denoting pooled standard error

### 5.3.3 Changes in heat flow – time curves

Power – time curves are presented for all calorimetric runs for each site in Figure 5.3, Figure 5.4 and Figure 5.5, with data from all isothermal runs presented in Figure 5.6 and Figure 5.7.



**Figure 5.3: Power – time curves produced by both glucose and water amended soil samples from the Fors arable site observed at: 2, 4, 6, 10, 16, 27 & 36 days after sample homogenisation**

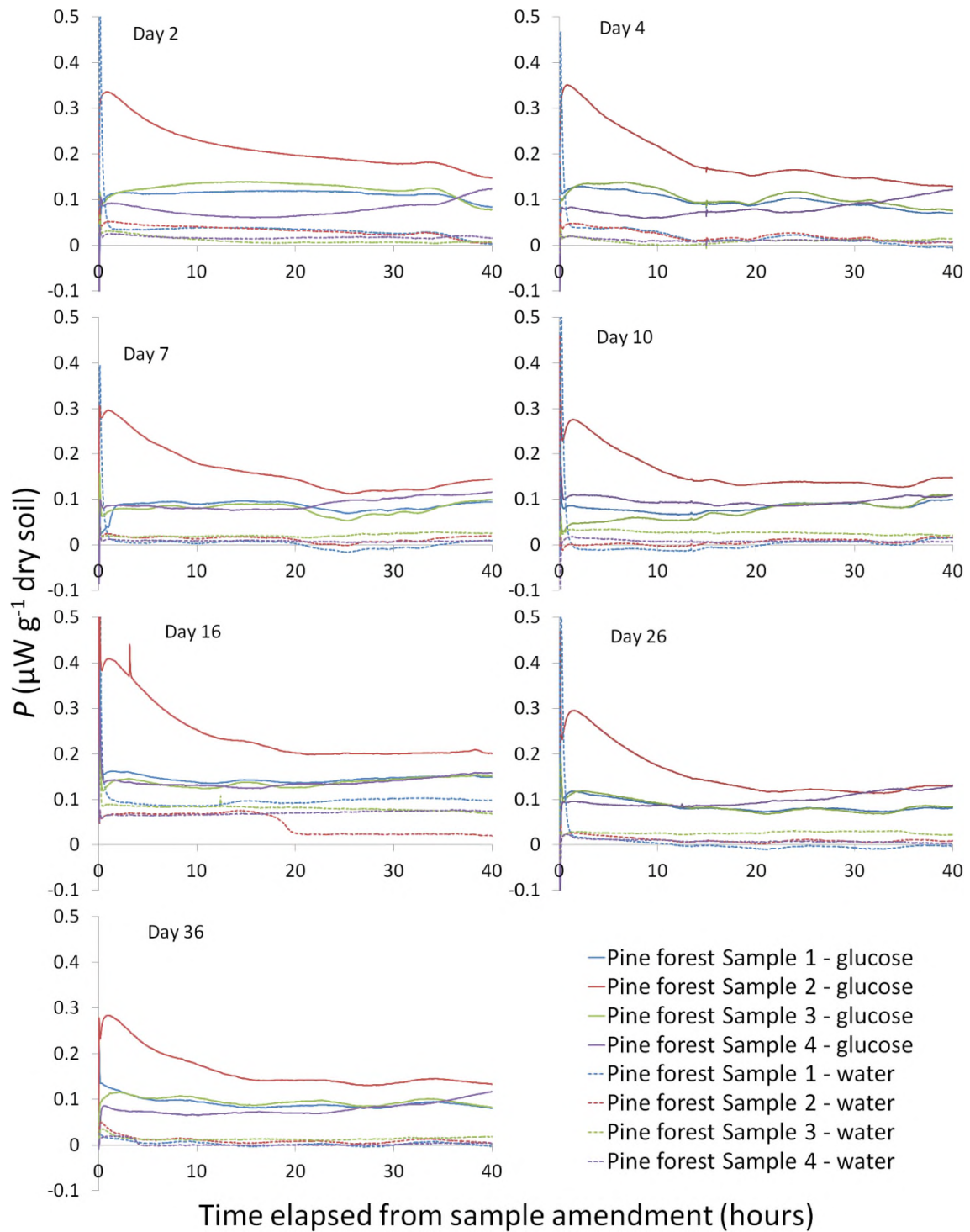


**Figure 5.4 Power – time curves produced by both glucose and water amended soil samples from the Jädraås pine forest site observed at: 2, 4, 7, 10, 16, 26 & 36 days after sample homogenisation**

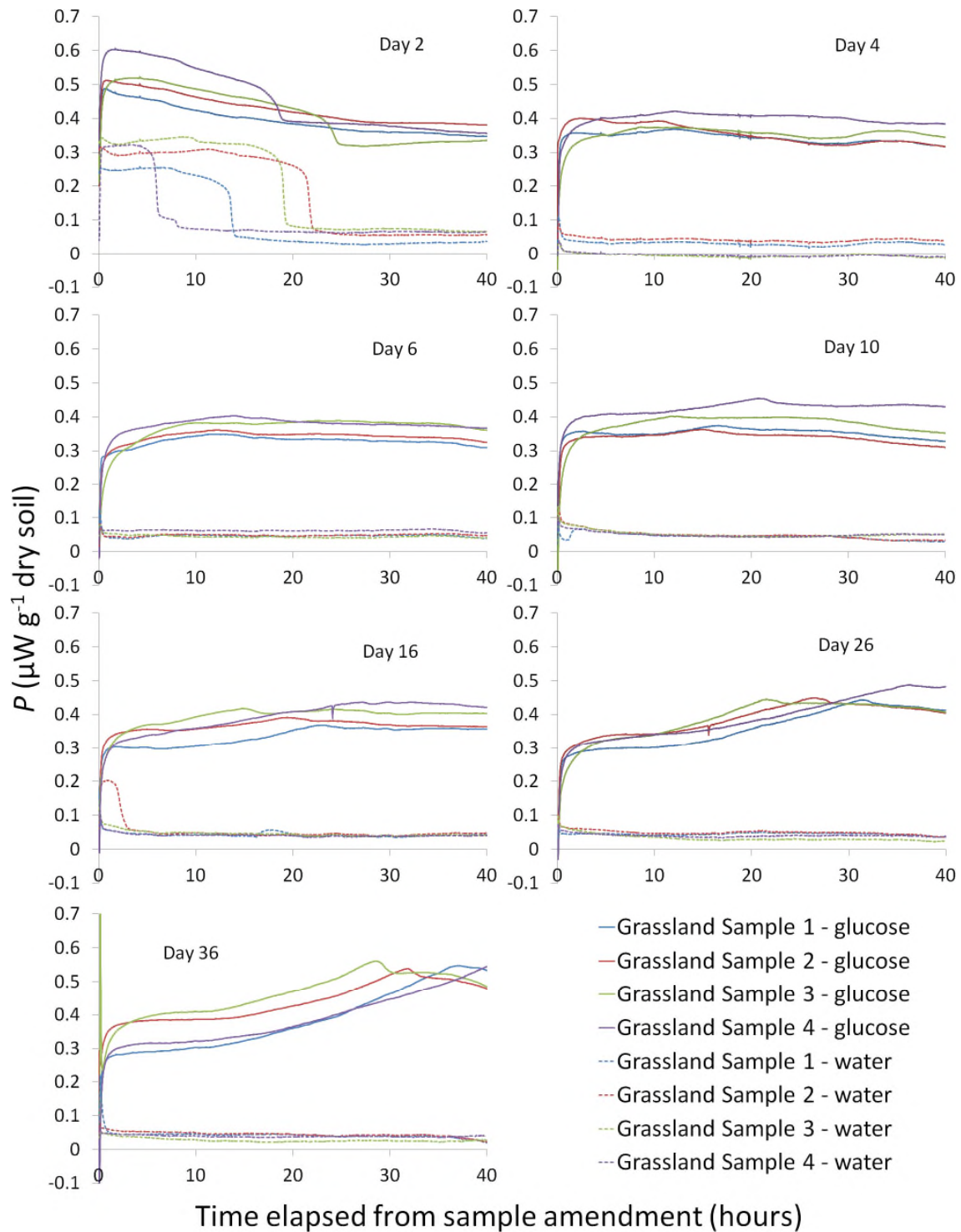


**Figure 5.5 Power – time curves produced by both glucose and water amended soil samples from the Nántuna grassland site observed at: 2, 4, 6, 10, 16, 26 & 36 days after sample homogenisation**

The nature of the power – time curves obtained from the arable samples remained similar on all occasions throughout the pre-incubation experiment,

despite minor variations in  $P_{\max}$  and  $tP_{\max}$  (Figure 5.3). The forest samples were also observed to maintain a similar power – time curve nature (Figure 5.4). In contrast, the power – time curves from the grassland samples changed in two key ways. After 2 days of pre-incubation the power – time curves had a period of elevated signal amplitude from 0 to between 6 and 24 hours, particularly prominent in the water amended samples (Figure 5.5). This was followed by a period of stability, with similarly shaped signals lacking a distinct peak, observed between 4 and 16 days after sample homogenisation. The power – time curves then began to change in nature after c. 26 days of pre-incubation, with the emergence of a peak occurring 22-35 hours after substrate addition, increasing to 27-42 hours for the run after 36 days of pre-incubation

Observed values of  $tP_{\max}$  remained constant for the arable samples, while a continuous increase in  $tP_{\max}$  was observed for the grassland soils (Figure 5.6b). Three of the samples from the forest samples showed no distinct peaks (Figure 5.4), as such values for  $P_{\max}$  were observed between <1 h to > 40 h, without any noticeable change in the fundamental shape of the power – time curve. The majority (86%) of values for  $tP_{\max}$  from the forest samples occurred either <3 h or >38 h after substrate addition, without any apparent trend, resulting in the large standard error for this dataset (Figure 5.6b). This starkly contrasts the results for  $P_{\max}$  (Figure 5.6a) which were shown by a Fisher LSD test to be statistically identical between treatments for the forest samples with no significant time effect ( $p>0.05$ ). The LSD test also indicated that the  $P_{\max}$  values of the grassland samples were similar at 6 to 16 days and 4, 10 & 16 days after sample homogenisation, with the repeated measures ANOVA confirming that



there was a time effect on  $P_{max}$  ( $p < 0.05$ ). A time effect was also evident for values of  $P_{max}$  from the arable soils, with measurements at 2 & 4 days being identified as statistically distinct from those at 16 to 36 days after sample homogenisation ( $p < 0.05$ ).

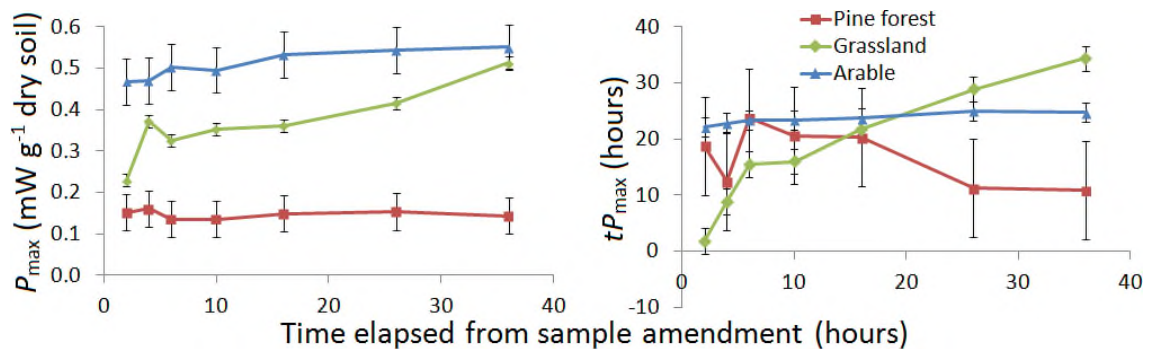


**Figure 5.6 Mean values for a) peak heat flow amplitude ( $P_{max}$ ) and b) time taken to reach peak heat flow amplitude ( $tP_{max}$ ) against pre-incubation time, with error bars denoting the pooled standard error for each series**

### 5.3.4 Enthalpy efficiency

Values for  $\eta_{eff}$  were constant throughout the experimental period with a few exceptions during the initial 6 days (grassland & arable) and at 36 days (grassland) after sample homogenisation (Figure 5.7). All observed values for  $\eta_{eff}$  from the forest samples were similar ( $p > 0.05$ ), whereas the arable samples produced similar results from 6 days after sample homogenisation ( $p > 0.05$ ). The grassland samples were statistically similar between 10 and 26 days after homogenisation ( $p > 0.05$ ).

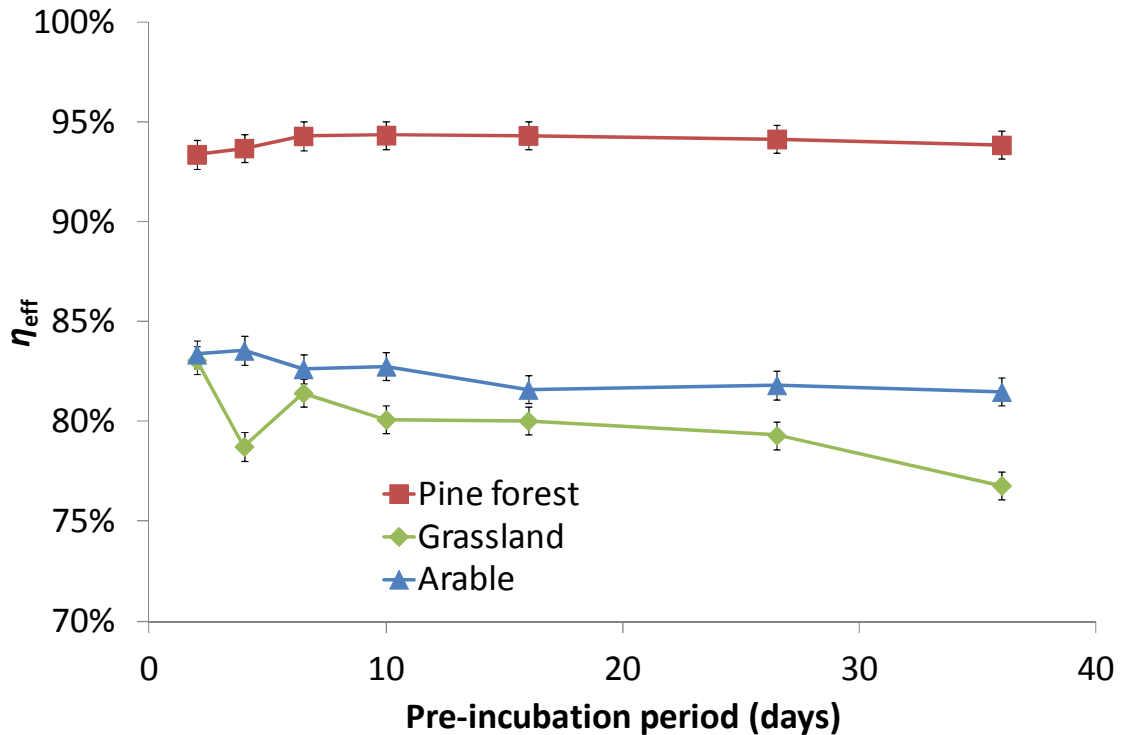


**Figure 5.7 Mean enthalpy efficiency ( $\eta_{\text{eff}}$ ) measured at 40 hours after substrate addition, with error bars denoting pooled standard error**

## 5.4 Discussion

The results from the PCA showed all three studied soils to be distinct from one another in terms of phenotypic structure, suggesting that all of the observed phenomena relate to a range of soil community contexts.

The C-mineralisation experiment undertaken to establish the concentration of glucose required to achieve microbial C-substrate saturation demonstrated that all the sampled soils were saturated by addition of between 2000 and 5000  $\mu\text{g}$  glucose-C  $\text{g}^{-1}$  dry soil. This corresponds to the findings of Anderson and Domsch (1978) who observed the microbial glucose-C saturation of two agricultural and one mixed forest soil at concentrations equivalent to c. 400,



1000 and 2600  $\mu\text{g glucose-C g}^{-1}$  soil solution respectively; and to West and Sparling (1986), who observed microbial respiratory saturation with glucose amendments of 1000 - 4000  $\mu\text{g glucose-C g}^{-1}$  dry soil. However, the C-saturation levels presented here were slightly higher than the findings of Anderson and Domsch (1975), who observed agricultural and forest soils reaching saturation at 200 - 400 and 400 - 1600  $\mu\text{g glucose-C g}^{-1}$  dry soil respectively, with forest litter saturating at 3200  $\mu\text{g glucose-C g}^{-1}$  dry mass.

Results indicated that C-saturation took place at c. 2000  $\mu\text{g glucose-C g}^{-1}$  dry soil in the grassland soil (Figure 5.2). The pretext of the SIHP index requires that the microbial community must be C-saturated throughout the entire length of the experiment, otherwise the results may be influenced by a fall in metabolic rate. Therefore it was decided to amend the calorimetry samples with 5000  $\mu\text{g glucose-C g}^{-1}$  dry soil, in order to guarantee glucose-C saturation of the microbial community throughout the whole period of isothermal calorimetric observation.

The unstable nature of the grassland power – time curve 2 days after sample homogenisation is likely due to disturbance during the sample homogenisation process creating aerobic conditions and making new sources of stored organic matter available (Müller-Stöver et al., 2012). The emergence of a peak in later runs may have been because of changes in microbial dynamics during consumption of the released organic matter. The arable and forest soils produced similar power – time curves at all instances throughout the experimental period, suggesting that ecosystems under low or structurally complex organic matter input regimes (e.g. needle litter) experience a less

severe reaction to disturbance, due to the lack of a sudden influx of labile organic matter. Therefore the window of opportunity for obtaining stable, reproducible signals may be longer in such soil ecosystems.

The highly variable results for  $tP_{\max}$  from the pine forest samples suggest that either the run time of 40 hours after substrate addition may have been insufficient to capture any distinct, stand alone peak, or that the microbial population was metabolising the glucose at maximum capacity without growing and that no stand alone peak could have been observed. Either way, drawing ecological conclusions by assessing the timing of absent peak amplitudes is redundant. However, this work aims to refine the methodology by assessing signal reproducibility; therefore the analysis is still meaningful in this instance as it allows for comparison with the seminal work of Núñez-Regueira et al. (1994). Due to the throughput limitations of analysing the samples with a single calorimeter, undertaking run times in excess of 40 hours would have proved impractical. Despite the large variations observed in  $tP_{\max}$ , the power – time curves in Figure 5.4 indicate that the forest soil produced signals of a highly replicable nature throughout the experimental period. This suggests that the observed trend was more due to the lack of a distinct peak in the signal from Field Replicates 1, 3 and 4.

The results for  $\eta_{\text{eff}}$  remained relatively stable for all soil types throughout the pre-incubation period, suggesting that although there may have been changes in the biomass during the experimental period, the efficiency of the microbial biomass was not affected.

## 5.5 Conclusions

The temporal changes in observed heat flows from the grassland soil add further weight to the argument that current methods of storing soils for a month or longer produce results no longer representative of the native microbial ecosystem that existed prior to sampling. As such, standard methods need to change in order to obtain representative observations from the microbial biomass *ex situ*.

The data indicate that results statistically similar in terms of peak amplitude could be obtained for all three sites from 6 to 16 days after sample homogenisation and that  $\eta_{\text{eff}}$  results were similar from 10 to 26 days. However, the results for  $tP_{\text{max}}$  were only able to demonstrate that there was a significant time effect on the grassland samples. As such it is recommended that in order to produce the most replicable and representative results, soil samples pre-incubated at 20°C should undergo isothermal microcalorimetric analysis 10 to 16 days after sample homogenisation.

## 6 Short term copper sulphate induced stress

*It is important to realise that in physics today, we have no knowledge of what energy is.*

– Richard Feynman

### 6.1 Introduction

Copper is an essential macronutrient necessary for a wide range of metabolic processes in both eukaryotes and prokaryotes, which occurs naturally in most soils (Lejon et al., 2007). However, when present at excessive concentrations it can begin to inhibit enzyme activity, hindering cellular metabolism. This can be highly problematic to land users, causing deteriorated plant health, reduced crop yields and can pose a threat to animal and human health (Cao & Hu, 2000; López Alonso et al., 2000; Loland & Singh, 2004).

Copper contamination can cause irreversible changes to the structure and function of the below ground microbial biomass. A substantial amount of research has been carried out into Cu contamination induced changes to both community structure and microbial activity. Changes in microbial community structure have been observed using phospholipid fatty acid (PLFA) profiling (Turpeinen et al., 2004; Frostegård et al., 1993), terminal restriction fragment length polymorphism (T-RFLP) (Tom-Petersen et al., 2003; Turpeinen et al., 2004), amplified ribosomal DNA restriction analysis (ARDRA) (Smit et al., 1997), polymerase chain reaction denaturing gradient gel electrophoresis (PCR-DGGE) profiling (Wakelin et al., 2010), *copA* DNA fingerprinting (Lejon et al., 2007), bacterial and fungal automated ribosomal intergenic spacer analysis

(ARISA) (Ranjard et al., 2006a; Ranjard et al., 2006b); while the influence of Cu contamination on microbial biomass and metabolic activity has been investigated by observations of ethylenediaminetetraacetic acid (EDTA) concentration (Ranjard et al., 2006a), chloroform labile biomass (Wang et al., 2007; Chander & Brookes, 1993; Ranjard et al., 2006a), litter decomposition rate (Berg et al., 1991), enzyme activity (Wang et al., 2007; Bogomolov et al., 1996) and substrate induced respiration measured by CO<sub>2</sub> mineralisation rate (Dumestre et al., 1999; Bogomolov et al., 1996) and heat production rate (Airoldi & Critter, 1996; Gruiz et al., 2010; Wang et al., 2010). As such, the impacts that Cu contamination has on the soil microbial community have been thoroughly investigated and are well understood (Bååth, 1989; Giller et al., 1998).

Recently isothermal microcalorimetry has been used to investigate the C-use dynamics of the soil microbial ecosystem, by investigating the thermodynamic response to fertilisation of the system with a C-substrate (Barros et al., 2011; Harris et al., 2012). As ecosystems, soil microbial communities will attempt to reach a steady state that minimises the production of entropy (Schneider & Kay, 1994). Any disruption to the ecosystem will cause the microbial community to counter or adapt to the changes in order to either re-establish the steady state or to reach a new steady state, resulting in the ecosystem being in a new or transient state that is not fully adapted to minimising entropy production (Addiscott, 1995).

A recent study by Harris et al. (2012) established a link between greater waste heat production rates and soil microbial communities subjected to long term

stress. In order to further develop understanding in this area, this study builds upon the in-depth understanding of the effects of Cu contamination of the soil microbial ecosystem, by investigating the relationship between waste heat production and recent lab contamination of soil samples with a Cu salt.

## **6.2 Materials and methods**

Due to stringent time limitations on using the isothermal microcalorimeter, a decision was made to run the experiment in two parts. The first aimed to assess the homogeneity of the sample, the reproducibility of power-time curves and how long an uncontaminated sample required to consume all the added glucose. The second phase of the experiment investigated the impact of Cu contamination on the thermal response of the soil microbial ecosystem. As samples from the two phases of the experiment were subjected to very different pre-incubation regimes, unfortunately they are not directly comparable and therefore may not contribute data to the same analysis (see Chapter 5). Nevertheless, relationships between the two datasets are presented and commented on.

### **6.2.1 Soils**

Soil samples were taken shortly after tillage from the long term fertility experiments site at Fors in Uppland, Sweden (60° 19' N, 17° 30' E), classified as a silty Udic Haploboroll soil (Calgren & Mattsson, 2001). Five field soil samples of c. 4 kg each were taken at the five points of a 'W' from a sampling area of c. 10 x 30 m located along the untreated field margin. The field samples were then placed into a single plastic bag and stored at 4°C prior to partial air

drying to adjust moisture content and subsequent mixing and passing through a 2 mm sieve to produce a single homogenised field sample. Samples from this were then taken for analysis of water holding capacity and gravimetric water content via the method of Rowell (1994).

### **6.2.2 Contamination of samples via Cu spiking**

For each of the 20 Cu contaminated mesocosms, sub samples of 500 g dry weight equivalent soil were taken from the single homogenised field sample and placed into a 1000 ml plastic pot. Lids were placed on top of the pots but not tightened, in order to allow gaseous exchange. Moisture losses were monitored by recording changes in weight and replenished by pipetting in DI water. The mesocosms were pre-incubated for 21 days at room temperature ( $20 \pm 2^\circ\text{C}$ ) to allow for recovery of the microbial ecosystem from the effects of sample homogenisation. Mesocosms were spiked with aqueous  $\text{CuSO}_4$  at concentrations of 1, 10, 100 & 1000 mg Cu  $\text{kg}^{-1}$  soil dry weight, with each Cu concentration having five replicate mesocosms. The mesocosms were then stored at room temperature ( $20 \pm 2^\circ\text{C}$ ) for a further 14 days prior to analysis, in order to allow the microbial ecosystems to react to, but not acclimatise to the  $\text{CuSO}_4$  contamination (Renella et al., 2002).

### **6.2.3 Microbial biomass-C**

Samples equivalent to 10 g dry weight each were taken from each mesocosm immediately prior to sample calorimetric analysis. All measurements were taken using the method of Vance et al. (1987) as outline in Chapter 3.3.

## 6.2.4 PLFA analysis

In order to assess the phenotypic differences between the microbial communities, soil samples were taken from each of the mesocosms prior to calorimetric analysis, freeze-dried then transported to Cranfield University, UK for phospholipid fatty acid (PLFA) analysis. This was undertaken via the method of (Frostegård et al., 1993b), outlined in Chapter 3.2.

Indicator fatty acids were used to calculate the fungal/bacterial ratio (Frostegård & Bååth, 1996), with the Mol % of 18:2 $\omega$ 6 as the fungal biomarker divided by the summed Mol % of *i*15:0, *ai*15:0, 15:0, *i*16:0, *i*17:0, *ai*17:0, *cyc*-17:0, and 19:0c as bacterial biomarkers (Frostegård & Bååth, 1996; Pawlett et al., 2013). The following molar ratios of specific PLFAs were used as indicators of ecological stress: Gram positive (*i*15:0, *ai*15:0, *i*16:0, *i*17:0 & *ai*17:0) / Gram negative (16:1 $\omega$ 7c, *cyc*-17:0, 18:1 $\omega$ 9c, 18:1 $\omega$ 7t & 19:0c) (Hueso et al., 2012; Feng & Simpson, 2009; Moore-Kucera & Dick, 2008; Frostegård et al., 2011), Saturated (14:0, 15:0, 16:0, 18:0 & 20:0) / Monounsaturated (16:1 $\omega$ 11t, 16:1 $\omega$ 7c, 16:1 $\omega$ 5, 17:1 $\omega$ 8c, 17:1 $\omega$ 8t, 17:1 $\omega$ 7, 18:1 $\omega$ 9c, 18:1 $\omega$ 7t, 18:1 $\omega$ 13 & 19:1 $\omega$ 6) (Moore-Kucera & Dick, 2008) and trans (17:1 $\omega$ 8t) / cis (17:1 $\omega$ 8c) (Frostegård et al., 2011).

## 6.2.5 pH

Triplicate samples from each mesocosm were air dried prior to pH analysis using an Orion 91-55 glass electrode pH meter (ExpotechUSA, Houston, TX, USA) via the method of Rowell (1994) outline in Chapter 3.5, calibrated with premixed buffers of pH 4.01 and 7.00.



## 6.2.6 Microcalorimetry

While the Cu contaminated samples were pre-incubating, eight samples of 3 g dry weight soil were taken from the remaining field sample after a storage period of 3 weeks at 5°C. These were placed into glass ampoules of 25 cm<sup>3</sup> volume, covered with micropore film in order to reduce moisture loss and pre-incubated for 24 hours at 20°C. All eight ampoules were capped with Admix syringes containing 100 µg D-glucose solution g<sup>-1</sup> dry soil, with a glucose C addition rate of 2 mg glucose C g<sup>-1</sup> dry soil. The samples were placed into the TAM Air isothermal microcalorimeter (TA Instruments, Sollentuna, Sweden) with thermostat set to 20.00°C and allowed c. 4 hours to reach thermal equilibrium with the instrument, before addition of the glucose solution via slow initial depression and repeated rapid flushing of the Admix syringes, in order to add the substrate drop wise. Values for heat flow rate, or power (*P*) and neat heat flow (*Q*) were recorded over a 130 hour period after glucose addition, the run was then terminated and the samples removed.

For the investigation of the Cu contaminated samples, each run consisted of 4 pairs of soil samples being examined, with each pair originating from the same mesocosm and consisting of one glucose amended sample and one water amended 'reference' sample. The order of the sample selection was strategically randomised to include one mesocosm from each of the four levels of Cu contamination in each run. The four 'reference samples' were amended with 100 µl deionised water g<sup>-1</sup> soil dry weight, bringing up the water holding capacity to 65%, while their four counterparts had 100 µl glucose solution g<sup>-1</sup> soil dry weight added, bringing the samples to 65% water holding capacity. The

glucose amended samples were supplied at a rate of 2 mg glucose C g<sup>-1</sup> soil dry weight. Samples of 3g dry weight soil were weighed into 25 cm<sup>3</sup> glass ampoules, which were then capped with either glucose solution or deionised water held in Admix syringes attached to the lid. The samples were then lowered into a TAM Air isothermal microcalorimeter (TA Instruments Sollentuna, Sweden), with thermostat set to 20.00°C, which was then sealed and allowed c. 4 hours to reach thermal equilibrium with the samples before substrate addition. Values for  $P$  and  $Q$  were recorded over runs of >100 hours after substrate addition and used to calculate  $\eta_{\text{eff}}$  and SIHP via Equations (12) and (13) respectively, via the method in Chapter 3.1. The calorimeter underwent a 30 minute signal baseline calibration both before and after each run.

### **6.2.7 Data analysis**

Statistical data analysis was carried out on all the collected datasets by use of a single factor one-way ANOVA, with a Fischer LSD test used to identify the presence of homogenous groups. The variance in phenotypic diversity of the samples' microbial communities was studied via constructing a principal component analysis (PCA) using the values of constituent molarity of known fatty acid methyl esters. Variance of principal component (PC) scores between treatments was assessed via a *post-hoc* one way ANOVA.

## 6.3 Results

### 6.3.1 Biomass & phenotypic profile

At two weeks after contamination there was an observed decrease in microbial biomass at the higher CuSO<sub>4</sub> concentration levels of 100 and 1000 mg Cu kg<sup>-1</sup> soil (Table 6.1). The F:B ratios were similar at 1, 100 and 1000 mg Cu kg<sup>-1</sup> soil, yet the PLFA results indicated a decrease in the proportion of fungal biomass at 10 mg Cu kg<sup>-1</sup> soil. These observations may indicate that the fungal biomass is vulnerable to CuSO<sub>4</sub> at a lower concentration, as a substantial reduction in the fungal biomass would only result in a slight reduction of the total chloroform labile biomass, as observed. This suggests that dieback of the fungal biomass occurs by 10 mg Cu kg<sup>-1</sup> soil, whereas bacterial dieback occurs between 10 and 100 mg Cu kg<sup>-1</sup> soil. The pH results showed that the samples contaminated with 1000 mg Cu kg<sup>-1</sup> were significantly ( $p < 0.001$ ) more acidic than the other samples. As such, soil acidification may have caused decreased F:B ratios for the most contaminated samples, although this is not evident from the F:B data in Table 6.1.

**Table 6.1 Mean chloroform labile biomass and fungal: bacterial PLFA index (F:B ratio) at each CuSO<sub>4</sub> contamination level**

CuSO <sub>4</sub> contamination (mg kg <sup>-1</sup> )	Mean biomass (µg C g <sup>-1</sup> soil)	Fungal: bacterial ratio	pH
1	345.15 (±17.9)	0.0561 (±0.0084)	7.28 (±0.035)
10	341.04(±17.8)	0.0376 (±0.0032)	7.25 (±0.027)
100	231.54(±22.5)	0.0682 (±0.0089)	7.21 (±0.019)
1000	92.97(±9.36)	0.0518 (±0.0037)	7.06 (±0.019)

The results from the PCA constructed from the PLFA analysis data (Figure 6.1a), showed that there was no phenotypic difference between mesocosms at different Cu concentration levels at the  $p = 0.10$  level. However, the PCA did indicate a variation in PC1 dependant on experimental batch number at the  $p = 0.005$  level, indicating that the period of time that the samples were kept in the refrigerator at 5°C had a greater effect on the phenotypic makeup, than the  $\text{CuSO}_4$  contamination concentration. A Fisher LSD test indicated that at the  $p = 0.05$  level, the phenotype of Batches 1-3 (Samples 1-12) were statistically homogeneous, while batches 4 and 5 were distinct from each other and batches 1-3. A second ANOVA analysis was run omitting samples from the final two batches (samples 13-20). This identified a  $\text{CuSO}_4$  contamination effect in PC3 at the  $p = 0.05$  level. However, a Fisher LSD test on the reduced dataset failed to establish a linier relationship between PC3 and  $\text{CuSO}_4$  concentration. The homogenous groups identified by the LSD test on PC3, are indicated by letters in Figure 6.1a, suggesting that concentration of the fungal biomarker 18:2 $\omega$ 6 was not unique in its variations between contamination levels. Additionally, the spread of individual PLFAs (Figure 6.1b) indicate that no particular PLFAs distinctively accounted for the variance observed, suggesting that all PLFA PLFA groups were effected by  $\text{CuSO}_4$  contamination.

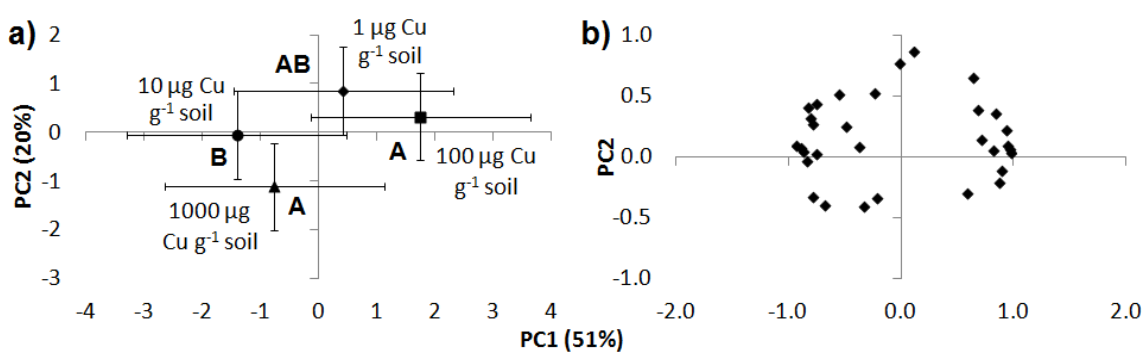


**Figure 6.1: Ordination of the first (PC1) and second (PC2) principal components constructed using the PLFA analysis data, showing; a) the phenotypic variance between Cu contamination levels, with bars denoting pooled standard error and letters indicating homogenous groups identified via an LSD test of the third (PC3) principal component, and b) individual loadings of all PLFAs identified in the analysis**

None of the PLFA bioindicators for stress, namely Gram positive / Gram negative, saturated / monounsaturated or trans / cis, showed a significant relation to CuSO<sub>4</sub> contamination levels nor either of the thermodynamic indices SIHP and  $\eta_{\text{eff}}$  when tested at the  $p=0.1$  level. However a significant stress effect was observed using the saturated / monounsaturated bioindicator against the sample batch indicator, indicating that batch number 4 (Samples 13-16) had proportionately higher levels of saturated PLFAs at a confidence level of  $p=0.01$ . This could indicate that the samples of batch number 4 may have undergone additional ecological stress compared to batches 1, 2, 3 & 5.

It is noteworthy that PLFA trans/cis values for environmental samples are typically  $<0.1$ , with levels significantly above this indicating environmental stress (Kaur et al., 2005). Although no clear relationship between the trans/cis ratio and CuSO<sub>4</sub> concentration or thermodynamic efficiency was observed, the values for this ratio were in the range of 0.19-1.00, with a mean of 0.51. This could indicate that all samples were under a high level of stress.

### **6.3.2 Power time curve of uncontaminated samples**

The power time curve produced by the non-lab contaminated soil samples took on an unexpected two peaked characteristic (Figure 6.2). The results showed remarkable similarities in curve characteristics, following a close grouping until

the secondary peak. After *c.* 70 hours the heat production rate of all the replicates fell rapidly, reaching a low heat output steady state, indicating that the samples had become anoxic (Vor et al., 2002). The point at which the samples became anoxic represented a  $Q_{total}$  value of between 100% and 122% of the  $\Delta H_c^0$  value for complete combustion with glucose of the 0.20 mmol oxygen available in the ampoule, supporting the observation by Vor et al. (2002) that 10-26% of the heat produced during the aerobic phase of excessive glucose amendment is attributable to anoxic or partially anoxic metabolism.

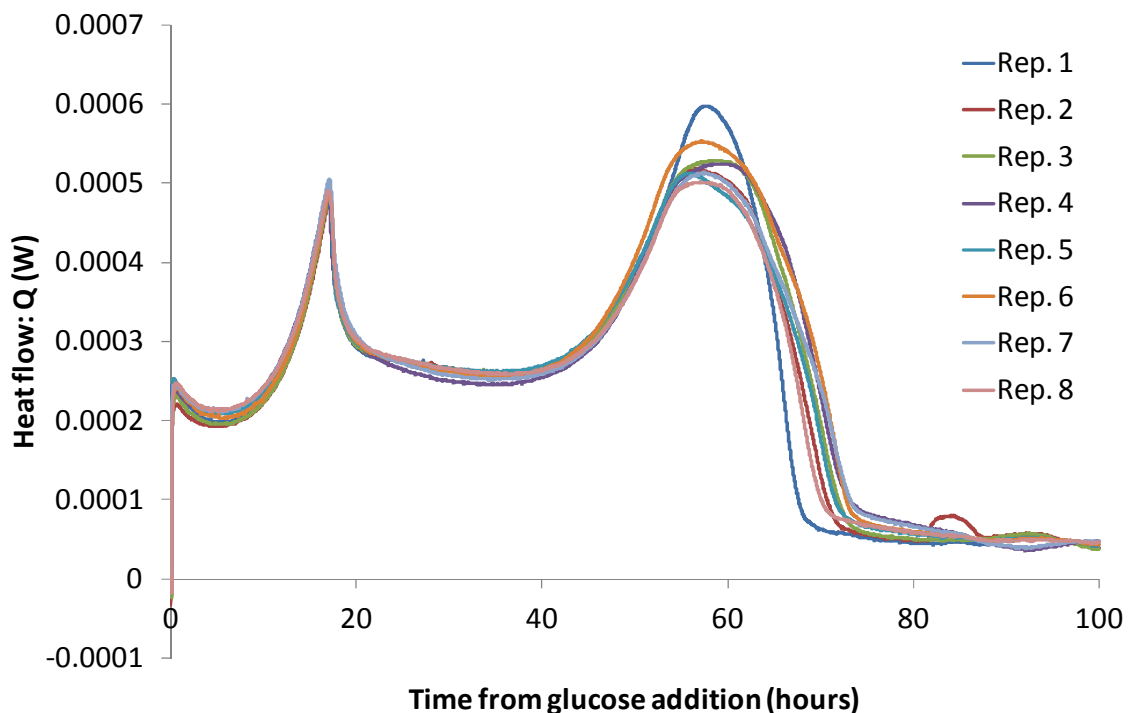


**Figure 6.2: Power/time curve recorded from 8 glucose amended samples of non-lab contaminated soil for 100 hours after substrate addition**

### 6.3.3 Power time curves of Cu contaminated samples

As with uncontaminated samples, the power – time curves of the  $CuSO_4$  contaminated samples produced a two peak signal. However, the secondary

peak appeared to be more influenced by  $\text{CuSO}_4$  levels than the primary peak (Figure 6.3). This is evidenced by the decline in amplitude of the secondary peak when Cu contamination is increased from 1 to 10  $\text{mg Cu kg}^{-1}$  soil, with the secondary peak becoming an indistinguishable shoulder at 100  $\text{mg Cu kg}^{-1}$  soil and completely vacant at 1000  $\text{mg Cu kg}^{-1}$  soil. A decrease in amplitude and a lengthening in the time taken to reach peak amplitude with increasing levels of Cu contamination can be observed in both the primary peak and, when present, the secondary peak (Figure 6.4). However this trend is only true of the contaminated samples, as the peak amplitudes of the uncontaminated samples were lesser than those contaminated with 1  $\text{mg Cu kg}^{-1}$  soil, despite time taken to reach peak amplitude remaining constant.

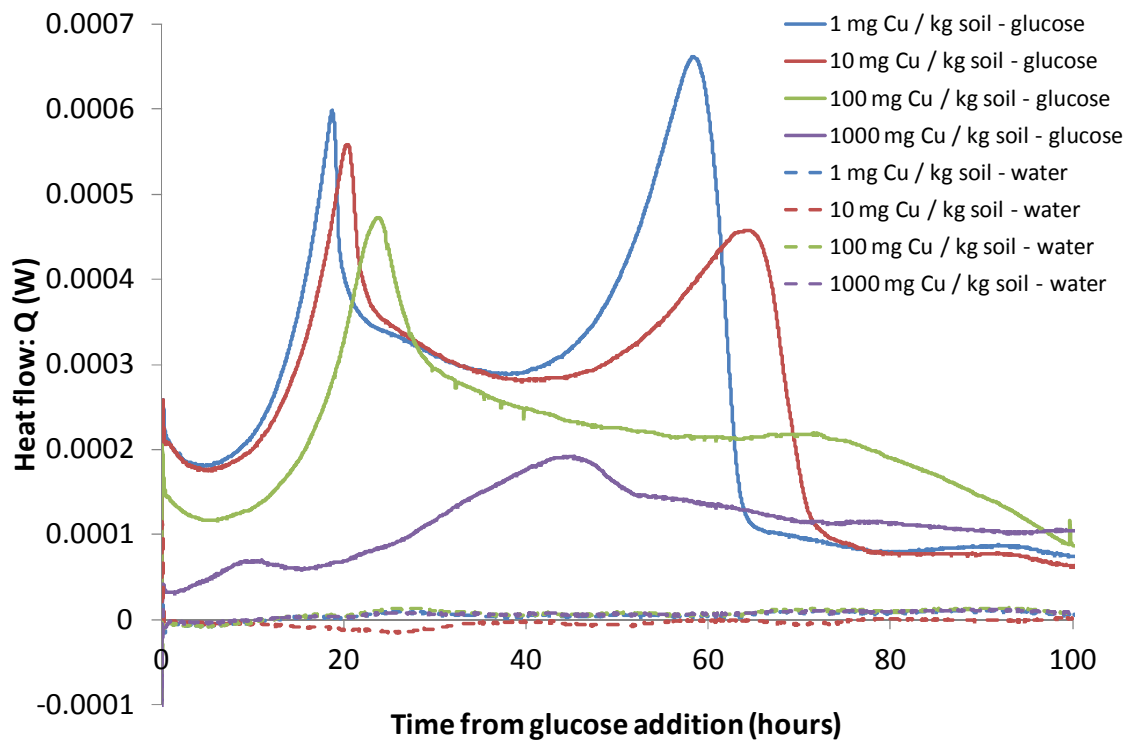


**Figure 6.3: Typical power/time curves for samples at each Cu contamination level, with both glucose and water amended samples from each replicate**

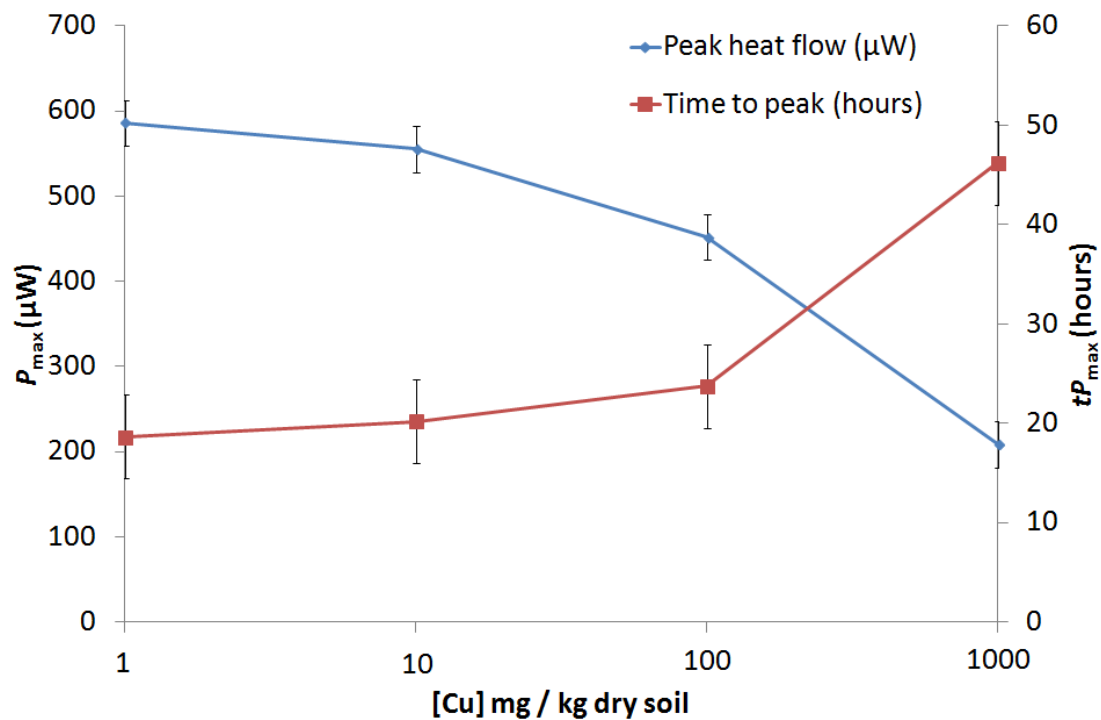


**Figure 6.4: Changes in primary peak amplitude and time taken to reach the primary peak due to increasing Cu contamination with bars denoting pooled standard error**

### 6.3.4 Enthalpy efficiency & SIHP

Values of  $\eta_{eff}$  were observed to increase along with Cu contamination (Figure 6.5), contrary to the expected observation. This was due to decreasing values of  $Q_{gluc}$  with increasing Cu contamination, possibly suggesting that the added glucose may have been incompletely metabolised. However when the same data was used to calculate SIHP (Figure 6.5) the values for waste heat production per unit biomass were shown to increase with Cu contamination, indicating that more waste heat was produced by the communities at higher Cu contamination levels. The observations for  $\eta_{eff}$  and SIHP would therefore appear to be contradictory, suggesting that further work may be required.



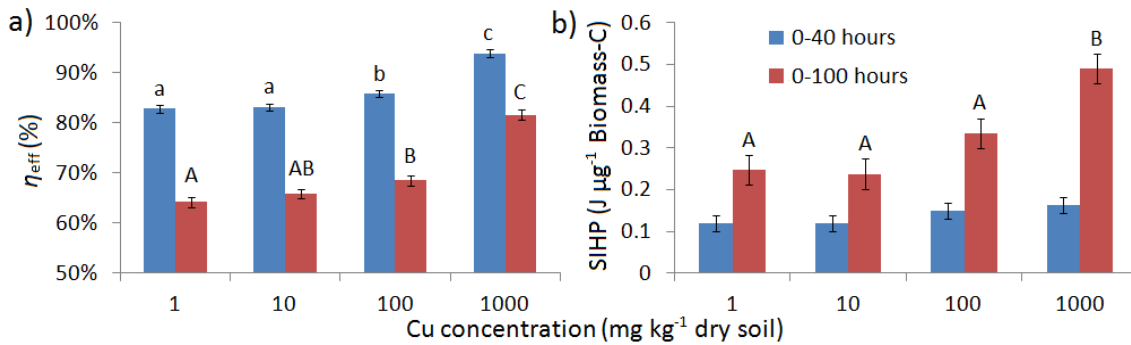


**Figure 6.5: Effect of Cu contamination on a)  $\eta_{eff}$  and b) SIHP with blue and red bars showing index values for 0-40 hours and 0-100 hours respectively, error bars denoting pooled standard error and letters indicating homogenous groups at the  $p = 0.05$  confidence level**

## 6.4 Discussion

In accordance with some ecosystem theory commentators (Schneider & Kay, 1994; Addiscott, 1995), the SIHP results indicated that the amount of waste heat produced per unit biomass increased with increasing  $\text{CuSO}_4$  contamination. This therefore establishes a link between short-term, lab-induced stress from metal contamination and reduced thermodynamic efficiency of the soil microbial community, supporting the findings of Harris et al. (2012) concerning long-term stress. However, due to the greater variance in chloroform labile biomass observations, the  $\eta_{eff}$  results did not correspond with the SIHP results as coherently as the results published in Harris et al. (2012), suggesting that a quantification of unmetabolised glucose may need to be integrated into the modified Batley Equation in future studies if there is a risk of this occurring.

It should be noted that the SIHP values increased at higher Cu concentrations, in accordance with decreasing biomass-C concentrations. It is most likely that these two observed trends were due to the detrimental effect of Cu on the metabolic processes of the microbial community, however it is also possible that

there is causation between the two trends. According to Jørgensen and Fath (2004) a reduction in the number of species present in the system will result in increased production of entropy, as dieback of certain organism groups will reduce the efficiency of energy and nutrient cycling, even if there is no loss of functionality. Conversely, a decrease in the thermodynamic efficiency of an individual organism may render it ecologically obsolete (Wilhelm et al., 2000), therefore contributing to a decrease in the total biomass concentration.

There was no apparent link between the phenotypic structure of the soil microbial community and the observed thermodynamic efficiency. The PLFA analysis showed that there were minor changes in the phenotypic structure of the soil samples at different levels of Cu contamination, notably the changes in the fungal biomarker 18:2 $\omega$ 6, however the communities were statistically indistinct. This could give an indication that the variations seen in both viable biomass and thermodynamic efficiency were due to the metabolic stress inflicted by the CuSO<sub>4</sub> contamination, rather than by fundamental changes to the biodiversity or functionality of the community. Other studies have reported changes in the microbial biomass, activity and genetic make-up of the soil microbial ecosystem due to short term contamination with metals which are not representative of long term contamination, indicating that two weeks after contamination samples had still not reached a new steady state adapted to Cu contamination (Renella et al., 2002; Ranjard et al., 2006b; Oorts et al., 2006). This short contamination period may be why none of the PLFA stress indicators showed a correlation to CuSO<sub>4</sub> concentrations, yet the trans/cis values indicated that all samples were stressed. Therefore it is likely that the changes

in PLFA profiling and thermodynamic efficiency were due to a soil ecosystem at differing levels of Cu-induced stress, rather than of several distinct steady-state ecosystems.

The double-peaked nature of the power-time curve is thought by the authors to be unique at the ecosystem level, as no mention of a similar occurrence could be found in the available literature. It is possible that the two peaks may represent a predominantly bacterial primary peak and a predominantly fungal secondary peak. This would go some way as to explaining why the secondary peak appears to undergo greater retardation due to Cu contamination, as the fungal biomass appeared to be susceptible to Cu at lower concentrations. However, many studies have found that metal contamination results in a microbial biomass shift towards fungal dominance (Wang et al., 2010b).

Other isothermal microcalorimetric studies (Wang et al., 2010b; Airoldi & Critter, 1996) also observed a reduction in peak amplitude due to contamination with  $\text{CuSO}_4$ , however the time at which the peak occurred appeared to remain consistent with the peak time of the uncontaminated samples, only increasing by c. 10% with contamination levels of up to  $1000 \text{ mg Cu kg}^{-1}$  soil. Previous isothermal microcalorimetric observations of lab-based soil contaminated with  $(\text{C}_2\text{H}_5\text{Hg})_2\text{HPO}_4$  and  $\text{H}_2\text{SeO}_4$  showed similar trends of decreased peak amplitudes and increased time taken to peak (Kawabata et al., 1983), trends that may reflect decreased population growth capacity and decreased population growth rate respectively within the soil microbial ecosystem. However, the observed increase in peak amplitude between uncontaminated soil and the  $1 \text{ mg Cu kg}^{-1}$  soil samples indicates that a small amount of  $\text{CuSO}_4$

may be able to slightly increase the microbial population carrying capacity of this soil and as such, that the soil may be depleted in either Cu or S, both of which are essential macronutrients. An increase in metabolic output due to low concentration  $\text{CuSO}_4$  has been reported previously in other experiments (Gruiz et al., 2010), indicating that  $\text{CuSO}_4$  may in fact act as a fertiliser when added at low concentrations.

## 6.5 Conclusions

Short term environmental stress due to  $\text{CuSO}_4$  contamination was indeed shown to increase the waste heat production of the soil microbial community, in accordance with the ideas of Addiscott (1995) and supporting the findings of Harris et al. (2012). The results of the enthalpy efficiency ratio ( $\eta_{eff}$ ) did not correspond to the results for SIHP, suggesting that the former analysis may need to account for unmetabolised substrate in some instances. Chloroform labile microbial biomass was observed to decrease with Cu contamination, with the fungal biomass appearing to be more susceptible at lower Cu concentrations, possibly contributing to the postulated 'fungal' secondary peak experiencing a greater level of Cu-contamination induced retardation than the postulated 'bacterial' primary peak. Additionally there was evidence that low levels of  $\text{CuSO}_4$  contamination may result in a fertilisation effect on the microbial community.

## 7 Ecosystem maturity

*The law that entropy always increases holds, I think, the supreme position among the laws of Nature. If someone points out to you that your pet theory of the universe is in disagreement with Maxwell's equations — then so much the worse for Maxwell's equations. If it is found to be contradicted by observation — well, these experimentalists do bungle things sometimes. But if your theory is found to be against the second law of thermodynamics I can give you no hope; there is nothing for it but to collapse in deepest humiliation.*

– Sir Arthur Stanley Eddington

### 7.1 Introduction

All living systems take low entropy energy and degrade it into higher entropy energy in order to sustain or add to their biomass or complexity (Addiscott, 2010; Lin, 2011). Odum, (1969) theorised that as ecosystems develop, they will transform from a state of 'high entropy' to one of 'low entropy', in order to produce and support as large and complex an organic structure as possible. By decreasing the waste energy production per unit biomass, ecosystems are able to invest more useful energy into biomass production (Schneider & Kay, 1994), allowing for a greater total biomass and a greater level of thermodynamic disequilibrium (See Chapter 1). As such, we should be able to observe a reduction in metabolic losses as an ecosystem develops (Insam & Haselwandter, 1989).

Due to the large timescales involved in ecosystem development, it is preferable to investigate areas that substitute 'space' for 'time'(Jenny, 1941; Pickett, 1989), where similar sites have undergone a similar perturbation at various points in time. Jenny (1941) termed such sites chronosequences, with areas of both natural (Merilä et al., 2002; Laliberté et al., 2012; DeLuca et al., 2002) and anthropogenic (Šourková et al., 2005; Baer et al., 2002) perturbations being used in subsequent studies. These typically follow a trend of rapid ecological succession, eventually followed by a more protracted period of retrogression (Wardle et al., 2004; Selmants & Hart, 2010).

Retreating glaciers have provided ecologists with a naturally perturbed chronosequence that allows investigation of freshly established ecosystems. In Europe the 16<sup>th</sup> to mid 19<sup>th</sup> century was marked by the expansion of mountain glaciers, known as the Little Ice Age, which peaked in c. 1850 (Mann, 2002). Since then, glaciers have retreated with a few short periods of re-advance, producing Vorfelds with moraines of varying surface age. Recently deglaciaded chronosequences have been studied in terms of vegetation development (Chapin et al., 1994; Burga, 1999), soil formation (Egli et al., 2006; He & Tang, 2008; Dümig et al., 2011) and development of the soil microbial biomass (Sigler et al., 2002; Tscherko et al., 2003; Knelman et al., 2012).

The use of chronosequences to assess how ecosystem development affects the thermodynamic efficiency of the below ground biomass was first attempted by Insam & Haselwandter (1989), who observed a decrease in the metabolic quotient ( $q\text{CO}_2$ ), a measurement of C-substrate induced  $\text{CO}_2$  produced per unit microbial biomass, along glacial Vorfelds in Austria and Canada. Wardle (1993)

built on this early work, observing a decrease in  $q\text{CO}_2$  between successional stages of forest and scrubland ecosystems in New Zealand. Wardle & Ghani (1995) found that  $q\text{CO}_2$  decreased over the first 250 years of primary succession on the Franz Josef Glacier chronosequence, before rising again in later phases. However, Wardle & Ghani (1995) went on to question the usefulness of the index, as it was found to respond unpredictably, often reacting more to ecosystem stress, rather than perturbations. Ohtonen et al. (1999) observed a decrease in  $q\text{CO}_2$  over the Lyman Glacier Vorfeld in Washington State, USA, while Merilä et al. (2002) found no conclusive trend in  $q\text{CO}_2$  on the Bothnian isostatic uplift in Western Finland.

To the author's knowledge there has been no use of calorimetric analysis to study chronosequence soils, however in a study on ecosystem disturbance, Barros et al. (2000) observed a higher rate of heat production per unit of added glucose-C in Amazonian soils that had remained as primary forest, with lower heat production (interpreted as greater efficiency) in neighbouring soils that had been converted to agricultural plantations. However, the observed trends may be due to fundamental issues with the methodology common to the issues in calculating  $\eta_{eff}$ . This is discussed in more detail in Chapter 8.

This chapter aims to use direct calorimetry of the soil microbial biomass in response to C-substrate addition, in order to test the null hypothesis that ecosystems become more thermodynamic efficient as they mature.

## 7.2 Materials and methods

### 7.2.1 Soil sampling

Soils samples were taken from a well studied chronosequence of glacial moraines along the Morteratsch Glacier Vorfeld, near St. Moritz, Switzerland in June of 2012 (Figure 7.1). The glacier Vorfeld lies in a almost straight, U-shaped valley with a North-South orientation (Figure 7.1). The glacial system lies in an area of relatively homogeneous geological makeup, consisting almost exclusively of granite and gneissic material (Egli et al., 2006). The valley has a current mean annual air temperature of *c.* +0.5°C and a mean annual precipitation of 1000-1300 mm (Egli et al., 2006).

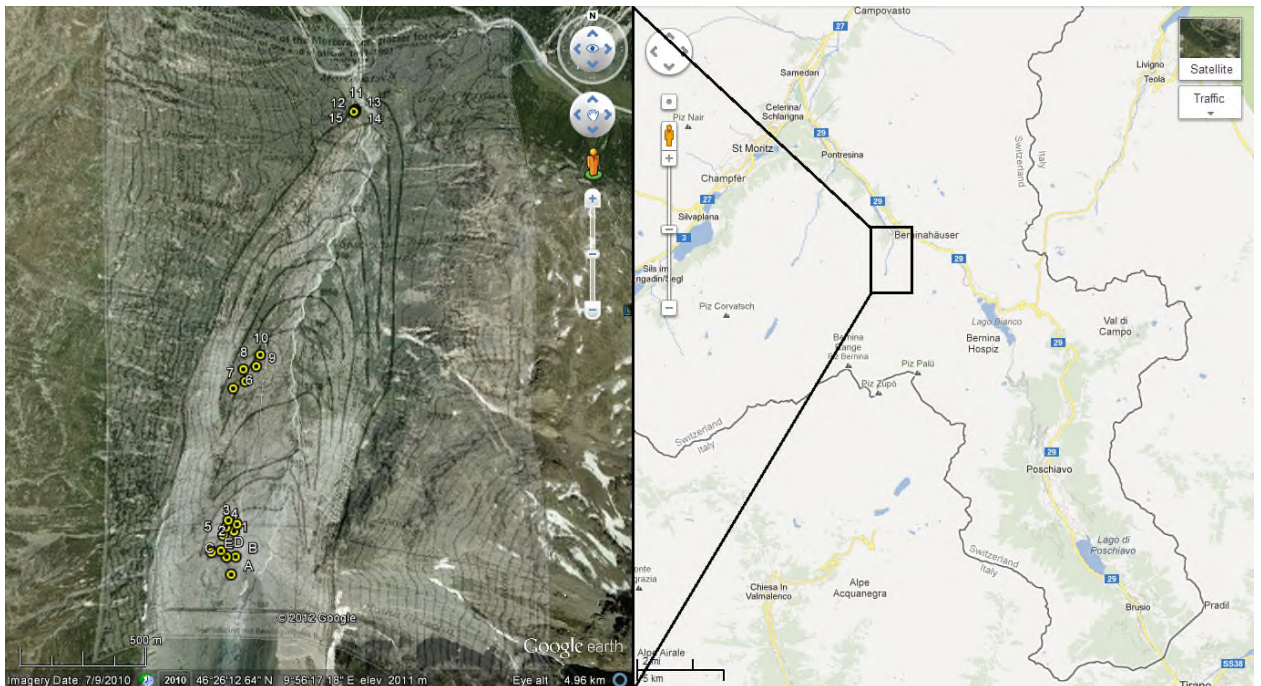


**Figure 7.1** Location of the sample site in SE Switzerland (Google Inc., 2011), showing approximate isochrones of equal surface age (from Burga, 1999) and the location of sampling sites (A-E & 1-15).



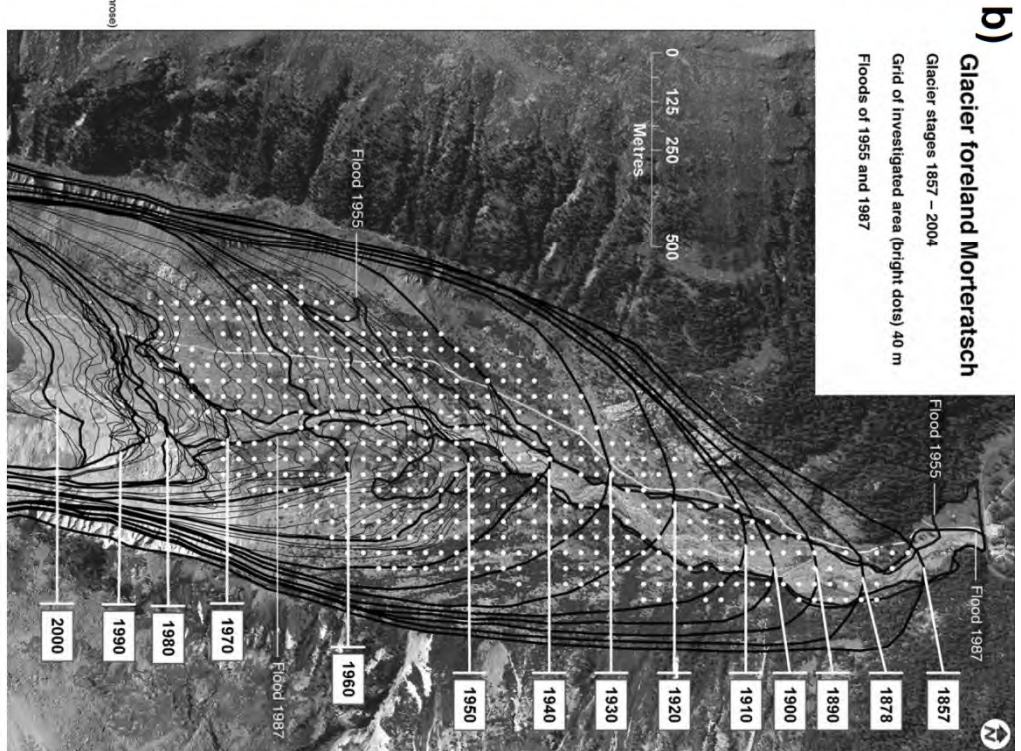
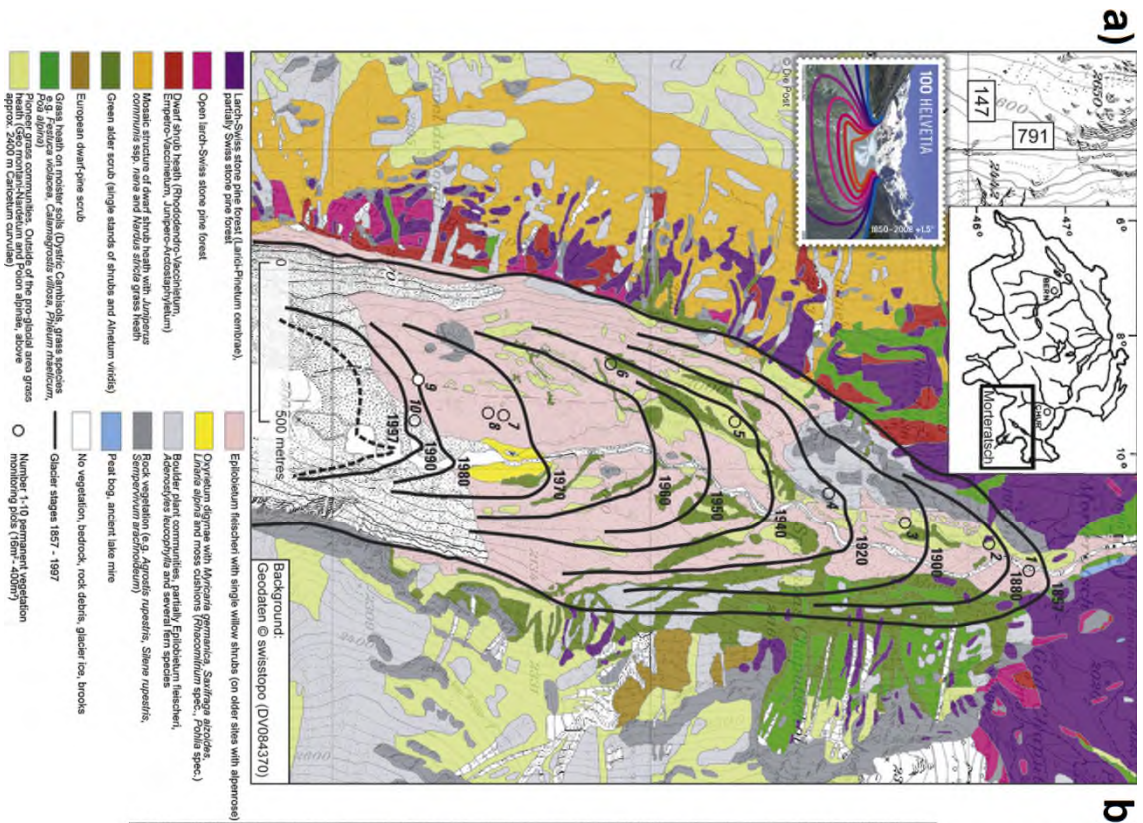


**Figure 7.2 Map of the Morteratsch Glacier Vorfeld, showing a) dominant vegetation types, and b) Isochrones showing retreat data (Burga et al., 2010)**

Samples were initially taken from 3 sampling areas (sample sites 1-15 in Figure 7.1) along moraines deposited in 2004-5, 1960-2 and 1857, representing surface ages of *c.* 8, *c.* 51 and *c.* 155 years respectively and distinct successional habitats. However, after the above ground ecosystem along the 2004-5 moraines was judged to be too well developed to represent an initial successional stage, an additional sample site was taken along the active moraine for the summer of 2012 (sample Sites A-E in Figure 7.1).

At each site an area of equal surface age was identified using data from publications of previous field studies along the Morteratsch Vorfeld along with retreat data published by the Swiss Glacier monitoring Network (<http://glaciology.ethz.ch/swiss-glaciers/>) and ground markers identifying the time that the glacier snout was at that location. After an area had been identified, its boundaries were plotted using a handheld GPS device (Garmin: Olathe, KS, USA). The GPS coordinates were fed into an Excel spreadsheet and a polygon of the sampling area produced. Excel's inbuilt random number generator function was then used to produce a grid coordinate within the North-South and East-West range of the sampling area. The first randomly-generated grid coordinate to fall within the sampling area polygon was then selected as the first sampling point at that site, with the remaining four sampling positions chosen by drawing a 'W' of best fit from this first point. This is shown in detail for the 1960-2 sampling site in Figure 7.3.



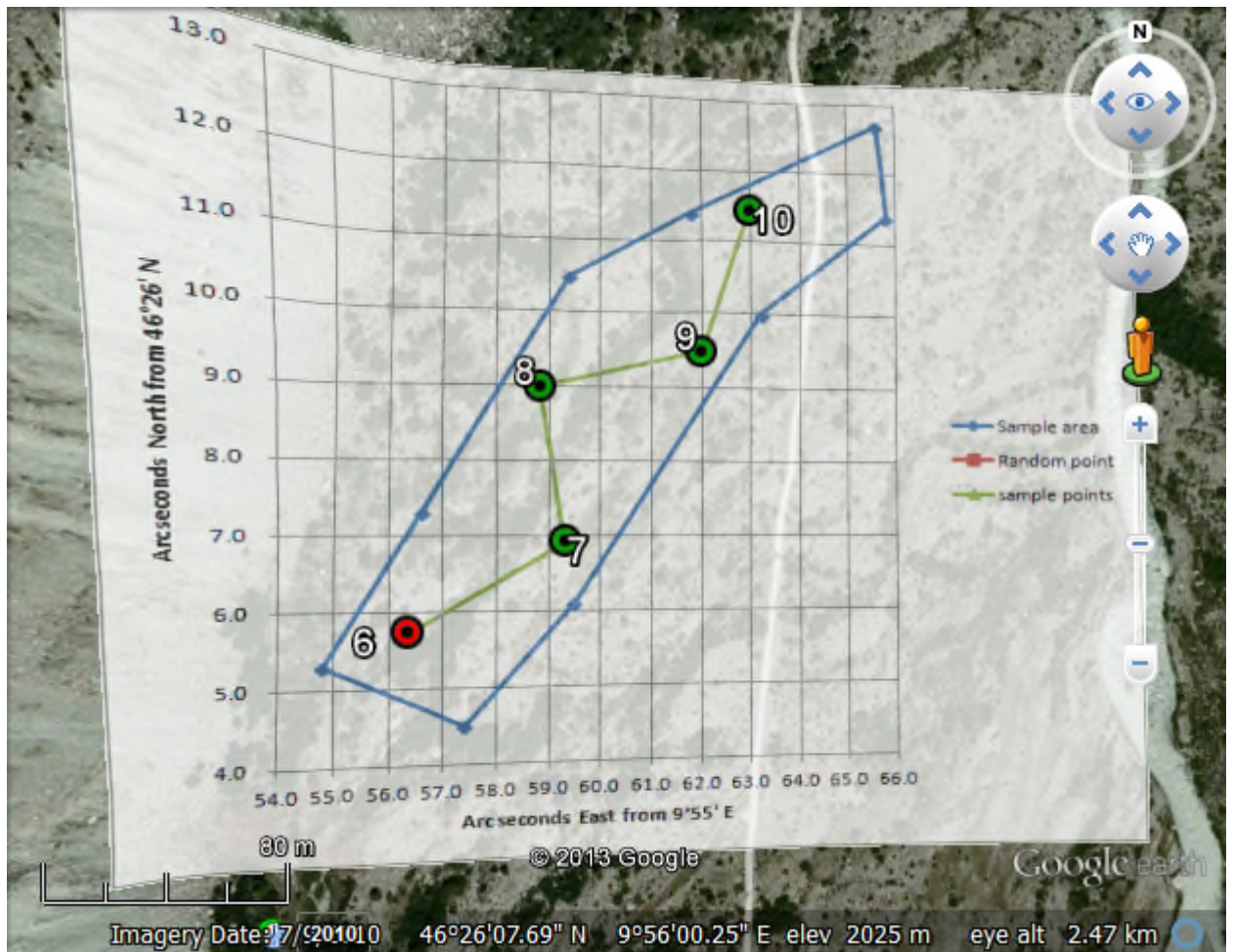


**Figure 7.3** Sampling polygon for the 1960-2 area, generated using GPS coordinates plotted into an MS Excel x-y plot, overlaid onto the Google Earth 3D terrain surface (Google Inc., 2011). Sampling positions are shown using Google Earth waypoints, with the red point (№6) identifying the randomly generated sampling position, with green points (№7-10) drawn from it as a ‘W’ of best fit.

At each site the exact location of soil sampling was chosen by throwing of a woollen jumper, backwards over the shoulder, in order to avoid sampling bias. An assessment of the vegetation was made at each sampling position, by marking a quadrant measuring 1.5 m by 1.5 m, centred on the sampling position, and recording all species of non-graminoid, non-bryophyta plants (i.e. excluding grasses & mosses). A record was also made of all trees and shrubs within a 5 m radius of the sampling position. Surface (7 cm) soil samples of c.

500 g were taken and placed into polyethylene bags; these were kept cool using freezer packs for transport back to the labs in Uppsala, Sweden.

### **7.2.2 Sample storage, homogenisation and pre-incubation**

Upon arrival at the labs in Uppsala, the samples were grouped into 5 batches of 4 samples each, selected using a random number generator. The selection process was arranged so that each batch would contain one sample from each of the 4 surface age bands, in order to minimise storage effects. Samples were homogenised 10 days prior to calorimetric analysis by passing through a 2 mm sieve before being mixed by hand. The first batch was homogenised the day after arrival, with homogenisation of subsequent batches staggered at 5 day intervals.

Prior to homogenisation samples were kept refrigerated at 4°C in the polythene sampling bags. After homogenisation samples were placed into pre-weighed 500 ml glass jars and pre-incubated at 20°C for 10 days prior to calorimetric analysis. Immediately after homogenisation sub-samples of soil were taken for determination of WHC & GWC via the method outline in Chapter 3.6 and 3.7.

The sample jars were weighed and, if needed, wetted or allowed to partially air dry in order to reach a GWC equivalent of at least 35% WHC, which would result in a GWC of c. 65% WHC after water or glucose solution additions calorimetric analysis. The jars were aerated every few days and the GWC topped up if needed. In order not to disturb the calorimetric signal, no water amendments were made during the 24 hours prior to sample analysis.

### **7.2.3 Calorimetric analysis**

Samples of 3 g dry soil weight equivalent were placed into glass ampoules for calorimetric analysis, as outlined in Chapter 3.1.

Two values for  $Q_{total}$  were taken for the calculation of the enthalpy efficiency ( $\eta_{eff}$ ) via Equation (12) in Chapter 3.1 and the substrate induced heat production (SIHP) using Equation (13) in Chapter 3.1:  $Q_{total}$  for T=0-40h to allow comparison with previous experiments and  $Q_{total}$  for T=0-100h, to ensure maximum glucose consumption.

Upon completion of the calorimetric analysis, the soil samples were freeze dried for use in the glucose oxidase assay

### **7.2.4 Biomass**

Samples for chloroform labile biomass were taken from the glass incubation jars c. 1 hour after removal of the calorimetric samples. Biomass was then determined using the chloroform fumigation-extraction method outlined in Chapter 3.3.

### **7.2.5 PLFA analysis**

Samples for PLFA analysis were taken simultaneously to the chloroform labile biomass samples and freeze dried for transport to the labs at Cranfield University, UK. PLFA analysis was then undertaken and a PCA constructed using the method outlined in Chapter 3.2. F:B ratios were calculated using the fungal biomarker 18:2 $\omega$ 6,9 and the bacterial biomarkers 15:0i, 15:0ai, 15:0, 16:0i, 17:0i, ai17:0, 17:0c and 19:0c (Frostegård & Bååth, 1996).

## 7.2.6 End-point glucose determination

Upon the completion of calorimetric runs, the ampoules were removed from the calorimeter and the contents flash frozen to  $-20^{\circ}\text{C}$ . The residual glucose content of the calorimetry samples was measured using a glucose oxidase assay kit (Sigma-Aldrich Inc., St. Louis, Missouri, USA), employing a methodology adapted from the technical bulletin supplied with the assay reagents (Glucose (GO) Assay Kit,).

The glass ampoules containing the soil samples (originally 3 g dry weight) were emptied into plastic centrifugation tubes of known mass, so that any loss of soil mass during transferral could be measured. The samples were suspended in 12 ml  $0.25\text{ M K}_2\text{SO}_4$  and laterally shaken at  $300\text{ oscillations min}^{-1}$  for 30 min, before being centrifuged at 2000 rpm for 2 min. The supernatant extract was filtered through a Whatman No. 4 filter paper and collected in a clean plastic bottle. The filtrate could then be diluted with additional  $0.25\text{ M K}_2\text{SO}_4$  if needed, with dilutions of 50%, 20%, 10%, and 5% being employed.

The assay reagent was prepared by mixing 500 units of glucose oxidase (*Aspergillus niger*), 100 purpurogallin units of peroxidase (horseradish), 4 mg o-dianisidine dihydrochloride and buffer salts in 40 ml of deionised water, as per the assay kit instructions.

A sample of 1 ml filtrate or diluted filtrate was amended with 2 ml of the assay reagent and placed in a water bath at  $37^{\circ}\text{C}$  away from the presence of light. After exactly 30 min the reaction was quenched by addition of 2 ml  $12\text{ N H}_2\text{SO}_4$ , before measurement of light absorbance at 540 nm wavelength. Absorbance

values were calibrated against a reagent blank containing 1 ml 0.25 M  $K_2SO_4$  with 2 ml of the assay reagent and 2 ml  $H_2SO_4$ .

Values for glucose concentration were determined by measuring absorbance at 540 nm of pre-determined glucose concentrations ranging from 0 to 0.08 mg glucose in 1 ml 0.25 M  $K_2SO_4$  and producing a simple regression of the results. This determined that the amount of glucose in the 1 ml sample =  $0.0626 \Delta A_{540}$  of the final product.

### **7.2.7 Total C and N**

Finely ground samples of c. 80 mg air dried soil were prepared for elemental analysis via the method outlined in Chapter 3.4, however several of the samples registered as below the detectable limit. These samples were then re-run with a sample of c. 500 mg air dried soil.

### **7.2.8 pH**

Samples of 10 g air dried soil were used for assessment of pH via the method outline in Chapter 3.5.

### **7.2.9 Statistical analysis**

For all results excluding the F:B and thermodynamic data comparison in Section 7.3.7, Statistical analysis was undertaken via a one-way ANOVA using site age as a categorical predictor, with samples grouped under a single approximate surface age at each sample site. Homogenous groups were identified via a *post-hoc* Fisher LSD test at the  $p=0.05$  significance level.



In Section 7.3.7, correlations between F:B ratios and thermodynamic indices were identified and quantified via a simple linear regression.

## 7.3 Results

### 7.3.1 Generic sample site and soil parameters

In terms of above ground vegetation, the sampling areas fell into 4 distinct ecological categories: vegetation free, pioneer communities, meadow/scrub and alpine forest (see Figure 7.4).

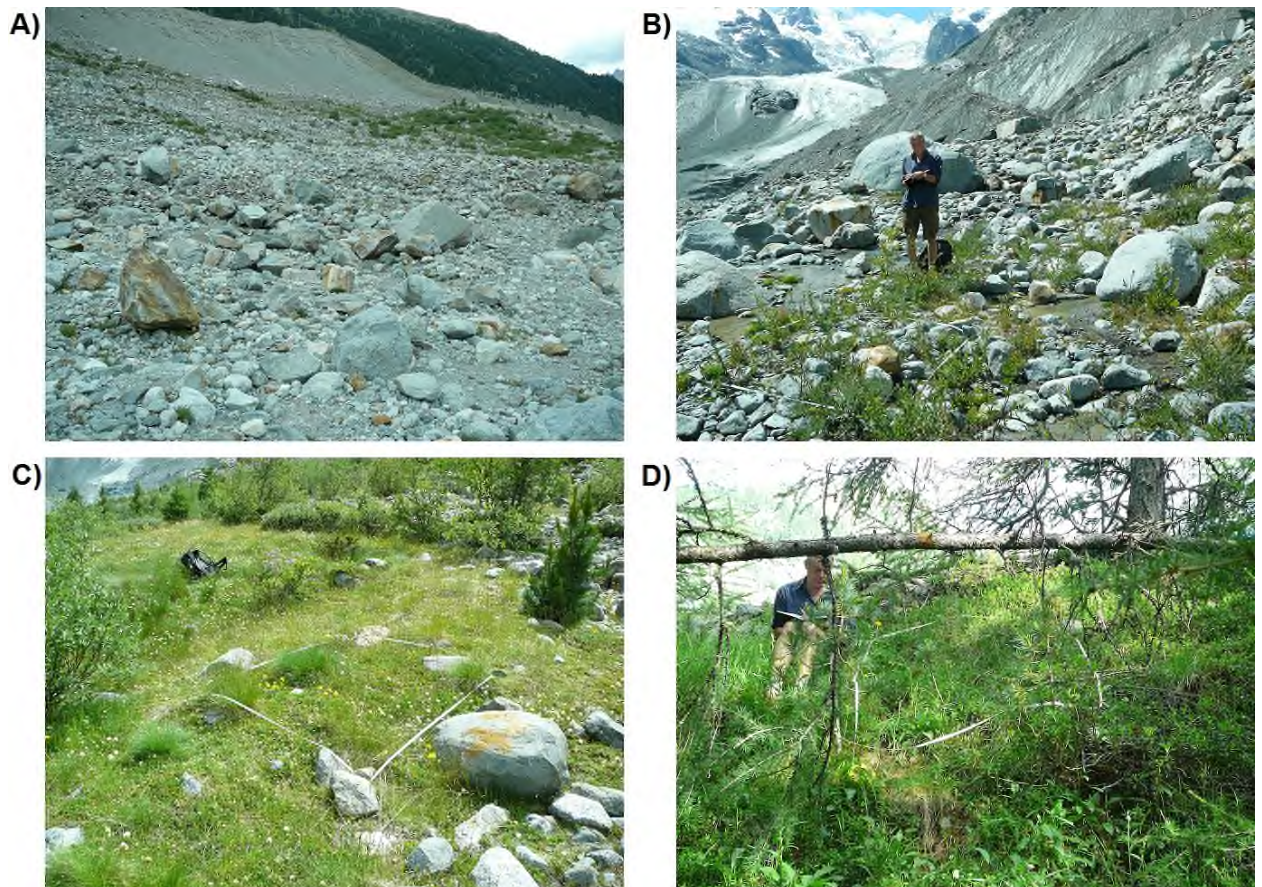


**Figure 7.4 Typical above ground ecosystem in each of the sampling areas, showing surface ages of: A) 0 years, B) 8 years, C) 51 years and D) 155 years.**



**Table 7.1 Approximate surface age, dominant vegetation type and soil characteristics of each sampling site**

Sample ID	Age: Ground markers & Burga (1999)†	Age: Burga et al. (2010)‡	Dominant vegetation type	Total soil C (mg g <sup>-1</sup> )	Total soil N (mg g <sup>-1</sup> )	C:N	WHC (g H <sub>2</sub> O g <sup>-1</sup> dry soil)	Soil pH	Biomass C (mg C g <sup>-1</sup> dry soil)
2012 a	<1	<9	Vegetation free	0.27	0.02	15.2	0.19	7.44	4.0
2012 b	1	<9	Vegetation free	0.27	0.03	9.1	0.19	6.63	1.9
2012 c	<1	<9	Vegetation free	0.23	0.02	10.2	0.21	6.64	20.7
2012 d	<1	<9	Vegetation free	0.27	0.02	11.3	0.17	6.35	8.6
2012 e	<1	<9	Vegetation free	0.23	0.03	8.9	0.13	6.51	-0.5
<b>mean</b>	<b>&lt;1</b>	<b>&lt;9</b>	<b>Vegetation free</b>	<b>0.25</b>	<b>0.02</b>	<b>10.9</b>	<b>0.18</b>	<b>6.72</b>	<b>6.9</b>
2004 a	10	11	Pioneer communities	0.74	0.07	11.0	0.22	6.42	35.2
2004 b	10	11	Pioneer communities	4.32	0.33	13.1	0.28	6.62	87.0
2004 c	8	10	Pioneer communities	1.33	0.05	29.6	0.22	6.57	54.0
2004 d	8	9	Pioneer communities	0.41	0.04	10.0	0.19	5.88	12.3
2004 e	7	<9	Pioneer communities	0.70	0.01	48.6	0.26	6.73	43.5
<b>mean</b>	<b>8.6</b>	<b>9.8</b>	<b>Pioneer communities</b>	<b>1.50</b>	<b>0.10</b>	<b>22.4</b>	<b>0.23</b>	<b>6.44</b>	<b>46.4</b>
1961 a	53	63	Pioneer communities	8.85	0.58	15.2	0.34	5.83	272.2
1961 b	51	61	Grassland	7.64	0.64	12.0	0.32	6.18	156.5
1961 c	53	63	Grassland	3.28	0.21	15.6	0.25	6.32	74.6
1961 d	51	61	Pioneer/Grassland	2.11	0.12	17.4	0.19	6.28	52.5
1961 e	51	62*	Grassland/Scrub	5.35	0.35	15.4	0.33	6.46	84.3
<b>mean</b>	<b>51.4</b>	<b>62</b>	<b>Pioneer/Grassland</b>	<b>5.45</b>	<b>0.38</b>	<b>15.1</b>	<b>0.29</b>	<b>6.21</b>	<b>128.0</b>
1857 a	155	155	Larch/pine forest	28.07	1.59	17.6	0.57	4.23	374.9
1857 b	155	155	Larch/pine forest	9.95	0.55	18.0	0.47	5.27	150.8
1857 c	155	155	Larch/pine forest	15.43	0.99	15.6	0.48	5.38	250.5
1857 d	155	155	Larch/pine forest	34.56	1.73	20.0	0.63	3.94	805.0
1857 e	155	155	Larch/pine forest	17.42	0.99	17.5	0.51	4.35	435.3
<b>mean</b>	<b>155</b>	<b>155</b>	<b>Larch/pine forest</b>	<b>21.09</b>	<b>1.17</b>	<b>17.8</b>	<b>0.53</b>	<b>4.63</b>	<b>403.3</b>

### Notes for Table 7.1:

\*According to Burga et al. (2010) the moraine was originally deposited in 1950, but the site was affected by a flash flood in 1955

†Burga (1999) only shows approximate location of isochrones for 1857 – 1997

‡Burga et al. (2010) only shows isochrones for 1857 – 2003

Values for C and N both showed a significant ( $p < 0.05$ ) age effect, with increases by several orders of magnitude over the course of the succession. However, the C:N ratio peaks after 8 years, with only the 0 years and 8 years sites found to be significantly ( $p < 0.05$ ) distinct from each other (see Table 7.1).

The WHC of the soil samples increased over the course of the successional gradient (see Table 7.1) with a highly significant age effect ( $p < 0.001$ ).

pH showed a significant ( $p < 0.01$ ) age effect, with the 151 year site being identified as statistically distinct from the earlier successional stages.

The biomass C results showed a significant ( $p < 0.05$ ) age effect with the 151 year site being identified as statistically distinct from the earlier successional stages.

The biomass C result for one of the samples returned a negative result. As such this sample was omitted from the SIHP index calculations and data analysis.

### 7.3.2 PLFA analysis and PCA

The PCA conducted used the PLFA results identified three homogenous groups ( $p < 0.05$ ) along PC1, with no statistically significant ( $p > 0.1$ ) variance identified along PC2. The homogenous groups identified along PC1, grouped the 51

years and 155 years sites as having similar phenotypes, with both the 8 years and 0 years sites identified as having a distinct phenotype from all other sites (Figure 7.5). This suggests that changes in the microbial phenotype are more pronounced during the earlier stages of succession.

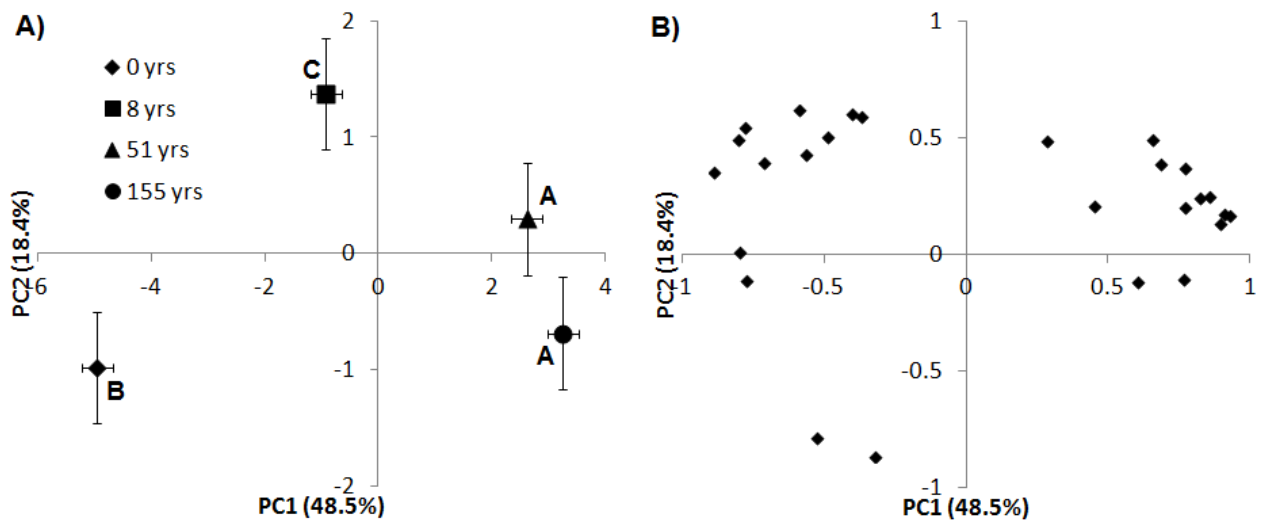


**Figure 7.5 Ordination of first (PC1) and second (PC2) principal components from the PLFA data, showing: A) phenotypic differences between the four sample sites, with bars denoting pooled standard error and letters denoting homogenous groups identified at the  $p=0.05$  level, and B) individual loading of all PLFAs identified by the PCA.**

The loadings of the individual PLFAs used in the PCA indicated that no single PLFA accounted for a great proportion of the observed variance and as such, the variations observed in the phenotype were broad-spectrum in nature.

### 7.3.3 Fungal: bacterial ratios

The ratios of the fungal and bacterial biomarkers identified homogenous groups that were distinct from each other ( $p<0.05$ ), however an age effect was

not clear, with F:B ratios peaking at 8 years and reaching a minimum at 155 years after de-glaciation.

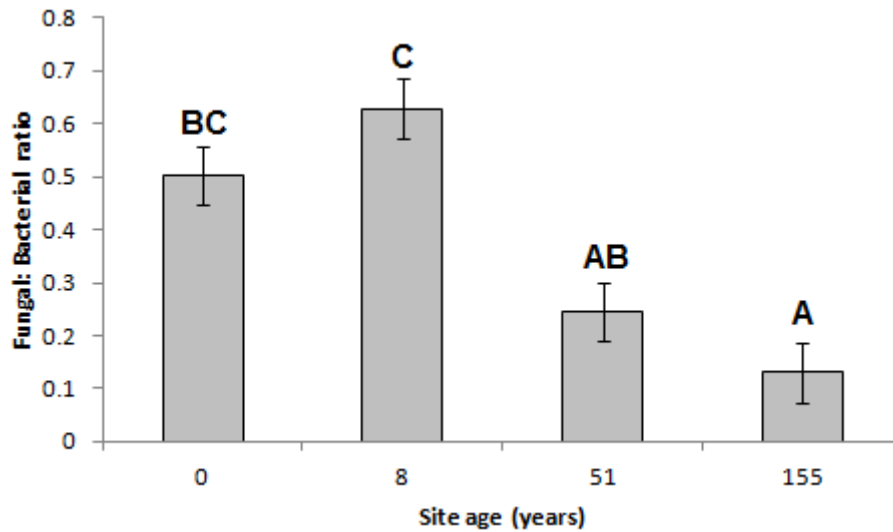


Figure 7.6 Ratios of fungal: bacterial biomarkers in the PLFA analysis, with error bars denoting pooled standard error and letters identifying homogenous groups.

### 7.3.4 Endpoint glucose determination

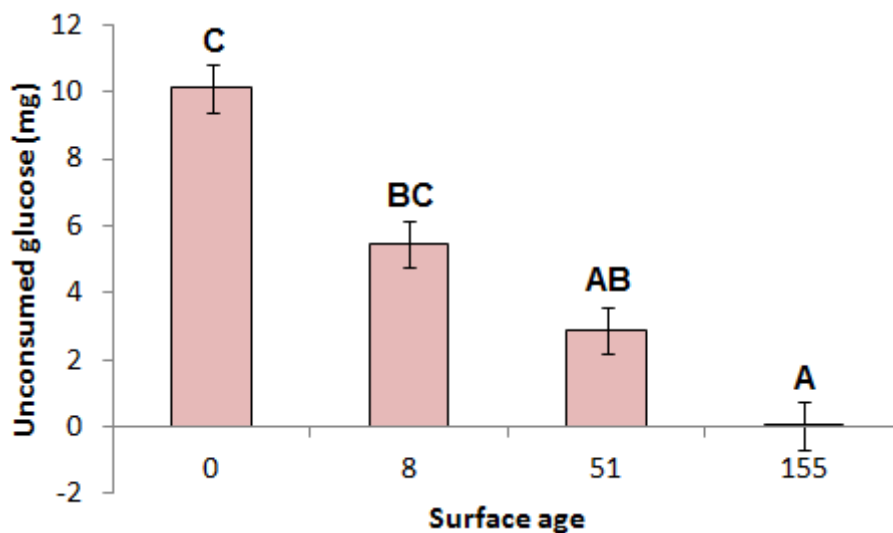


Figure 7.7 Glucose remaining in samples after removal from the calorimeter, as determined by a glucose oxidase assay, with bars denoting pooled standard error and homogenous groups identified by letters.

The amount of glucose that remained unconsumed in the calorimetric samples showed a very strong age effect ( $p < 0.005$ ) with almost complete consumption of the added glucose by all samples at the 151 years site and very low consumption by samples from the 0 years site. The quantity of unconsumed glucose showed a negative correlation with the  $\log_{10}$  value of the microbial biomass-C, with an  $r^2$  value of 0.715 (3 sf), indicating that the microbes in the early successional stage were able to ingest more glucose per unit biomass than microbes in later successional stages.

However, despite the highly significant effect there was an issue with the results from the glucose oxidase assay. Two of the samples in the assay, one from 0 years site and one from the 8 years site, produced results indicating that there was more glucose present in the sample than the 15.00 mg that had been added. As such these two results have been omitted from further analysis using the glucose oxidase results (see Section 7.3.5.1). Omission of these two results from the data presented in Figure 7.7 had little effect on the statistical significance, with  $p$  remaining below 0.005, identical homogenous groups being identified for the reduced dataset and a slight reduction in the pooled standard error.

### **7.3.5 Enthalpy efficiency**

Values of  $\eta_{eff}$  for both  $T=0-40$  h and  $T=0-100$  h showed a highly significant ( $p < 0.005$ ) age effect, with homogenous groups identifying that opposing ends of the successional gradient were statistically distinct (Figure 7.8).

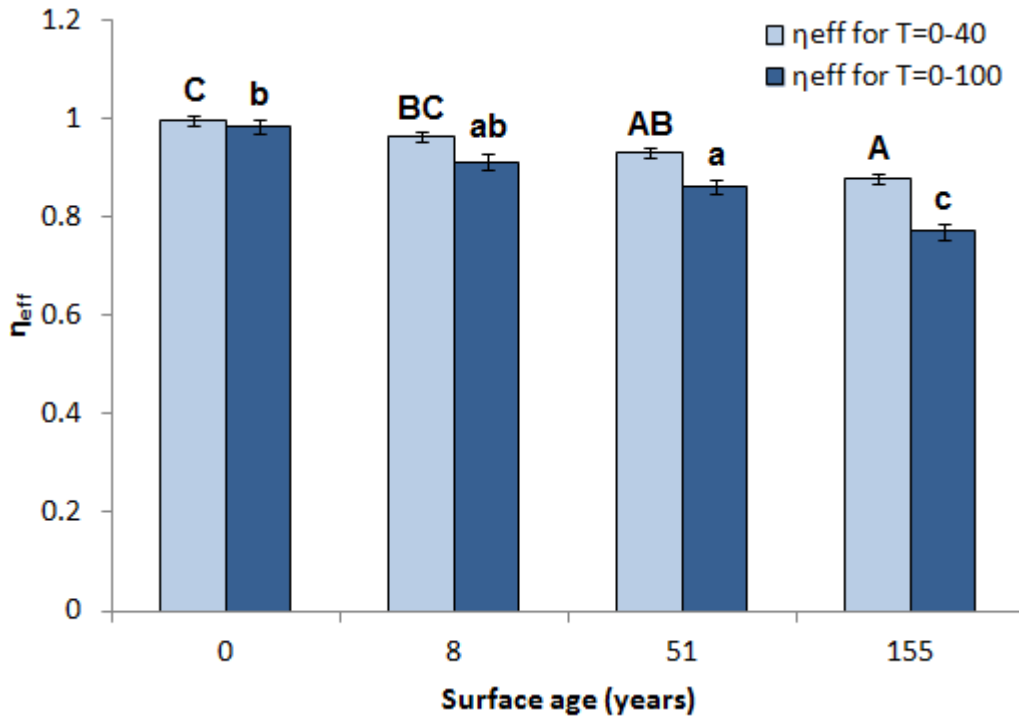


Figure 7.8 Mean enthalpy efficiency ( $\eta_{eff}$ ) for surface age groups after 40 and 100 hours calorimeter run time, with bars denoting pooled standard error and homogenous groups marked with letters (upper case: T=0-40; lower case: T=0-100).

### 7.3.5.1 Accounting for unconsumed glucose

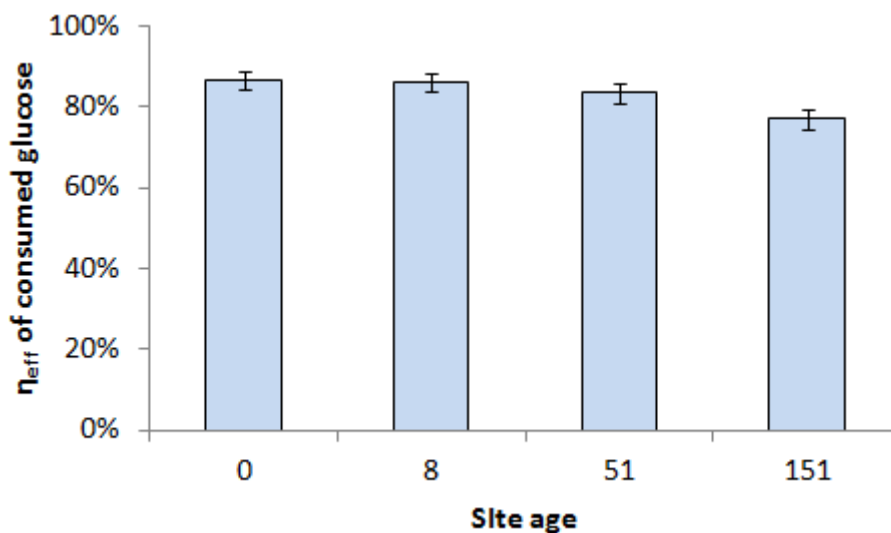
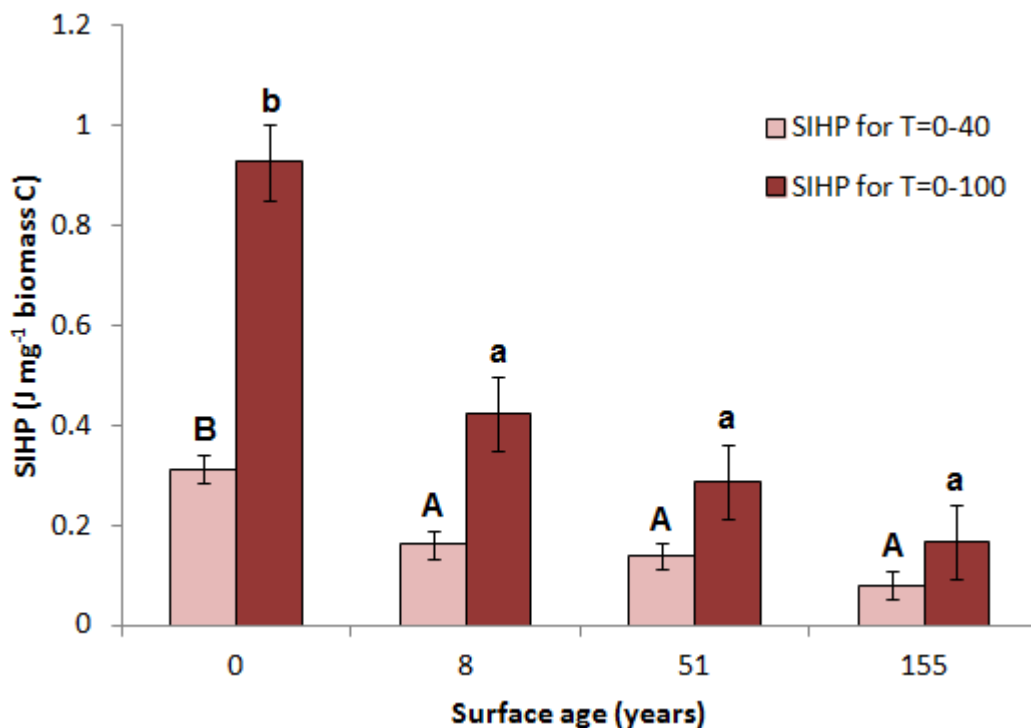


Figure 7.9 Mean enthalpy efficiency ( $\eta_{eff}$ ) for surface age groupings after 100 hours calorimeter run time, accounting for unconsumed glucose. Bars denoting pooled standard error.

Values for  $\eta_{eff}$  calculated using  $\Delta H^0$  values for glucose that could not be recovered by  $K_2SO_4$  solution extraction, as determined by a glucose oxidase assay, were observed to decrease with increasing surface age (Figure 7.9), however the relationship was not statistically significant ( $p>0.1$ ). A Fisher LSD test conducted on the data failed to identify any statistically distinct homogenous groups at a  $p=0.1$  level.

### 7.3.6 Substrate induced heat production (SIHP)



**Figure 7.10 Mean substrate induced heat production (SIHP) for surface age groups after 40 and 100 hours calorimeter run time, with bars denoting pooled standard error and homogenous groups marked with letters (upper case: T=0-40; lower case: T=0-100). One sample with a negative biomass value was omitted from the analysis.**

Values for SIHP for T=0-40 h displayed a slight age effect ( $p<0.1$ ), with homogenous groups identified at the  $p=0.1$  level indicating that values for the 0 year site were distinct from those of the 8 to 155 year sites (Figure 7.10). SIHP

results for T=0-100 h showed a significant age effect ( $p < 0.05$ ), with values for the 0 years site identified as distinct from those of 8 to 155 years (Figure 7.10).

### 7.3.7 Fungal dominance and thermodynamic efficiency

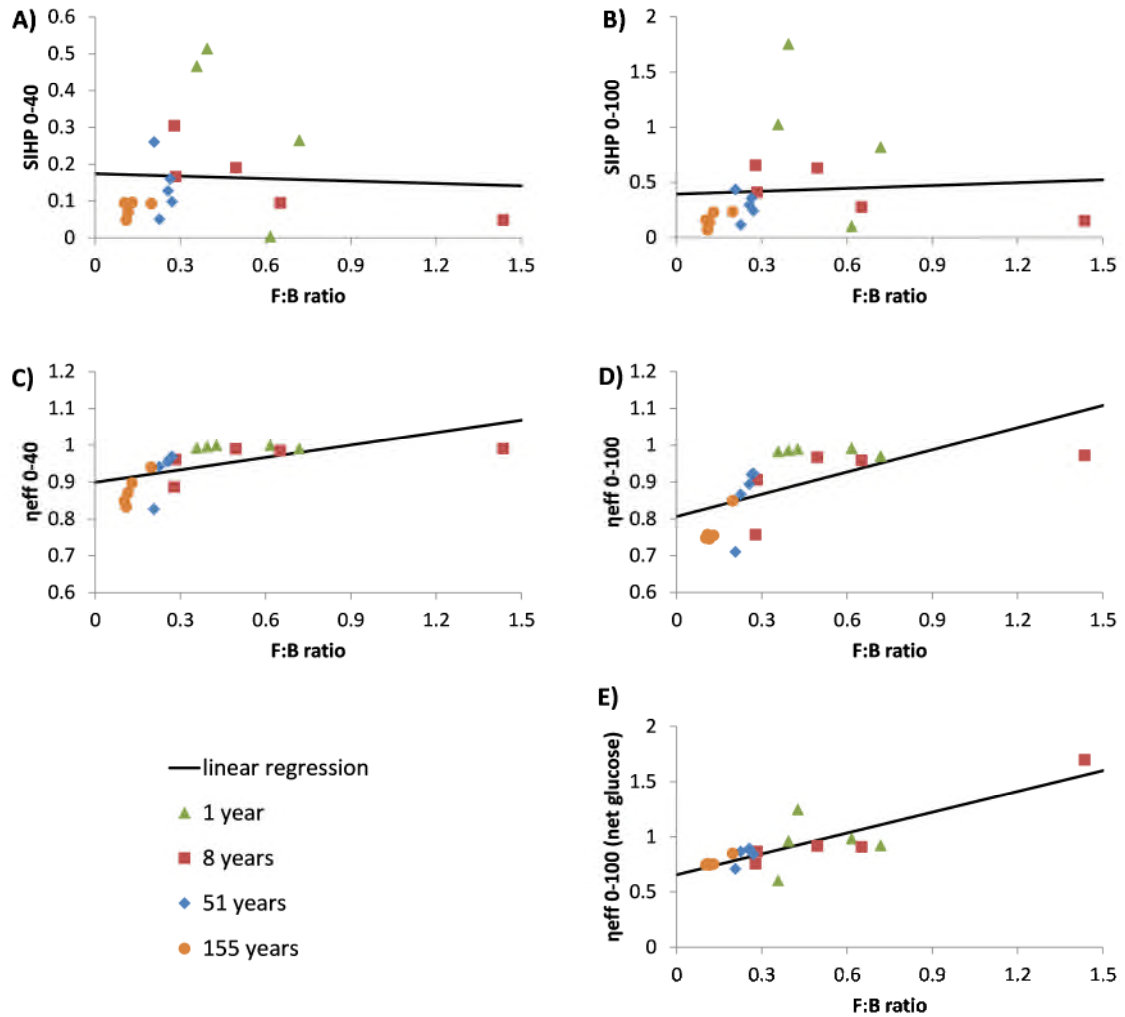


**Figure 7.11 Modelled relationship between fungal: bacterial ratios and thermodynamic indices, namely: A) SIHP for T=0-40h, B) SIHP for T=0-100h, C) enthalpy efficiency for T=0-40h, D) enthalpy efficiency for T=0-100h and E) enthalpy efficiency for T=100h, accounting for unconsumed glucose. Data point styles denote surface age of sample.**

Assessment of statistical relationships between F:B ratios and the thermodynamic indices via significance simple regression, identified relationships between F:B and  $\eta_{eff}$  for T=0-40 h ( $p < 0.01$ ), F:B and  $\eta_{eff}$  for T=0-



100 h ( $p < 0.005$ ) and F:B and  $\eta_{eff}$  using  $\Delta H^0$  for unrecovered glucose at T=0-100 h ( $p < 0.001$ ). No statistically significant ( $p > 0.5$ ) was identified between F:B ratios and either SHIP for T=0-40 h nor SHIP for T=0-100 h.

Relationships between surface age, F:B ratios and thermodynamic indices were modelled using a simple regression (Figure 7.11), showing that for all three of the  $\eta_{eff}$  indices, there is a trend of increasing fungal dominance corresponding to an increase in  $\eta_{eff}$ , most pronounced at the c. 51 year site. The two graphs modelling the relationship between surface age, F:B ratios and SHIP both show a sharp inflection point in SHIP at 20-40 years surface age, where SHIP decreases with increasing fungal dominance, however beyond this point SHIP increases relative to both surface age and fungal dominance.

## 7.4 Discussion

There was a disparity between the approximate surface ages published in Burga (1999), Burga et al. (2010) and those obtained from onsite markings (see Figure 7.1 & 7.2 and Table 7.1). The isochrones published in Burga et al. (2010) appear to have been subject to more thorough research, however the absolute surface age at the sampling points is not of great importance within the scope of the hypothesis tested in this chapter. It is more important that the sites represent differing stages of ecological development.

The increases in total soil C, total soil N, WHC, and microbial biomass-C over successional time followed a well-documented and understood pattern (Jenny, 1941; Egli et al., 2006; He & Tang, 2008; Lin, 2011).

However, C:N ratios indicated that C sequestration rates were not in line with N fixation throughout the chronosequence, with N-fixation playing a greater role in c. 0 years sites, before a relative surge of C fixation at the c. 8 years site.

A gradual decrease in pH over a glacial chronosequence, followed by distinctively lower pH values at the terminal moraine has been observed in other studies (He & Tang, 2008; Grice, 2010). In both cases the lower pH was associated with a greater level of mineral decomposition at the terminal moraine than would have been expected from sites along the chronosequence. This led Grice (2010) to conclude that both the pH and mineralogy of the terminal moraine may be influenced by material which was pushed along the valley floor during glacial re-advance. As such the soils developing on terminal moraines may be considered to be much older than the age of the moraine's deposition, as the material will have undergone pedogenesis *ex-situ*.

The PCA of the PLFA results indicated that changes in the microbial phenotype were more pronounced during the early phases of succession, potentially indicating that either the succession of the soil microbial biomass follows that of the above ground biomass, or that, just like plants (Chapin et al., 1994), pioneering microbes put themselves at a competitive disadvantage by developing the soil.

It would be expected for F:B ratios to peak during the mid-successional grassland-type ecosystem, due to greater production of root exudates prior to fungal symbionts becoming dominant in the rhizosphere with the introduction of woody plants (Harris, 2009). However, the F:B ratio peaked during the pioneer

communities type ecosystem (Figure 7.6), indicating that fungal symbionts may have become dominant earlier than anticipated.

The indication from the glucose oxidase assay that not all the glucose had been ingested by the microbial biomass, even 100 hours after substrate addition, is an important finding and should affect how results from the previous chapters are interpreted, especially when calculating values for  $\eta_{eff}$ .

The  $\eta_{eff}$  results indicated that metabolic efficiency decreased with increasing surface age, contrary to the hypothesis and yet again juxtaposing the SIHP results. However this trend was reduced in amplitude and no longer statistically robust after the unmetabolised glucose was accounted for. This indicates that the methodology for producing the  $\eta_{eff}$  index may be flawed and as such not suitable for assessing thermodynamic efficiency in its current form. Modification of the data collection method for  $\eta_{eff}$  may allow this index to provide useful data in future experiments. However, the fact that  $\eta_{eff}$  has once again shown the opposite of what was expected and of the SIHP results obtained from the same data, may provide some new insight into the energetic workings of ecosystems. This is discussed more in Chapter 8.

Similarly to some studies on  $qCO_2$ , the SIHP showed a decrease in the metabolic wastage per unit biomass over the chronosequence (Insam & Haselwandter, 1989), adding weight to Odum's (1969) theory that immature ecosystems produce more entropy than mature ones. The differences in SIHP had a greater amplitude after 100 hours, yet statistical analysis only identified the 0 years ecosystem as different to the three older sites, whereas the results

for 40 hours, although less robust, showed a more continuous trend of change along the length of the chronosequence (see Figure 7.10). This may indicate that the SIHP value for the 0 year site has been influenced by the inefficient process of microbial population growth during the 40-100 hour period, therefore skewing the results.

As a correlation was observed between  $\eta_{eff}$  and the F:B ratio, but not between SIHP and the F:B ratio it is not clear whether there is a connection between F:B ratios and thermodynamic efficiency, due to the problems highlighted with the  $\eta_{eff}$  index. However, it may be stated that the thermodynamic efficiency ( $\eta_{eff}$ ) was observed to increase in samples with greater fungal dominance.

## 7.5 Conclusions

It has been empirically demonstrated that soil microbial communities in the early stages of ecosystem development produce more waste heat per unit biomass than soil microbial communities in later stages of the same developmental chronosequence. As such there is good evidence to suggest that the soil microbial community has become more thermodynamically efficient over the course of ecosystem development along the Morteasch Glacier Vorfield.

There was an observed positive correlation between the  $\eta_{eff}$  of the soil microbial ecosystem and fungal dominance, however it is not clear if this relates to thermodynamic efficiency.

Again the  $\eta_{eff}$  and SIHP indexes provided apparently conflicting results, indicating that there may be issues with the method of data collection or processing, especially as efforts to improve the  $\eta_{eff}$  index proved to produce

statistically non-robust results. Given further research, the non-agreement of these two indexes may lead to new insights into the thermodynamic workings of below ground ecosystems or improvements in the measurement of thermodynamic efficiency in ecology.

## 8 General discussion and conclusions

*In this house we obey the laws of thermodynamics!*

– Homer Simpson

### 8.1 Summary

In Chapter 1 the aims of this study were outlined as building on the work of Harris et al. (2012) by investigating the theory that ecosystems would minimise entropy production per unit biomass in order to allow a greater total biomass from the flow of available energy (Odum, 1969). This was carried out by the testing of three key hypotheses:

1. The thermodynamic efficiency of the soil microbial biomass increases as ecosystem development takes place along a successional gradient.
2. The thermodynamic efficiency of the soil microbial biomass will decrease when subjected to ecological stress.
3. The thermodynamic efficiency of the soil microbial biomass will be greater when the fungal biomass is dominant than when the bacterial biomass dominates.

An additional aim of the project was outlined in Chapter 2; to introduce a standardised operating procedure for the isothermal calorimetric analysis of soil samples, in order to bring the research discipline in line with methodologies employed within the broader domain of soil microbiology.

These aims were realised by the comparison of existing work with the experimental results of four experimental projects, aimed at improving and

standardising the isothermal microcalorimetric method for soil microbial analysis (Chapters 4 & 5), assessing the thermodynamic efficiency of the soil microbial biomass subject to ecosystem stress arising from contamination with metals (Chapters 4 & 6), assessing of the thermodynamic efficiency of the soil microbial biomass in relation to fungal dominance (Chapters 7) and assessing the thermodynamic efficiency of the soil microbial biomass during ecological succession (Chapter 7).

## **8.2 Comment on the methodology**

### **8.2.1 Improvements to the isothermal calorimetric method**

The review of studies employing isothermal calorimetry for the study of soil science, presented in Chapter 2, identified that the majority of available literature had employed a methodology for the preparation, storage and pre-incubation of soil samples due for isothermal calorimetric analysis that was based on practices from two decades ago, that was unsuitable for accurate and timely signal capture. Most studies were working on the findings of Núñez-Regueira et al. (1994a), who identified that storing of soil at 4°C produced ‘important changes of the metabolic activity of soil microorganisms’, with later comments that storing the soil at 4°C for up to three months ‘ensured satisfactory reproducibility of the measurements’ (Núñez-Regueira et al., 1994b).

As mentioned above, this finding lead to the introduction of a secondary aim for this project; to introduce a new standardised method. An experiment was set up in order to test how pre-incubation of samples at 20°C for 2 to 36 days

beforehand influenced the accuracy of isothermal calorimetric measurements at 20°C. The results indicated that a pre-incubation period of 10-16 days prior to isothermal calorimetric analysis was optimal, similar to standard methodologies in other areas of soil microbiology (Powlson & Jenkinson, 1976; Wang et al., 2001; Creamer et al., 2009).

Pre-incubation of soil samples for 10-16 days at the same temperature as the isothermal calorimetric analysis was subsequently employed in all later experiments constituting this project. The idea of changing the standard methodology generated some interest at the XVII International Society of Biological Calorimetry Conference, 2012 in Leipzig and the suggestions have been adopted in a recent publication (Herrmann et al., 2014).

### **8.2.2 Calculation of $\eta_{eff}$**

Barros et al. (2000, 2001) assessed the thermodynamic efficiency of the soil microbial biomass using the metabolic enthalpy change,  $\Delta H_{met}$ , an index calculated in a similar way to  $\eta_{eff}$ , expressed as the enthalpy change per mol added glucose (see Chapter 2). Barros et al. (2001) criticized the usefulness of the  $\Delta H_{met}$  index, due to its key assumption of complete consumption of the added glucose, stating that this is difficult to demonstrate. Barros et al. (2001) observed a tenfold increase in glucose amendment resulted in an eightfold decrease in  $\Delta H_{met}$ , and commented that the results of a previous study (Barros et al., 1997) did not allow for the intended calculation of  $\Delta H_{met}$ , as the power-time curve failed to return to a stable baseline within the observational window, preventing the procurement of a reliable value for  $Q_{total}$ . This statement is also



true of the grassland soils in Chapter 5, the most contaminated samples in Chapter 6 and the earliest successional stages in Chapter 7, indicating that values for  $\eta_{\text{eff}}$  may be unreliable.

Wang et al. (2010b) attempted to overcome this key issue by using an egg membrane biosensor to measure dissolved glucose in real time, demonstrating that all available glucose was consumed during calorimetric observations. Similarly, an end-point glucose oxidase assay was used to determine residual glucose in the calorimetry samples in Chapter 7 and semi-successfully in Chapter 6, in that it was able to determine the absence of glucose in the 1, 10 & 100 mg Cu kg<sup>-1</sup> soil samples and the presence of glucose in the 1000 mg Cu kg<sup>-1</sup> soil samples at a concentration above the maximum measurable value.

The findings of Wang et al. (2010a; b, 2014) have shown that values for  $\Delta H_{\text{met}}$  decrease when the microbial biomass is subjected to stress from contamination with metals (Wang et al., 2010b) and pesticides (Wang et al., 2010a, 2014), suggesting that this is caused by restraint of metabolic activities under stress. As  $\Delta H_{\text{met}}$  is an inverse analogue of  $\eta_{\text{eff}}$  (see Chapter 2), this indicates that ecological stress increases the thermodynamic efficiency of the soil microbial biomass, supporting the findings of Chapters 5, 6 & 7, while contradicting the second key hypothesis. Even when remaining glucose is taken into account, the evidence remains counter to Odum's (1969) theory and the findings of Harris et al. (2012).

### **8.2.2.1 No accounting for biomass**

An additional issue with the  $\eta_{\text{eff}}$  index is that it does not take the microbial biomass into account, therefore assuming that a small and large biomass will have the same in response to fertilisation with a finite quantity of C-substrate. The  $\eta_{\text{eff}}$  index operates on the premise of a Carnot heat engine, where all energy is converted to work (biomass production) or heat (Chapter 1), so results may be influenced by whether glucose-C is stored by the biomass in substrate form or degraded before being converted into new biomass. However it is likely that glucose-C degradation dominates (Harris et al., 2012).

Chen et al. (2011) proposed calculating values of  $\Delta H_{\text{met}}$  per unit biomass, however it is not clear how this could be applied to the dimensionless  $\eta_{\text{eff}}$  index. Instead, it may be of more value to improve the  $\eta_{\text{eff}}$  index by amending the microbial biomass with a standard quantity of C-substrate per unit biomass.

### **8.2.2.2 C-substrate saturation and O<sub>2</sub> depletion**

Possibly the greatest hindrance to the successful use of the  $\eta_{\text{eff}}$  index was the quantity of glucose added. The SIHP index requires the soil microbial biomass to be under C-substrate saturation throughout the period of observation, as the heat production per unit biomass can be reduced by substrate scarcity. The  $\eta_{\text{eff}}$  index on the other hand requires complete exhaustion of the C-substrate by the biomass. These two requirements are not easily compatible. From the results of Harris et al. (2012), the SIHP index was given precedence over the  $\eta_{\text{eff}}$  index, therefore the calorimetric method was adapted to ensure glucose-C saturation (Chapter 5), resulting in amendments of 2 mg glucose-C g<sup>-1</sup> dry soil being used.

Vor et al. (2002) calculated that a 25 ml ampoule with a 5 g soil sample contained enough O<sub>2</sub> to metabolise 6 mg glucose. If we assume that the solid and liquid fraction of the 3 g dry weight soil sample account for c. 1 cm<sup>3</sup>, then the 20 ml ampoule used here should contain c. 0.16 mmol O<sub>2</sub> gas, assuming it was prepared at 293 K and 100 Pa, and that 21% of the headspace gas was O<sub>2</sub>. This would only be enough to completely combust c. 2 mg glucose-C (c. 5 mg glucose), therefore we can assume that at most one third of the total 6 mg glucose-C amendment was metabolised to CO<sub>2</sub> and H<sub>2</sub>O before the sample became anoxic.

While it is possible to calculate  $\eta_{\text{eff}}$  in anoxic conditions using the TAM Air calorimeter, the experiment would not have been possible within the time period available. Additionally, a mixture of oxic and anoxic conditions should not be used for the calculation of one  $\eta_{\text{eff}}$  value.

### **8.2.3 Calculation of SIHP**

The calculation of heat production related to biomass is not completely novel. Sparling (1981a; b, 1983) compared heat production with biomass-C as determined by ATP concentration, substrate induced respiration and chloroform fumigation extraction and fumigation respiration, observing a strong link between heat output and microbial biomass. This led Sparling (1983) to produce a figure of 180.05 mW g<sup>-1</sup> biomass-C for glucose induced heat production, to be used for estimation of the total soil microbial biomass (see Chapter 2). Both Sparling (1983) and later work by Raubuch & Beese (1999) only measured heat production of the initial few hours after glucose addition in

order to avoid microbial growth, as both specifically aimed to use the method as an alternative means of calculating a microbial biomass figure: for this reason the SIHP is different, as it aims to stimulate microbial growth in order to observe how efficient this process is.

The use of heat production per unit biomass was first linked to the concept of biotic efficiency by Barros et al. (2003) as the cell specific heat rate,  $J_{Q/N}$ . However the soil microbial biomass estimates were made using the most probable number method from colony forming units, an outdated and highly inaccurate method of microbial biomass determination (Ritz, 2007).

In this respect the SIHP index gives genuinely new insights into how the laws of thermodynamics are manifested in ecology. Unlike the enthalpy efficiency index,  $\eta_{\text{eff}}$  (Harris et al., 2012) and the calorespirometric ratio,  $R_q/R_{\text{CO}_2}$  (Barros et al., 2010, 2011), it is the only measurement that is able to directly quantify the waste heat production of a complex ecological community on a *per unit biomass* basis, thereby allowing accurate comment on the entropy production per unit biomass of an ecosystem. In this respect, the SIHP index has allowed Odum's (1969) theory of ecosystems developing to minimise entropy production per unit biomass to be empirically tested for the first time.

### **8.3 Thermodynamic efficiency**

From the points discussed above it is evident that the enthalpy efficiency index,  $\eta_{\text{eff}}$ , requires further development before it can offer any robust commentary on the thermodynamic efficiency of soil microbial communities. As such this section

will deal with the conclusions that can be drawn from results obtained using the SIHP index in relation to the three key hypotheses.

### **8.3.1 Relationship with ecosystem maturity**

The SIHP results obtained from samples taken along the Morteratsch glacial chronosequence in Switzerland showed a statistically robust trend of decreasing waste heat production per unit biomass over the course of ecological succession (Chapter 7). Calorimetric results showed a statistically significant trend in decreasing SIHP with increasing surface age from observations at both 40 and 100 hours after C-substrate addition, supporting Odum's (1969) theory and the first key hypothesis:

1. The thermodynamic efficiency of the soil microbial biomass increases as ecosystem development takes place along a successional gradient.

The findings of Chapter 7 corresponded with the results for metabolic quotient,  $q\text{CO}_2$ , obtained by Insam & Haselwandter (1989), Wardle (1993) and Wardle & Ghani (1995), which showed a decrease in the  $\text{CO}_2$  mineralisation per unit biomass during ecological succession glacial chronosequences in Austria, Canada and New Zealand. However, the usefulness of this index has been called into question, as several studies reported inverse trends or conflicting results (Wardle & Ghani, 1995; Ohtonen et al., 1999; Merilä, 2003). As such, it may be worthwhile making observations of SIHP on other successional chronosequences, in order to robustly test the first key hypothesis before it can be accepted with confidence.

### 8.3.2 Relation to ecological stress

Soil samples subjected to long term metal contamination due to close proximity to the Gusums Bruk brass mill in Sweden showed significantly ( $p < 0.05$ ) higher SIHP levels at 64 hours after substrate addition than those at a distance of greater than a few hundred meters (Chapter 4). This indicates that long-term metal induced stress increases the production of waste heat per unit biomass. Short term  $\text{CuSO}_4$  induced stress was observed to significantly ( $p < 0.05$ ) increase SIHP at contamination levels of  $1000 \text{ mg Cu kg}^{-1}$  dry soil, despite a slight ( $p > 0.5$ ) decrease in SIHP with contamination of up to  $10 \text{ mg Cu kg}^{-1}$  dry soil (Chapter 6). The slight decrease was possibly due to fertilisation of the microbial biomass with  $\text{H}_2\text{SO}_4\text{-S}$ , thereby reducing ecological stress. Stress induced by both long term and short term metal contamination caused a statistically significant increase in SIHP at the highest levels of concentration. This implies that entropy production per unit biomass is greater in microbial communities highly stressed by metal contamination, thereby supporting the second key hypothesis:

2. The thermodynamic efficiency of the soil microbial biomass will decrease when subjected to ecological stress.

Harris et al. (2012) provides additional evidence to support that this hypothesis is also true for ecological stress induced by soil nutrient input regimes. More evidence for this can be obtained from a re-interpretation of the data presented in Sparling (1983) and Raubuch & Beese (1999). There is also additional

evidence to suggest that stress from acidity decreases thermodynamic efficiency (Herrmann et al., 2011).

### **8.3.3 Relation to fungal dominance**

There was no statistically significant evidence or observed correlation in the results produced in this project to support or reject the third key hypothesis:

3. The thermodynamic efficiency of the soil microbial biomass will be greater when the fungal biomass is dominant than when the bacterial biomass dominates.

It is likely that any influence that fungal dominance played in the total heat production per unit biomass of the microbial community was outweighed by the primary variables which were being tested, i.e. metal contamination (Chapter 6) and ecological development (Chapter 7). A further experiment was planned to manipulate the fungal dominance in samples from the same parent sample, via sterilisation and re-inoculation. However, unfortunately it was not possible to analyse these samples calorimetrically.

## **8.4 Suggestions for future work**

As stated above, this work using the SIHP index is the first to measure waste heat production per unit biomass in an ecological community. As such, this has opened up many new areas for future study as well as highlighting key areas requiring further investigation. In reference to the three key hypotheses, there are three main areas that require more investigation:

1. SIHP vs. ecosystem development in different locations and contexts

2. SIHP vs. different types of ecological stress
3. SIHP vs. different ecological strategies, such as r/K .e.g. fungal/bacterial dominance, possibly in the context of biomass/diversity dilution experiments.

It has also been mentioned that the  $\eta_{\text{eff}}$  may yet prove to be useful in providing new insights into the three areas mentioned above. As such, it is a suggestion of this study that a measure of  $\eta_{\text{eff}}$  where samples are amended on a mass of C-substrate per unit mass of microbial biomass-C could be employed in future studies attempting to measure thermodynamic efficiency of the soil microbial biomass. It is also a recommendation that amendment of samples on a g C-substrate per g microbial biomass-C basis may further improve the accuracy of the SIHP index, as oversaturation with glucose-C can inhibit total metabolic rate (see Chapter 5).

There would be great scientific merit in combining techniques previously used to observe maximisation of entropy production (see Chapter 1) with analogous measurements of SIHP. If this were employed over the course of a successional gradient, such as in Chapter 7, then it may be possible to observe ecosystems developing to maximise total entropy production, while minimising entropy production per unit biomass, as suggested in Chapter 1.

## **8.5 Concluding remarks**

The question printed on the front cover of this thesis asks:

*Is the thermodynamic efficiency of soil microbial communities related to ecosystem maturity and stress?*



From the body of work presented here, we can say that there is good evidence that it is. Results have indicated that soil microbial communities produce more waste heat per unit biomass in the early stages of ecological succession and under conditions of ecological stress induced by metal contamination. This implies that soil microbial communities will develop mechanisms to reduce entropic losses, thereby driving efficiency in a thermodynamic scene.

This provides empirical evidence supporting Odum's (1969) theory that ecosystems will develop mechanisms to reduce entropic losses and contradicting the theory of Schneider & Kay (1994) and Schneider & Sagan (2005) that life *is* a manifestation of the second law of thermodynamics that exists to degrade energetic gradients to the fullest extent. Instead it is proposed that life *does* manifest the second law of thermodynamics, as all processes must, yet produces the maximum total biomass within an energetic gradient by maximising energy capture (resulting in maximisation of total entropy production) while minimising energy loss (achieved by minimisation of entropy production per unit biomass).

The work presented here confirms that soil microbial systems are ideal candidates for testing some of these broad ecological principles and theories – and at a pace unsustainable in larger systems. This area warrants further work and investigation, and could prove an effective tool in advancing fundamental understanding of key ecosystem processes and evolutionary pressures.

## References

- Addiscott, T.M. 1995. Entropy and sustainability. *European Journal of Soil Science* **46**, 161–168.
- Addiscott, T.M. 2010. Entropy, non-linearity and hierarchy in ecosystems. *Geoderma* **160**, 57–63.
- Ahamadou, B., Huang, Q., Chen, W., Wen, S., Zhang, J.J., Mohamed, I., Cai, P., & Liang, W. 2009. Microcalorimetric assessment of microbial activity in long-term fertilization experimental soils of Southern China. *FEMS Microbiology Ecology* **70**, 30–9
- Airoldi, C. 1998. O uso de calorimetria em ecologia. *Química Nova* **21**, 635–641
- Airoldi, C., & Critter, S.A.M. 1996. The inhibitor effect of copper sulphate on microbial glucose degradation in red latosol soil. *Thermochimica Acta* **288**, 73–82.
- Airoldi, C., & Prado, A.G.S.S. 2002. The inhibitory biodegradation effects of the pesticide 2,4-D when chemically anchored on silica gel. *Thermochimica Acta* **394**, 163–169
- Åkerblom, S., Bååth, E., Bringmark, L., & Bringmark, E. 2007. Experimentally induced effects of heavy metal on microbial activity and community structure of forest mor layers. *Biology and Fertility of Soils* **44**, 79–91
- Albers, B.P.B.B.P., Beese, F., & Hartmann, A. 1995. Flow-microcalorimetry measurements of aerobic and anaerobic soil microbial activity. *Biology and Fertility of Soils* **19**, 203–208
- Alberts, B., Bray, D., Lewis, J., Raff, M., Walter, P., Hopkin, K., Johnson, A., & Roberts, K. 2012. *Essential Cell Biology*, 3rd Edition. Garland Science, New York and Abingdon.
- Alef, K., Beck, T., Zelles, L., & Kleiner, D. 1988. A comparison of methods to estimate microbial biomass and N-mineralization in agricultural and grassland soils. *Soil Biology and Biochemistry* **20**, 561–565.
- Almqvist, H. 2010. The legacy of the mill. MSc Thesis. SLU: Sweden 54.
- Anderson, J.P.E., & Domsch, K.H. 1975. Measurement of bacterial and fungal contributions to respiration of selected agricultural and forest soils. *Canadian Journal of Microbiology* **21**, 314–322.

- Anderson, J.P.E., & Domsch, K.H. 1978. A physiological method for the quantitative measurement of microbial biomass in soils. *Soil Biology and Biochemistry* **10**, 215–221.
- Anderson, T., & Domsch, K.H. 1985. Maintenance carbon requirements of actively-metabolizing microbial populations under in situ conditions. *Soil Biology and Biochemistry* **17**, 197–203.
- Aoki, I. 1989. Holological study of lakes from an entropy viewpoint - Lake Mendota. *Ecological Modelling* **45**, 81–93.
- Aoki, I. 1995. Entropy production in living systems: from organisms to ecosystems. *Thermochimica Acta* **250**, 359–370.
- Atkins, P.W. 2000. Atkins' Physical Chemistry. 6th ed. OUP Oxford, Oxford.
- Bååth, E. 1989. Effects of heavy metals in soil on microbial processes and populations (a review). *Water Air and Soil Pollution* **47**, 335–379.
- Bååth, E., Arnebrant, K., & Nordgren, a. 1991. Microbial biomass and ATP in smelter-polluted forest humus. *Bulletin of Environmental Contamination and Toxicology* **47**, 278–82
- Baer, S.G., Kitchen, D.J., Blair, J.M., & Rice, C.W. 2002. Changes in ecosystem structure and function along a chronosequence of restored grasslands. *Ecological Applications* **12**, 1688–1701.
- Barja, M.I., Núñez-Regueira, L., & Nu, L. 1999. Microcalorimetric measurements of the influence of glucose concentration on microbial activity in soils. *Soil Biology and Biochemistry* **31**, 441–447
- Barja, M.I., Proupín-Castiñeiras, J., Núñez-regueira, L., & Proupin, J. 1997. Microcalorimetric study of the effect of temperature on microbial activity in soils. *Thermochimica Acta* **303**, 155–159
- Barros, N. 2003. Comments on the paper titled "Use of microcalorimetry to study microbial activity during the transition from oxic to anoxic conditions." *Biology and Fertility of Soils* **38**, 124–125.
- Barros, N., Airoidi, C., Simoni, J.A.J. a. J.D.A., Ramajo, B., Espina, A., & García, J.R. 2006. Calorimetric determination of the effect of ammonium-iron (II) phosphate monohydrate on Rhodic Eutrudox Brazilian soil. *Thermochimica Acta* **441**, 89–95
- Barros, N., & Feijóo, S. 2003. A combined mass and energy balance to provide bioindicators of soil microbiological quality. *Biophysical Chemistry* **104**, 561–572

- Barros, N., Feijóo, S., & Álvarez, J.M. 2008a. A thermodynamic model and software to assess the contribution of land use to global warming. *International Journal of Low Carbon Technologies* **3**, 24–31.
- Barros, N., Feijóo, S., Balsa, R., & Feijóo, S. 1997. Comparative study of the microbial activity in different soils by the microcalorimetric method. *Thermochimica Acta* **296**, 53–58
- Barros, N., Feijóo, S., & Fernández, S. 2003. Microcalorimetric determination of the cell specific heat rate in soils: relationship with the soil microbial population and biophysic significance. *Thermochimica Acta* **406**, 161–170
- Barros, N., Feijóo, S., Fernández, S., Simoni, J.D.A., & Airolidi, C. 2000. Application of the metabolic enthalpy change in studies of soil microbial activity. *Thermochimica Acta* **356**, 1–7.
- Barros, N., Feijóo, S., & Hansen, L.D. 2011. Calorimetric determination of metabolic heat, CO<sub>2</sub> rates and the calorespirometric ratio of soil basal metabolism. *Geoderma* **160**, 542–547.
- Barros, N., Feijóo, S., Salgado, J., Ramajo, B., García, J.R.R., & Hansen, L.D. 2008b. The dry limit of microbial life in the Atacama Desert revealed by calorimetric approaches. *Engineering in Life Sciences* **8**, 477–486
- Barros, N., Feijóo, S., Simoni, J.A.D.A., Airolidi, C., Ramajo, B., Espina, A., & García, J.R. 2008c. A mass and energy balance to provide microbial growth yield efficiency in soil: sensitivity to metal layering phosphates. *Journal of Thermal Analysis and Calorimetry* **93**, 657–665.
- Barros, N., Feijóo, S., Simoni, A., Critter, S.A.M., & Airolidi, C. 2001. Interpretation of the metabolic enthalpy change,  $\Delta H_{\text{met}}$ , calculated for microbial growth reactions in soils. *Journal of Thermal Analysis* **63**, 577–588.
- Barros, N., Feijoo, S., Simoni, J.A., Prado, A.G.S., Barboza, F.D., & Airolidi, C. 1999. Microcalorimetric study of some Amazonian soils. *Thermochimica Acta* **328**, 99–103.
- Barros, N., Gallego, M., & Feijóo, S. 2004. Calculation of the Specific Rate of Catabolic Activity (Ac) from the Heat Flow Rate of Soil Microbial Reactions Measured by Calorimetry: Significance and Applications. *Chemistry and Biodiversity* **1**, 1560–1568
- Barros, N., Gallego, M., & Feijóo, S. 2007a. Sensitivity of calorimetric indicators of soil microbial activity. *Thermochimica Acta* **458**, 18–22
- Barros, N., Gomez-Orellana, I., Feijóo, S., & Balsa, R. 1995. The effect of soil moisture on soil microbial activity studied by microcalorimetry. *Thermochimica Acta* **249**, 161–168.

- Barros, N., Ramajo, B., & García, J.R. 2009. The effect of solid-liquid effluents from anaerobic digesters on soil microbial activity: A calorimetric study. *Journal of Thermal Analysis and Calorimetry* **95**, 831–835.
- Barros, N., Salgado, J., & Feijóo, S. 2007b. Calorimetry and soil. *Thermochimica Acta* **458**, 11–17
- Barros, N., Salgado, J., Rodríguez-Añón, J.A., Proupín-Castiñeiras, J., Villanueva-López, M., & Hansen, L.D. 2010. Calorimetric approach to metabolic carbon conversion efficiency in soils: Comparison of experimental and theoretical models. *Journal of Thermal Analysis and Calorimetry* **99**, 771–777
- Bastow, J. 2012. Succession, resource processing, and diversity in detrital food webs. p. 117–135. *In* Soil Ecology and Ecosystem Services. Wall, D.H., Bardgett, R.D., Behan-Pelletier, V., Herrick, J.E., Jones, T.H., Ritz, K., Six, J., Strong, D.R., Van der Putten, W.H. (eds.),. Oxford University Press.
- Battley, E.H. 1960. Enthalpy Changes Accompanying the Growth of *Saccharomyces cerevisiae* (Hansen). *Physiologia Plantarum* **13**, 628–640
- Battley, E.H. 1995. A reevaluation of the thermodynamics of growth of *Saccharomyces cerevisiae* on glucose, ethanol, and acetic acid. *Canadian Journal of Microbiology* **41**, 388–98.
- Begon, M., Townsend, C.R., & Harper, J.L. 2006. Ecology: From Individuals to Ecosystems. 4th ed. Blackwell Publishing, Malden, MA.
- Bengtsson, G., & Rundgren, S. 1988. The Gusum case: a brass mill and the distribution of soil Collembola. *Canadian Journal of Zoology* **66**, 1518–1526.
- Berg, B., Ekbohm, G., Söderström, B., & Staaf, H. 1991. Reduction of decomposition rates of scots pine needle litter due to heavy-metal pollution. *Water Air and Soil Pollution* **59**, 165–177.
- Blagodatskaya, E., Blagodatsky, S., Anderson, T.-H., & Kuzyakov, Y. 2014. Microbial growth and carbon use efficiency in the rhizosphere and root-free soil. *PLoS ONE* **9**, e93282.
- Bligh, E.G., & Dyer, W.J. 1959. A rapid method of total lipid extraction and purification. *Canadian Journal of Biochemistry and Physiology* **37**, 911–917.
- Blundell, S.J., & Blundell, K.M. 2009. Concepts in Thermal Physics. 2nd ed. Oxford University Press, Oxford, UK.
- Bogomolov, D.M., Chen, S.K., Parmelee, R.W., Subler, S., & Edwards, C.A. 1996. An ecosystem approach to soil toxicity testing: a study of copper contamination in laboratory soil microcosms. *Applied Soil Ecology* **4**, 95–105

- Bölter, M. 1994. Microcalorimetry and CO<sub>2</sub>-evolution of soils and lichens from Antarctica. *Polar Biology* **7**, 209–220.
- Brady, N.C., & Weil, R.R. 2008. *The Nature and Properties of Soils*. 14th ed. Prentice Hall, Upper Saddle River, New Jersey, USA.
- Braissant, O., Wirz, D., Göpfert, B., & Daniels, A.U. 2010. Use of isothermal microcalorimetry to monitor microbial activities. *FEMS Microbiology Letters* **303**, 1–8
- Brunsell, N. a., Schymanski, S.J., & Kleidon, A. 2011. Quantifying the thermodynamic entropy budget of the land surface: is this useful? *Earth System Dynamics* **2**, 87–103.
- Buchholz, A.C., & Schoeller, D. a. 2004. Is a calorie a calorie? *The American Journal of Clinical Nutrition* **79**, 899S–906S.
- Burga, C.A. 1999. Vegetation development on the glacier forefield Morteratsch (Switzerland). *Applied Vegetation Science* **2**, 17–24.
- Burga, C. a., Krüsi, B., Egli, M., Wernli, M., Elsener, S., Ziefle, M., Fischer, T., & Mavris, C. 2010. Plant succession and soil development on the foreland of the Morteratsch glacier (Pontresina, Switzerland): Straight forward or chaotic? *Flora - Morphology, Distribution, Functional Ecology of Plants* **205**, 561–576.
- Cabral, M.E.S., & Sigstad, E.E. 2011. A new approach to determine soil microbial biomass by calorimetry. *Journal of Thermal Analysis and Calorimetry* **104**, 23–29
- Calgren, K., & Mattsson, L. 2001. Swedish soil fertility experiments. *Acta Agriculturae Scandinavica* **51**, 49–76.
- Cao, Z., & Hu, Z. 2000. Copper contamination in paddy soils irrigated with wastewater. *Chemosphere* **41**, 3–6
- Cenciani, K., Freitas, S., Auxiliadora, S., Critter, M., & Airoidi, C. 2011. Enzymatic activity measured by microcalorimetry in soil amended with organic residues. *Revista Brasileira de Ciência do Solo* **35**, 1167–1175.
- Chambers, J.Q., Tribuzy, E.S., Toledo, L.C., Crispim, B.F., Higuchi, N., Santos, J. dos, Araujo, A.C., Kruijt, B., Nobre, A.D., & Trumbore, S.E. 2004. Respiration from a tropical forest ecosystem: partitioning of sources and low carbon use efficiency. *Ecological Applications* **14**, 72–88.
- Chander, K., & Brookes, P.C. 1993. Residual effects of zinc, copper and nickel in sewage sludge on microbial biomass in a sandy loam. *Soil Biology and Biochemistry* **25**, 1231–1239.

Chapin, F.S.I., Walker, L.R., Fastie, C.L., & Sharman, L.C. 1994. Mechanisms of primary succession following deglaciation at Glacier Bay, Alaska. *Ecological Monographs* **64**, 149–175.

Chen, K., Yao, J., Qi, S., Zheng, S., Luo, Y., Záray, G., Wang, F., Mohammad, R., & Choi, M.M.F. 2011. Characterization of depth-related microbial community activities in freshwater sediment by combined method. *Geomicrobiology Journal* **28**, 328–334.

Chen, H., Yao, J., Wang, F., Choi, M.M.F., Bramanti, E., & Zaray, G. 2009. Study on the toxic effects of diphenol compounds on soil microbial activity by a combination of methods. *Journal of Hazardous Materials* **167**, 846–51

Chen, H., Yao, J., Wang, F., Zhou, Y., Chen, K., Zhuang, R.S., & Zaray, G. 2010. Investigation of the Acute Toxic Effect of Chlorpyrifos on *Pseudomonas putida* in a Sterilized Soil Environment Monitored by Microcalorimetry. *Archives of Environmental Contamination and Toxicology* **58**, 587–593

Chen, H., Zhuang, R., Yao, J., Wang, F., & Qian, Y. 2013. A comparative study on the impact of phthalate esters on soil microbial activity. *Bulletin of Environmental Contamination and Toxicology* **91**, 217–23

Coûteaux, M.-M., Raubuch, M., & Berg, M. 1998. Response of protozoan and microbial communities in various coniferous forest soils after transfer to forests with different levels of atmospheric pollution. *Biology and Fertility of Soils* **27**, 179–188.

Creamer, R.E., Bellamy, P., Black, H.I.J., Cameron, C.M., Campbell, C.D., Chamberlain, P., Harris, J.A., Parekh, N., Pawlett, M., Poskitt, J., Stone, D., & Ritz, K. 2009a. An inter-laboratory comparison of multi-enzyme and multiple substrate-induced respiration assays to assess method consistency in soil monitoring. *Biology and Fertility of Soils* **45**, 623–633

Creamer, R.E., Bellamy, P., Black, H.I.J., Cameron, C.M., Campbell, C.D., Chamberlain, P., Harris, J.A., Parekh, N., Pawlett, M., Poskitt, J., Stone, D., & Ritz, K. 2009b. An inter-laboratory comparison of multi-enzyme and multiple substrate-induced respiration assays to assess method consistency in soil monitoring. *Biology and Fertility of Soils* **45**, 623–633

Critter, S.A.M., & Airoidi, C. 2001. Application of Calorimetry to Microbial Biodegradation Studies of Agrochemicals in Oxisols. *Journal of Environmental Quality* **30**, 954–959.

Critter, S.A.M., Freitas, S.S., & Airoidi, C. 2001. Calorimetry versus respirometry for the monitoring of microbial activity in a tropical soil. *Applied Soil Ecology* **18**, 217–227

- Critter, S.A.M., Freitas, S.S., & Airoidi, C. 2002a. Comparison between microorganism counting and a calorimetric method applied to tropical soils. *Thermochimica Acta* **394**, 133–144
- Critter, S.A.M., Freitas, S.S., & Airoidi, C. 2002b. Microbial biomass and microcalorimetric methods in tropical soils. *Thermochimica Acta* **394**, 145–154
- Critter, S.A.M., Freitas, S.S., & Airoidi, C. 2004a. Comparison of microbial activity in some Brazilian soils by microcalorimetric and respirometric methods. *Thermochimica Acta* **410**, 35–46
- Critter, S.A.M., Freitas, S.S., & Airoidi, C. 2004b. Microcalorimetric measurements of the metabolic activity by bacteria and fungi in some Brazilian soils amended with different organic matter. *Thermochimica Acta* **417**, 275–281
- Critter, S.A.M., Simoni, J.D.A., & Airoidi, C. 1994. Microcalorimetric study of glucose degradation in some Brazilian soils. *Thermochimica Acta* **232**, 145–154.
- Dahlin, S., & Witter, E. 1998. Can the low microbial biomass C-to-organic C ratio in an acid and a metal contaminated soil be explained by differences in the substrate utilization efficiency and maintenance requirements? *Soil Biology and Biochemistry* **30**, 633–641.
- Darwin, C. 1859. *On the Origin of Species*. Wordsworth Editions Ltd.
- DeLuca, T.H., Nilsson, M.-C., & Zackrisson, O. 2002. Nitrogen mineralization and phenol accumulation along a fire chronosequence in northern Sweden. *Oecologia* **133**, 206–214.
- Dhatfield. 2008. Cell membrane detailed diagram 4. *Wikipedia* Available at [http://en.wikipedia.org/wiki/File:Cell\\_membrane\\_detailed\\_diagram\\_4.svg](http://en.wikipedia.org/wiki/File:Cell_membrane_detailed_diagram_4.svg) (verified 5 August 2013).
- Dowling, N.J.E., Widdel, F., & White, D.C. 1986. Phospholipid ester-linked fatty acid biomarkers of acetate-oxidizing sulphate-reducers and other sulphide-forming bacteria. *Journal of General Microbiology* **132**, 1815–1825.
- Drong, K., Lamprecht, I., Motzkus, C., & Schaarschmidt, B. 1991. Calorimetric investigations of pollution by xenobiotics. *Thermochimica Acta* **193**, 125–134
- Dumestre, A., Sauve, S., McBride, M., Baveye, P., & Berthelin, J. 1999. Copper speciation and microbial activity in long-term contaminated soils. *Archives of Environmental Contamination and Toxicology* **36**, 124–131.
- Dümig, A., Smittenberg, R., & Kögel-Knabner, I. 2011. Concurrent evolution of organic and mineral components during initial soil development after retreat of the Damma glacier, Switzerland. *Geoderma* **163**, 83–94.



Dyckmans, J., Flessa, H., Lipski, A., Potthoff, M., & Beese, F. 2006. Microbial biomass and activity under oxic and anoxic conditions as affected by nitrate additions. *Journal of Plant Nutrition and Soil Science* **169**, 108–115

Dziejowski, J.E. 1995. Calorimetric and respirometric characteristics of the decomposition of animal wastewaters in soil. *Thermochimica Acta* **251**, 37–43.

Dziejowski, J.E., & Białobrzewski, I. 2011. Calorimetric studies of solid wastes, sewage sludge, wastewaters and their effects on soil biodegradation processes. *Journal of Thermal Analysis and Calorimetry* **104**, 161–168.

Egli, M., Wernli, M., Kneisel, C., & Haerberli, W. 2006. Melting glaciers and soil development in the proglacial area Morteratsch (Swiss Alps): I. Soil type chronosequence. *Arctic, Antarctic and Alpine Research* **38**, 499–509.

Feng, X., & Simpson, M.J. 2009. Temperature and substrate controls on microbial phospholipid fatty acid composition during incubation of grassland soils contrasting in organic matter quality. *Soil Biology and Biochemistry* **41**, 804–812

Folkesson, L. 1984. Deterioration of the moss and lichen vegetation in a forest polluted by heavy metals. *Ambio* **13**, 37–39.

Fradette, S., Rho, D., Samson, R., LeDuy, A., Rho, S.F.D., & Leduy, R.S.A. 1994. Microcalorimetry as a diagnostic and analytical tool for the assessment of biodegradation of 2,4-D in a liquid medium and in soil. *Applied Microbiology and Biotechnology* **42**, 432–439.

Frostegård, Å., & Bååth, E. 1996. The use of phospholipid fatty acid analysis to estimate bacterial and fungal biomass in soil. *Biology and Fertility of Soils* **22**, 59–65.

Frostegård, Å., Bååth, E., & Tunlid, A. 1993a. Shifts in the structure of soil microbial communities in limed forests as revealed by phospholipid fatty acid analysis. *Soil Biology and Biochemistry* **25**, 723–730.

Frostegård, Å., Tunlid, A., & Bååth, E. 1993b. Phospholipid fatty acid composition, biomass, and activity of microbial communities from two soil types experimentally exposed to different heavy metals. *Applied and Environmental Microbiology* **59**, 3605–3617.

Frostegård, Å., Tunlid, A., & Bååth, E. 1996. Changes in microbial community structure during long-term incubation in two soils experimentally contaminated with metals. *Soil Biology and Biochemistry* **28**, 55–63.

Frostegård, Å., Tunlid, A., & Bååth, E. 2011. Use and misuse of PLFA measurements in soils. *Soil Biology and Biochemistry* **43**, 1621–1625

- Gai, N., Yang, Y., Li, T., Yao, J., Wang, F., & Chen, H. 2011. Effect of lead contamination on soil microbial activity measured by microcalorimetry. *Chinese Journal of Chemistry* **29**, 1541–1547
- Ge, T., Nie, S., Tong, C., Xiao, H., & Qin, H. 2012. Microcalorimetric studies for microbial activity of three vegetable soils. *Journal of Food, Agriculture & Environment* **10**, 930–932.
- Ge, T., Nie, S., Wu, J., Shen, J., Xiao, H., Tong, C., Huang, D., Hong, Y., & Iwasaki, K. 2011. Chemical properties, microbial biomass, and activity differ between soils of organic and conventional horticultural systems under greenhouse and open field management: a case study. *Journal of Soils and Sediments* **11**, 25–36
- Giller, K.E., Witter, E., & Mcgrath, S.P. 1998. Toxicity of heavy metals to microorganisms and microbial processes in agricultural soils: a review. *Soil Biology and Biochemistry* **30**, 1389–1414.
- Glucose (GO) Assay Kit. Saint Louis, Missouri, USA.
- Google Inc. 2011. Google Earth. Available at <http://www.google.com/earth/index.html>.
- Grice, S.M. 2010. An assessment of ecosystem development over time in the Morteratsch Valley, Switzerland. BSc Thesis, University of Reading: UK.
- Gruiz, K., Feigl, V., Hajdu, C., & Tolner, M. 2010. Environmental toxicity testing of contaminated soil based on microcalorimetry. *Environmental Toxicology* **25**, 479–486.
- Guo, H., Yao, J., Cai, M., Qian, Y., Guo, Y., Richnow, H.H., Blake, R.E., Doni, S., & Ceccanti, B. 2012. Effects of petroleum contamination on soil microbial numbers, metabolic activity and urease activity. *Chemosphere* **87**, 1273–80
- Hågvar, S. 1998. The relevance of the Rio-Convention on biodiversity to conserving the biodiversity of soils. *Applied Soil Ecology* **9**, 1–7.
- Harris, J.A. 2009. Soil microbial communities and restoration ecology: facilitators or followers? *Science* **325**, 573–574
- Harris, J. a., Ritz, K., Coucheney, E., Grice, S.M., Lerch, T.Z., Pawlett, M., & Herrmann, A.M. 2012. The thermodynamic efficiency of soil microbial communities subject to long-term stress is lower than those under conventional input regimes. *Soil Biology and Biochemistry* **47**, 149–157.
- Hassan, W., Chen, W., Cai, P., & Huang, Q. 2013a. Estimation of enzymatic, microbial, and chemical properties in Brown soil by microcalorimetry. *Journal of Thermal Analysis and Calorimetry* **116**, 969–988

Hassan, W., Chen, W., Huang, Q., & Mohamed, I. 2013b. Microcalorimetric evaluation of soil microbiological properties under plant residues and dogmatic water gradients in Red soil. *Soil Science and Plant Nutrition* **59**, 858–870

He, L., & Tang, Y. 2008. Soil development along primary succession sequences on moraines of Hailuoguo Glacier, Gongga Mountain, Sichuan, China. *Catena* **72**, 259–269.

Heilmann, B., & Beese, F. 1992. Miniaturized method to measure carbon dioxide production and biomass of soil microorganisms. *Soil Science Society of America Journal* **56**, 596–598

Heilmann, B., Lebuhn, M., & Beese, F. 1995. Methods for the investigation of metabolic activities and shifts in the microbial community in a soil treated with a fungicide. *Biology and Fertility of Soils* **19**, 186–192

Herrmann, A.M., Coucheney, E., & Nunan, N. 2014. Isothermal microcalorimetry provides new insight into terrestrial carbon cycling. *Environmental Science & Technology* **48**, 4344–52

Herrmann, A.M., Grice, S.M., Ritz, K., & Harris, J.A. 2011. Thermodynamic principles of soil organic matter decomposition in a changing world. *Mineralogical Magazine* **75**, 1016.

Hillel, D. 1998. *Environmental Soil Physics: Fundamentals, Applications and Environmental Considerations*. Waltham, MA, USA. Academic Press Inc.

Hodson, M.E. 2004. Heavy metals--geochemical bogey men? *Environmental Pollution* **129**, 341–3

Holdaway, R.J., Sparrow, A.D., & Coomes, D. A. 2010. Trends in entropy production during ecosystem development in the Amazon Basin. *Philosophical transactions of the Royal Society of London. Series B, Biological Sciences* **365**, 1437–1447.

Hong, Z., Rong, X., Cai, P., Liang, W., & Huang, Q. 2011. Effects of Temperature, pH and Salt Concentrations on the Adsorption of *Bacillus subtilis* on Soil Clay Minerals Investigated by Microcalorimetry. *Geomicrobiology Journal* **28**, 686–691

Hueso, S. 2012. Severe drought conditions modify the microbial community structure, size and activity in amended and unamended soils. *Soil Biology and Biochemistry* **50**, 167-173

Hund, K., Zelles, L., Scheunert, I., & Korte, F. 1988. A critical estimation of methods for measuring side-effects of chemicals on microorganisms in soils. *Chemosphere* **17**, 1183–1188.

Insam, H., & Haselwandter, K. 1989. Metabolic quotient of the soil microflora in relation to plant succession. *Oecologia* **79**, 174–178.

Jenny, H. 1941. Factors of soil formation: a system of quantitative pedology. McGraw-Hill, New York, USA.

Jenny, H. 1980. The soil resource: origin and behavior. Springer-Verlag, New York, USA.

Jørgensen, S.E., & Fath, B.D. 2004. Application of thermodynamic principles in ecology. *Ecological Complexity* **1**, 267–280.

Kashian, D.M., Romme, W.H., Tinker, D.B., Turner, M.G., & Ryan, M.G. 2013. Postfire changes in forest carbon storage over a 300-year chronosequence of *Pinus contorta*-dominated forests. *Ecological Monographs* **83**, 49–66.

Katchalsky, A., & Curran, P.F. 1967. Nonequilibrium Thermodynamics in Biophysics. Harvard University Press, Cambridge, MA, USA.

Kaur, Amrit, Chaudhary, A., Kaur, Amarjeet, Choudhary, R., & Kaushik, B. 2005. Phospholipid fatty acid – A bioindicator of environment monitoring and assessment in soil ecosystem. *Current Science* **89**, 1103-1112

Kawabata, T., Yamanoand, H., & Takahashi, K. 1983. An attempt to characterize calorimetrically the inhibitory effect of foreign substances on microbial degradation of glucose in soil. *Agricultural and Biological Chemistry* **47**, 1281–1288.

Keiblinger, K.M., Hall, E.K., Wanek, W., Szukics, U., Hämmerle, I., Ellersdorfer, G., Böck, S., Strauss, J., Sterflinger, K., Richter, A., & Zechmeister-Boltenstern, S. 2010. The effect of resource quantity and resource stoichiometry on microbial carbon-use-efficiency. *FEMS Microbiology Ecology* **73**, 430–440.

Kimura, T., & Takahashi, K. 1985. Calorimetric studies of soil microbes: quantitative relation between heat evolution during microbial degradation of glucose and changes in microbial activity in soil. *Journal of General Microbiology* **131**, 3083–3089

Kleidon, A. 2004. Beyond Gaia: Thermodynamics of Life and Earth System Functioning. *Climatic Change* **66**, 271–319.

Kleidon, A., Malhi, Y., & Cox, P.M. 2010. Maximum entropy production in environmental and ecological systems. *Philosophical Transactions of the Royal Society of London. Series B, Biological Sciences* **365**, 1297–302.

Klier, C., Grundmann, S., Gayler, S., & Priesack, E. 2008. Modelling the Environmental Fate of the Herbicide Glyphosate in Soil Lysimeters. *Water Air and Soil Pollution: Focus* **8**, 187–207

Knelman, J.E., Legg, T.M., O'Neill, S.P., Washenberger, C.L., González, A., Cleveland, C.C., & Nemergut, D.R. 2012. Bacterial community structure and function change in association with colonizer plants during early primary succession in a glacier forefield. *Soil Biology and Biochemistry* **46**, 172–180.

Koga, K., Suehiro, Y., Matsuoka, S.-T., & Takahashi, K. 2003. Evaluation of growth activity of microbes in tea field soil using microbial calorimetry. *Journal of Bioscience and Bioengineering* **95**, 429-434.

Konno, T. 1976. Application of microcalorimetry to the study of soil microorganisms. *Netsu Sokutei* **3**, 148–151. (in Japanese, translated at <https://translate.google.com/>)

Konno, T. 1979. Dojō no seibutsu kassei o hakaru. *Kagaku To Seibutsu* **17**, 574–579. (in Japanese translated at <https://translate.google.com/>)

Kreutzer, K., & Zelles, L. 1986. Die Auswirkungen von saurer Beregnung und Kalkung auf die mikrobielle Aktivität im Boden. *Forstwissenschaftliches Centralblatt* **105**, 314–317.

Kuperman, R.G., & Carreiro, M.M. 1997. Soil heavy metal concentrations, microbial biomass and enzyme activities in a contaminated grassland ecosystem. *Soil Biology and Biochemistry* **29**, 179–190.

Laliberté, E., Turner, B.L., Costes, T., Pearse, S.J., Wyrwoll, K.-H., Zemunik, G., & Lambers, H. 2012. Experimental assessment of nutrient limitation along a 2-million-year dune chronosequence in the south-western Australia biodiversity hotspot. *Journal of Ecology* **100**, 631–642.

Lamprecht, I., Motzkus, C., Schaarschmidt, B., & Coenen-Stass, D. 1990. Pentachlorophenol - an environmental pollutant: Microcalorimetric investigations of an ecological model system. *Thermochimica Acta* **172**, 87–94.

Lantmäteriet. 2013. Kartsök och ortnamn. Lantmäteriet, Gävle, Sweden. Available at <http://kso.lantmateriet.se/kartsok/kos/index.html> (verified 20 August 2013).

Laor, Y., Raviv, M., & Borisover, M. 2004. Evaluating microbial activity in composts using microcalorimetry. *Thermochimica Acta* **420**, 119–125

Lehr, S., Scheunert, I., & Beese, F. 1996. Mineralization of free and cell-wall-bound isotopurone in soils in relation to soil microbial parameters. *Soil Biology and Biochemistry* **28**, 1–8

Lejon, D.P.H., Nowak, V., Bouko, S., Pascault, N., Mougél, C., Martins, J.M.F., & Ranjard, L. 2007. Fingerprinting and diversity of bacterial copA genes in response to soil types, soil organic status and copper contamination. *FEMS Microbiology Ecology* **61**, 424–37

Levy, W., Radl, V., Ruth, B., Schmid, M., Munch, J.C., & Schroll, R. 2007. Harsh summer conditions caused structural and specific functional changes of microbial communities in an arable soil. *European Journal of Soil Science* **58**, 736–745.

Liang, S., Ynag, L., Jiang, S., Yu, X., Xia, Y., Ian, Y., & Lu, Z. 2014. Microcalorimetric study of microbial activity changes of Acrisol in subtropical China under three different land management. *African Journal of Agricultural Research* **9**, 1740–1752.

Likens, G.E. 1992. *The ecosystem approach: its use and abuse*. Ecology Institute, Oldendorf/Luhe, Germany

Lin, H. 2011. Three Principles of Soil Change and Pedogenesis in Time and Space. *Soil Science Society of America journal* **75**, 2049–2070.

Lindahl, B.D., de Boer, W., & Finlay, R.D. 2010. Disruption of root carbon transport into forest humus stimulates fungal opportunists at the expense of mycorrhizal fungi. *The ISME Journal* **4**, 872–81

Ljungholm, K., Norén, B., & Odham, G. 1980. Microcalorimetric and gas chromatographic studies of microbial activity in water leached, acid leached and restored soils. *Oikos* **34**, 98–102.

Ljungholm, K., Norén, B., Sköld, R., & Wadsö, I. 1979a. Use of Microcalorimetry for the Characterization of Microbial Activity in Soil. *Oikos* **33**, 15–23

Ljungholm, K., Norén, B., & Wadsö, I. 1979b. Microcalorimetric Observations of Microbial Activity in Normal and Acidified Soils. *Oikos* **33**, 24–30

Lloyd, S. 2004. Going into reverse. *Nature* **430**, 971.

Loland, J.Ø., & Singh, B.R. 2004. Copper contamination of soil and vegetation in coffee orchards after long-term use of Cu fungicides. *Nutrient Cycling in Agroecosystems* **69**, 203–211.

López Alonso, M., Benedito, J.L., Miranda, M., Castillo, C., Hernández, J., & Shore, R.F. 2000. The effect of pig farming on copper and zinc accumulation in cattle in Galicia (north-western Spain). *Veterinary Journal (London, England : 1997)* **160**, 259–66

Lotka, A.J. 1922. Contribution to the energetics of evolution. *Proceedings of the National Academy of Sciences of the United States of America* **8**, 147–151.

Maier, R.M., Pepper, I.L., & Gerba, C.P. 2009. *Environmental Microbiology*, Second Edition. 2nd ed. Academic Press, Burlington, MA.

Mann, M.E. 2002. Little Ice Age. p. 504–509. *In* Encyclopedia of Global Environmental Change. Cuff D. & Goudie A. S. (eds). Oxford University Press, Oxford, UK.

Manzoni, S., Taylor, P., Richter, A., Porporato, A., & Agren, G.I. 2012. Environmental and stoichiometric controls on microbial carbon-use efficiency in soils. *The New Phytologist* **196**, 79–91.

Medina, S., Raviv, M., Saadi, I., & Laor, Y. 2009. Methodological aspects of microcalorimetry used to assess the dynamics of microbial activity during composting. *Bioresource Technology* **100**, 4814–20

Merilä, P. 2003. Soil microbial dynamics and the condition of Norway spruce on the Bothnian land-uplift coast. PhD Thesis. University of Helsinki: Finland

Merilä, P., Strömmer, R., & Fritze, H. 2002. Soil microbial activity and community structure along a primary succession transect on the land-uplift coast in western Finland. *Soil Biology and Biochemistry* **34**, 1647–1654.

Moore-Kucera, J., & Dick, R.P. 2008. PLFA Profiling of Microbial Community Structure and Seasonal Shifts in Soils of a Douglas-fir Chronosequence. *Microbial Ecology* **55**, 500-511

Mortensen, U., Norén, B., & Wadsö, I. 1973. Microcalorimetry in the Study of the Activity of Microorganisms. *Bulletins from the Ecological Research Committee* **17**, 189–197.

Müller-Stöver, D., Hauggaard-Nielsen, H., Eriksen, J., Ambus, P., & Johansen, A. 2012. Microbial biomass, microbial diversity, soil carbon storage, and stability after incubation of soil from grass–clover pastures of different age. *Biology and Fertility of Soils* **48**, 371–383

Nordgren, A., Bååth, E., & Söderström, B. 1988. Evaluation of soil respiration characteristics to assess heavy metal effects on soil microorganisms using glutamic acid as a substrate. *Soil Biology and Biochemistry* **20**, 949–954.

Núñez-Regueira, L., Barros, N., & Barja, M.I. 1994a. Effect of storage of soil at 4°C on the microbial activity studied by microcalorimetry. *Journal of Thermal Analysis* **41**, 1379–1383.

Núñez-Regueira, L., Barros, N., & Barja, M.I. 1994b. A kinetic analysis of the degradation of glucose by soil microorganisms studied by microcalorimetry. *Thermochimica Acta* **237**, 73–81

Núñez-Regueira, L., Proupín-Castiñeiras, J., Rodríguez-Añón, J. a., Villanueva-López, M., & Núñez-Fernández, O. 2006a. Design of an experimental procedure to assess soil health state. *Journal of Thermal Analysis and Calorimetry* **85**, 271–277

- Núñez-regueira, L., Rodr, J.A., Proup, J., Núñez-Fernández, O., Rodríguez-Añón, J.A., & Proupín-Castiñeiras, J. 2002. The influence of some physicochemical parameters on the microbial growth in soils. *Thermochimica Acta* **394**, 123–131.
- Núñez-Regueira, L., Rodríguez-Añón, J. a., Proupín-Castiñeiras, J., & Núñez-Fernández, O. 2005. Influence of the agricultural exploitation processes on the productivity capacity control of soils: design of an experimental procedure. *Journal of Thermal Analysis and Calorimetry* **80**, 35–41.
- Núñez-Regueira, L., Rodríguez-Añón, J. a., Proupín-Castiñeiras, J., & Núñez-Fernández, O. 2006b. Microcalorimetric study of changes in the microbial activity in a humic Cambisol after reforestation with eucalyptus in Galicia (NW Spain). *Soil Biology and Biochemistry* **38**, 115–124
- Núñez-Regueira, L., Rodríguez-Añón, J. a., Proupín-Castiñeiras, J., Villanueva-López, M., & Núñez-Fernández, O. 2006c. Study of the influence of different forest species on the microbial activity in soils. *Journal of Thermal Analysis and Calorimetry* **84**, 7–13
- Odum, E.P. 1969. The strategy of ecosystem development. *Science* **164**, 262–270.
- Odum, H.T. 2007. *Environment, Power, and Society for the Twenty-First Century: The Hierarchy of Energy*. Columbia University Press, New York, USA.
- Ohtonen, R., Fritze, H., Pennanen, T., Jumpponen, A., & Trappe, J. 1999. Ecosystem properties and microbial community changes in primary succession on a glacier forefront. *Oecologia* **119**, 239–246.
- Oliveira, D. a., Barros, N., & Airoidi, C. 2008. Calorimetric investigation of m-methoxyphenol effect on *Chromobacterium violaceum* activity in soil. *Thermochimica Acta* **471**, 86–89
- Oorts, K., Bronckaers, H., & Smolders, E. 2006. Discrepancy of the microbial response to elevated copper between freshly spiked and long-term contaminated soils. *Environmental Toxicology and Chemistry / SETAC* **25**, 845–53
- Pamatmat, M.M., & Bhagwat, A.M. 1973. Anaerobic Metabolism in Lake Washington Sediments. *Limnology and Oceanography* **18**, 611–627.
- Pawlett, M., Ritz, K., Dorey, R. A, Rocks, S., Ramsden, J., & Harris, J.A. 2013. The impact of zero-valent iron nanoparticles upon soil microbial communities is context dependent. *Environmental Science and Pollution Research International* **20**, 1041–9.



- Petersen, S.O., & Klug, M.J. 1994. Effects of Sieving, Storage, and Incubation Temperature on the Phospholipid Fatty Acid Profile of a Soil Microbial Community. *Applied and Environmental Microbiology* **60**, 2421–2430.
- Pickett, S.T.A. 1989. Space-for-Time Substitution as an Alternative to Long-Term Studies. p. 110–135. *In* Long-Term Studies in Ecology: Approaches and Alternatives. Springer-Verlag, New York, USA.
- Plante, A.F., Fernández, J.M., & Leifeld, J. 2009. Application of thermal analysis techniques in soil science. *Geoderma* **153**, 1–10
- Powlson, D.S., & Jenkinson, D.S. 1976. The effects of biocidal treatments on metabolism in soil-II. Gamma irradiation, autoclaving, air-drying and fumigation. *Soil Biology and Biochemistry* **8**, 179–188.
- Prado, A.G.S., & Airoldi, C. 1999. The influence of moisture on microbial activity of soils. *Thermochimica Acta* **332**, 71–74.
- Prado, A.G.S., & Airoldi, C. 2000. Effect of the pesticide 2,4-D on microbial activity of the soil monitored by microcalorimetry. *Thermochimica Acta* **349**, 17–22
- Prado, A.G.S.S., & Airoldi, C. 2001. Microcalorimetry of the degradation of the herbicide 2,4-D via the microbial population on a typical Brazilian red Latosol soil. *Thermochimica Acta* **371**, 169–174
- Prado, A.G.S.S., & Airoldi, C. 2002. The toxic effect on soil microbial activity caused by the free or immobilized pesticide diuron. *Thermochimica Acta* **394**, 155–162
- Prado, A.G.S., Evangelista, S.M., SouzaDe, J.R., Matos, J.G.S., Souza, M. a. a., Oliveira, D. a., & Airoldi, C. 2011. Effect of the irrigation with residual wastewaters on microbial soil activity of the ornamental flowers (*Dahlia pinnata*) cultures monitored by isothermal calorimetry. *Journal of Thermal Analysis and Calorimetry* **106**, 431–436
- Priesack, E., & Kisser-Priesack, G.M. 1993. Modelling diffusion and microbial uptake of <sup>13</sup>C-glucose in soil aggregates. *Geoderma* **56**, 561–573.
- Ranjard, L., Echairi, A., Nowak, V., Lejon, D.P.H., Nouaïm, R., & Chaussod, R. 2006a. Field and microcosm experiments to evaluate the effects of agricultural Cu treatment on the density and genetic structure of microbial communities in two different soils. *FEMS Microbiology Ecology* **58**, 303–15.
- Ranjard, L., Lignier, L., & Chaussod, R. 2006b. Cumulative Effects of Short-Term Polymetal Contamination on Soil Bacterial Community Structure. *Applied and Environmental Microbiology* **72**, 1684–1687.

Raubuch, M., & Beese, F. 1995. Pattern of microbial indicators in forest soils along an European transect. *Biology and Fertility of Soils* **19**, 362–368.

Raubuch, M., & Beese, F. 1999. Comparison of microbial properties measured by O<sub>2</sub> consumption and microcalorimetry as bioindicators in forest soils. *Soil Biology and Biochemistry* **31**, 949–956.

Raubuch, M., & Joergensen, R.G. 2002. C and net N mineralisation in a coniferous forest soil: the contribution of the temporal variability of microbial biomass C and N. *Soil Biology and Biochemistry* **34**, 841–849

Ren, Y., Zhang, P., Yan, D., Yan, Y., Chen, L., Qiu, L., Mei, Z., & Xiao, X. 2012. Application of microcalorimetry of *Escherichia coli* growth and discriminant analysis to the quality assessment of a Chinese herbal injection (Yinzhihuang). *Acta Pharmaceutica Sinica B* **2**, 278–285.

Renella, G., Chaudri, a. . M., & Brookes, P.C. 2002. Fresh additions of heavy metals do not model long-term effects on microbial biomass and activity. *Soil Biology and Biochemistry* **34**, 121–124

Ritz, K. 2007. The plate debate: cultivable communities have no utility in contemporary environmental microbial ecology. *FEMS Microbiology Ecology* **60**, 358–362

Rodríguez-Añón, J. a., Proupín-casti, J.Ô., Nú, O.Ô., Proupín-Castiñeiras, J., Villanueva-López, M., & Núñez-Fernández, O. 2007. Development of an experimental procedure to analyse the “soil health state” by microcalorimetry. *Journal of Thermal Analysis and Calorimetry* **87**, 15–19

Rong, X., Huang, Q., Jiang, D., Cai, P., & Liang, W. 2007. Isothermal Microcalorimetry: A Review of Applications in Soil and Environmental Sciences. *Pedosphere* **17**, 137–145

Rowell, D.L. 1994. *Soil Science: Methods and Applications*. 1st ed. Prentice Hall, Upper Saddle River, New Jersey, USA.

Rühling, Å., Bååth, E., Nordgren, A., & Söderström, B. 1984. Fungi in metal-contaminated soil near the Gusum brass mill, Sweden. *Ambio* **13**, 34–36.

Saetre, P., & Stark, J.M. 2005. Microbial dynamics and carbon and nitrogen cycling following re-wetting of soils beneath two semi-arid plant species. *Oecologia* **142**, 247–60.

Salgado, J., Villanueva, M., Núñez-Fernández, O., Proupín-Castiñeiras, J., Barros, N., Rodríguez-Añón, J. a., & Villanueva-López, M. 2009. Calorimetric seasonal characterization of culture and pasture soils. *Journal of Thermal Analysis and Calorimetry* **98**, 293–298

Scheunert, I., Attar, A., & Zelles, L. 1995. Ecotoxicological effects of soil-bound pentachlorophenol residues on the microflora of soils. *Chemosphere* **30**, 1995–2009

Schneider, E.D., & Kay, J.J. 1994. Life as a manifestation of the second law of thermodynamics. *Mathematical and Computer Modelling* **19**, 25–48.

Schneider, E.D., & Sagan, D. 2005. *Into the Cool: Energy Flow, Thermodynamics, and Life*. University of Chicago Press, Chicago, USA.

Schrödinger, E. 1944. *What is Life?* Cambridge University Press, Croyden, UK.

Schymanski, S.J., Kleidon, A., Stieglitz, M., & Narula, J. 2010. Maximum entropy production allows a simple representation of heterogeneity in semiarid ecosystems. *Philosophical transactions of the Royal Society of London. Series B, Biological sciences* **365**, 1449–55.

Selmants, P.C., & Hart, S.C. 2010. Phosphorus and soil development: does the Walker and Syers model apply to semiarid ecosystems? *Ecology* **91**, 474–84.

Sigler, W. V., Crivii, S., & Zeyer, J. 2002. Bacterial succession in glacial forefield soils characterized by community structure, activity and opportunistic growth dynamics. *Microbial Ecology* **44**, 306–16.

Sigstad, E.E., Bejas, M.A., Amoroso, M.J., Garc, C.I., & García, C.I. 2002. Effect of deforestation on soil microbial activity A worm-composite can improve quality? A microcalorimetric analysis at 25 °C. *Thermochimica Acta* **394**, 171–178.

Sigstad, E.E., Schabes, F.I., & Tejerina, F. 2013. A calorimetric analysis of soil treated with effective microorganisms. *Thermochimica Acta* **569**, 139–143

Sindhøj, E., Hansson, A., Andr, O., Kätterer, T., Marissink, M., & Pettersson, R. 2000. Root dynamics in a semi-natural grassland in relation to atmospheric carbon dioxide enrichment, soil water and shoot biomass. *Plant and Soil* **223**, 253–263.

Six, J., Frey, S.D., Thiet, R.K., & Batten, K.M. 2006. Bacterial and Fungal Contributions to Carbon Sequestration in Agroecosystems. *Soil Science Society of America Journal* **70**, 555.

Skopp, J., Jawson, M. D. & Doran, J. W. 1990. Steady-state aerobic microbial activity as a function of soil water content. *Soil Science Society of America Journal* **54**, 16-19-1625

Smit, E., Leeflang, P., & Wernars, K. 1997. Detection of shifts in microbial community structure and diversity in soil caused by copper contamination using

amplified ribosomal DNA restriction analysis. *FEMS Microbiology Ecology* **23**, 249–261.

Šourková, M., Frouz, J., Fettweis, U., Bens, O., Hüttl, R.F., & Šantrůčková, H. 2005. Soil development and properties of microbial biomass succession in reclaimed post mining sites near Sokolov (Czech Republic) and near Cottbus (Germany). *Geoderma* **129**, 73–80.

Sparling, G.P. 1981a. Microcalorimetry and other methods to assess biomass and activity in soil. *Soil Biology and Biochemistry* **13**, 93–98.

Sparling, G.P. 1981b. Heat output of the soil biomass. *Soil Biology and Biochemistry* **13**, 373–376.

Sparling, G.P. 1983. Estimation of microbial biomass and activity in soil using microcalorimetry. *Journal of Soil Science* **34**, 381–390.

Sparling, G.P., Fermor, T.R., & Wood, D.A. 1982. Measurement of the microbial biomass in composted wheat straw, and the possible contribution of the biomass to the nutrition of *Agaricus bisporus*. *Soil Biology and Biochemistry* **14**, 609–611.

Spencer, H. 1864. *The Principles of Biology*, Volume 1. Williams and Norgate, London, UK.

Stein, S., Selesi, D., Schilling, R., Pattis, I., Schmid, M., & Hartmann, A. 2005. Microbial activity and bacterial composition of H<sub>2</sub>-treated soils with net CO<sub>2</sub> fixation. *Soil Biology and Biochemistry* **37**, 1938–1945.

Stenger, R., Priesack, E., & Beese, F. 1996. In situ studies of soil mineral N fluxes: Some comments on the applicability of the sequential soil coring method in arable soils. *Plant and Soil* **183**, 199–211

Strickland, M.S., & Rousk, J. 2010. Considering fungal:bacterial dominance in soils – Methods, controls, and ecosystem implications. *Soil Biology and Biochemistry* **42**, 1385–1395.

Tancho, A., Merckx, R., Schoovaerts, R., & Vlassak, K. 1995. Relation between substrate-induced respiration and heat loss from soil samples treated with various contaminants. *Thermochimica Acta* **251**, 21–28.

Teeling, H., & Cypionka, H. 1997. Microbial degradation of tetraethyl lead in soil monitored by microcalorimetry. *Applied Microbiology and Biotechnology* **48**, 275–279

Tissot, P. 1999. Calorimetric study of the bioremediation of a polluted soil. *Journal of Thermal Analysis and Calorimetry* **57**, 303–312.

- Tom-Petersen, A., Leser, T.D., Marsh, T.L., & Nybroe, O. 2003. Effects of copper amendment on the bacterial community in agricultural soil analyzed by the T-RFLP technique. *FEMS Microbiology Ecology* **46**, 53–62.
- Tscherko, D., Rustemeier, J., Richter, A., Wanek, W., & Kandeler, E. 2003. Functional diversity of the soil microflora in primary succession across two glacier forelands in the Central Alps. *European Journal of Soil Science* **54**, 685–696.
- Tunlid, A., & Hoitink, H. 1989. Characterization of bacteria that suppress *Rhizoctonia* damping-off in bark compost media by analysis of fatty acid biomarkers. *Applied and Environmental Microbiology* **55**, 1368–1374.
- Turpeinen, R., Kairesalo, T., & Häggblom, M.M. 2004. Microbial community structure and activity in arsenic-, chromium- and copper-contaminated soils. *FEMS Microbiology Ecology* **47**, 39–50.
- Tyler, G. 1984. The Impact of Heavy Metal Pollution on Forests: A Case Study of Gusum, Sweden. *Ambio* **13**, 18–24.
- Ulanowicz, R.E., & Hannon, B.M. 1987. Life and the Production of Entropy. *Proceedings of the Royal Society B: Biological Sciences* **232**, 181–192.
- Vallino, J.J. 2010. Ecosystem biogeochemistry considered as a distributed metabolic network ordered by maximum entropy production. *Philosophical transactions of the Royal Society of London. Series B, Biological Sciences* **365**, 1417–27.
- Vance, E.D., Brookes, P.C., & Jenkinson, D.S. 1987. An extraction method for measuring soil microbial biomass C. *Soil Biology and Biochemistry* **19**, 703–707.
- Vor, T., Dyckmans, J., Flessa, H., & Beese, F. 2002. Use of microcalorimetry to study microbial activity during the transition from oxic to anoxic conditions. *Biology and Fertility of Soils* **36**, 66–71.
- Wadsö, L. 2005. Applications of an eight-channel isothermal conduction calorimeter for cement hydration studies. *Cement International* **3**, 94–101.
- Wadsö, I. 2009. Characterization of microbial activity in soil by use of isothermal microcalorimetry. *Journal of Thermal Analysis and Calorimetry* **95**, 843–850.
- Wadsö, L. 2010. Operational issues in isothermal calorimetry. *Cement and Concrete Research* **40**, 1129–1137.
- Wadsö, I., & Goldberg, R.N. 2001. Standards in isothermal microcalorimetry (IUPAC Technical Report). *Pure and Applied Chemistry* **73**, 1625–1639.

- Wakelin, S.A., Chu, G., Lardner, R., Liang, Y., & McLaughlin, M. 2010. A single application of Cu to field soil has long-term effects on bacterial community structure, diversity, and soil processes. *Pedobiologia* **53**, 149–158
- Wang, W.J., Chalk, P., Chen, D., & Smith, C.. 2001a. Nitrogen mineralisation, immobilisation and loss, and their role in determining differences in net nitrogen production during waterlogged and aerobic incubation of soils. *Soil Biology and Biochemistry* **33**, 1305–1315
- Wang, W.J., Chalk, P.M., Chen, D., & Smith, C.J. 2001b. Nitrogen mineralisation, immobilisation and loss, and their role in determining differences in net nitrogen production during waterlogged and aerobic incubation of soils. *Soil Biology and Biochemistry* **33**, 1305–1315
- Wang, Y., Shi, J., Wang, H., Lin, Q., Chen, X., & Chen, Y. 2007. The influence of soil heavy metals pollution on soil microbial biomass, enzyme activity, and community composition near a copper smelter. *Ecotoxicology and Environmental Safety* **67**, 75–81.
- Wang, F., Yao, J., Chen, H., Chen, K., Trebše, P., Zaray, G., & Trebse, P. 2010a. Comparative toxicity of chlorpyrifos and its oxon derivatives to soil microbial activity by combined methods. *Chemosphere* **78**, 319–26
- Wang, F., Yao, J., Chen, H., Yi, Z., & Choi, M.M.F. 2014. Influence of short-time imidacloprid and acetamiprid application on soil microbial metabolic activity and enzymatic activity. *Environmental Science and Pollution Research International*
- Wang, F., Yao, J., Si, Y., Chen, H., Russel, M., Chen, K., Qian, Y., Zaray, G., Bramanti, E., & Bramanti, Æ.E. 2010b. Short-time effect of heavy metals upon microbial community activity. *Journal of Hazardous Materials* **173**, 510–516.
- Wardle, D. A. 1993. Changes in the microbial biomass and metabolic quotient during leaf litter succession in some New Zealand forest and scrubland ecosystems. *Functional Ecology* **7**, 346–355.
- Wardle, D. A., & Ghani, A. 1995. A critique of the microbial metabolic quotient (qCO<sub>2</sub>) as a bioindicator of disturbance and ecosystem development. *Soil Biology and Biochemistry* **27**, 1601–1610.
- Wardle, D. A., Walker, L.R., & Bardgett, R.D. 2004. Ecosystem properties and forest decline in contrasting long-term chronosequences. *Science* **305**, 509–513.
- Waring, B.G., Weintraub, S.R., & Sinsabaugh, R.L. 2014. Ecoenzymatic stoichiometry of microbial nutrient acquisition in tropical soils. *Biogeochemistry* **117**, 101–113.

- West, A.W., & Sparling, G.P. 1986. Modifications to the substrate-induced respiration method to permit measurement of microbial biomass in soils of differing water contents. *Journal of Microbiological Methods* **5**, 177–189.
- White, E.P., Thibault, K.M., & Xiao, X. 2012. Characterizing species abundance distributions across taxa and ecosystems using a simple maximum entropy model. *Ecology* **93**, 1772–8.
- Wilhelm, T., Brüggemann, R., & Bru, R. 2000. Goal functions for the development of natural systems. *Ecological Modelling* **132**, 231–246.
- Wirén-Lehr, S. von, Scheunert, I., & Dörfler, U. 2002. Mineralization of plant-incorporated residues of <sup>14</sup>C-isoproturon in arable soils originating from different farming systems. *Geoderma* **105**, 351–366.
- Wu, J., Joergensen, R.G., Pommerening, B., Chaussod, R., & Brookes, P.C. 1990. Measurement of soil microbial biomass C by fumigation-extraction: an automated procedure. *Soil Biology and Biochemistry* **22**, 1167–1169.
- Yamano, H., & Takahashi, K. 1983. Temperature effect on the activity of soil microbes measured from heat evolution during the degradation of several carbon sources. *Agricultural and Biological Chemistry* **47**, 1493– 1499.
- Yamano, H., Takahashi, K., Chemistry, B., & Prefecture, O. 1983. Temperature Effect on the Activity of Soil Microbes Measured from Heat Evolution during the Degradation of Several Carbon Sources. *Agricultural and Biological Chemistry* **47**, 1493–1499.
- Yao, J., Tian, L., Wang, Y., Djah, A., Wang, F., Chen, H., Su, C., Zhuang, R.S., Zhou, Y., Choi, M.M.F., Bramanti, Æ.E., & Bramanti, E. 2008. Microcalorimetric study the toxic effect of hexavalent chromium on microbial activity of Wuhan brown sandy soil: an *in vitro* approach. *Ecotoxicology and Environmental Safety* **69**, 289–95
- Yao, J., Wang, F., Tian, L., Zhou, Y., Chen, H., Chen, K., Gai, N., Zhuang, R.S., Maskow, Æ.T., Ceccanti, B., Zaray, G., & Maskow, T. 2009. Studying the toxic effect of cadmium and hexavalent chromium on microbial activity of a soil and pure microbe: A microcalorimetric method. *Journal of Thermal Analysis and Calorimetry* **95**, 517–524.
- Yao, J., Xu, C., Wang, F., Tian, L., Wang, Y., Chen, H., Yong, Z., Choi, M.M.F., Bramanti, Æ.E., Maskow, Æ.T., Bramanti, E., & Maskow, T. 2007. An *in vitro* microcalorimetric method for studying the toxic effect of cadmium on microbial activity of an agricultural soil. *Ecotoxicology* **16**, 503–509
- Zelles, L. 1999. Fatty acid patterns of phospholipids and lipopolysaccharides in the characterisation of microbial communities in soil : a review. *Biology and Fertility of Soils* **29**, 111–129

- Zelles, L., Adrian, P., Bai, Q.Y., Stepper, K., Adrian, M. V., Fischer, K., Maier, A., & Ziegler, A. 1991. Microbial activity measured in soils stored under different temperature and humidity conditions. *Soil Biology and Biochemistry* **23**, 955–962.
- Zelles, L., Scheunert, I., & Korte, F. 1986. Comparison of Methods to Test Chemicals for Side Effects on Soil Microorganisms. *Ecotoxicology and Environmental Safety* **12**, 53–69
- Zelles, L., Scheunert, I., & Kreutzer, K. 1987a. Effect of artificial irrigation, acid precipitation and liming on the microbial activity in soil of a spruce forest. *Biology and Fertility of Soils* **4**, 137–143.
- Zelles, L., Scheunert, I., & Kreutzer, K. 1987b. Bioactivity in limed soil of a spruce forest. *Biology and Fertility of Soils* **3**, 211–216.
- Zelles, L., Stepper, K., & Zsolnay, a. 1990. The effect of lime on microbial activity in spruce (*Picea abies* L.) forests. *Biology and Fertility of Soils* **9**, 78–82
- Zhang, J., Gurkan, Z., & Jørgensen, S.E. 2010. Application of eco-exergy for assessment of ecosystem health and development of structurally dynamic models. *Ecological Modelling* **221**, 693–702
- Zhang, Y., Yang, Z., & Li, W. 2006. Analyses of urban ecosystem based on information entropy. *Ecological Modelling* **197**, 1–12.
- Zheng, S., Hu, J., Chen, K., Yao, J., Yu, Z., & Lin, X. 2009. Soil microbial activity measured by microcalorimetry in response to long-term fertilization regimes and available phosphorous on heat evolution. *Soil Biology and Biochemistry* **41**, 2094–2099.
- Zheng, S., Yao, J., Zhao, B., & Yu, Z. 2007. Influence of agricultural practices on soil microbial activity measured by microcalorimetry. *European Journal of Soil Biology* **43**, 151–157.
- Zhuang, R.S., Chen, H., Yao, J., Li, Z., Burnet, J.E., & Choi, M.M.F. 2011. Impact of beta-cypermethrin on soil microbial community associated with its bioavailability: a combined study by isothermal microcalorimetry and enzyme assay techniques. *Journal of Hazardous Materials* **189**, 323–328